A Comparison Between Synchronous CDMA and Orthogonal Frequency Division Multiplexing (OFDM) for Fixed Broadband Wireless Access

Shital Ratilal Chheda

Thesis submitted to the Faculty of the
Virginia Polytechnic Institute and State University
in partial fulfillment of the requirements for the degree of

Master of Science
in
Electrical Engineering

Charles W. Bostian, Chair
Ira Jacobs
Dennis G. Sweeney

April 15, 2002
Blacksburg, Virginia

Keywords: CDMA, OFDM, synchronous, broadband, wireless, 3G, Non-Line-of-Sight (NLOS), orthogonal, VOFDM, SCDMA

A Comparison Between Synchronous CDMA and Orthogonal Frequency Division Multiplexing (OFDM) for Fixed Broadband Wireless Access

Shital Ratilal Chheda

(ABSTRACT)

The growth of broadband Internet access has paved the way for the development of many new technologies. As the cost of implementing broadband access soars, the best alternative will be to use fixed wireless for these services. This thesis addresses the possibility of 3rd Generation (3G) mobile cellular wireless systems as the basis for fixed broadband wireless service. Two of the 3G technologies aimed at providing fixed broadband wireless access are Time Division Synchronous Code Division Multiple Access (TD-SCDMA) and Orthogonal Frequency Division Multiplexing (OFDM).

This thesis aims to provide a preliminary study on using TD-SCDMA and OFDM for broadband wireless systems. Currently, there is not enough theory and information to establish the feasibility of using either of these technologies for broadband wireless access. First, the basic features and background on synchronous CDMA and OFDM are presented for the reader to better understand these technologies. Then, an example TD-SCDMA system is described, and some analytical and experimental results are presented. Finally, TD-SCDMA's technologies, along with this system's attributes, are compared analytically to that of Vector OFDM (VOFDM).

Acknowledgements

First of all, I would like to thank my advisor, Dr. Charles Bostian, for all his support during the course of my research and thesis. His dedication to the improvement of the wireless communications program at Virginia Tech was instrumental in my continued education. The Center for Wireless Telecommunications (CWT) provided me with the resources and support necessary to pursue my research and complete my thesis properly. The time spent and advice lent by Dr. Ira Jacobs and Dr. Dennis Sweeney reviewing this thesis, helping with my research, and participating as part of my thesis committee is very much appreciated. I would also like to thank Tim Gallagher for his continued help and advice with my research. Also, the administrative support from the other faculty and staff of CWT is appreciated.

I would also like to thank my sponsor, the Center for Innovate Technology (CIT) and especially Jean Woods for spearheading and funding this project. I would also like to thank Navini Networks and especially Phillip Levy and Walter Marusak for allowing me to use their system and field trial data for my thesis. Without their Ripwave system details and experiment results, this thesis would have not been possible. Finally, I would like to thank nTelos and especially Steve Garber and Noel Munson for their support of this research and thesis.

It has been my pleasure to work with the Graduate Research Assistants in the CWT graduate labs. Their technical advice and constant source of entertainment made coming to work a pleasure on even the busiest of days. I wish them all the best in their future endeavors.

Finally, I would like to thank my family. My parents Ratilal and Rekha Chheda and my sister Jeenal supported my decision to return to Virginia Tech for my Masters degree. Without their continued support and encouragement I would not have had the resolve to complete this degree.

Contents

List of Figures

List of Tables

Chapter 1

Introduction

There is no doubt that wireless data service is in demand. Already the industry is seeing data traffic in wireless networks begin to overtake voice, as it did in the wireline world a few years back. The opportunities for new services are boundless. However, the technical challenges of deploying high-speed data in a mobile or fixed broadband environment, when added to the high cost of spectrum and a jittery market, have the potential to slow the rollout of third generation networks. In the meantime, wireless network operators face the same issues as always – increasing revenue, growing their customer base, and generating profit.

1.1 Need for Wireless Broadband

The growing convergence of the technologies of voice, data, and video entertainment is driving the need for flexible broadband communications direct to small businesses and to the home. Upgrading the copper based local loop (currently the major bottleneck) to provide this capability is possible, but doing so will be both slow and very expensive. In some rural areas, it will be impossible. In these circumstances, wireless networks have a number of key advantages. In particular, they are less expensive and can be installed more quickly than their wired counterparts. In a wired network, the majority of the cost has to be expended on central plant and cabling before subscribers can be connected and revenue can be earned. With a wireless network, the radio base station has to be installed in advance, but the customer premises equipment is only installed when new customers are added to the system [1]. In addition to these major advantages of lower initial costs and rapid deployment, wireless broadband access makes it easy to upgrade to a newer infrastructure. There is also the ability to define service types [for Quality of Service (QOS) purposes] based on the type of users (residential / small businesses) and there is inherent flexibility in dynamic bandwidth allocations.

1.2 Market Situation

No single application is seen to be the driving force in the broadband wireless market. Most believe that it will be necessary to offer a range of services that will be easily adapted to new requirements as the market develops. Some initial applications will be high-speed Internet access, remote LAN access, file and data transfer, and video conferencing. Within a few years, applications such as desk-to-desk video, tele-medicine, interactive CAD, or collaborative working might be commonplace for broadband wireless technology. Figure 1.1 from [1] shows how this scenario might develop in terms of time scales and required bit rates.

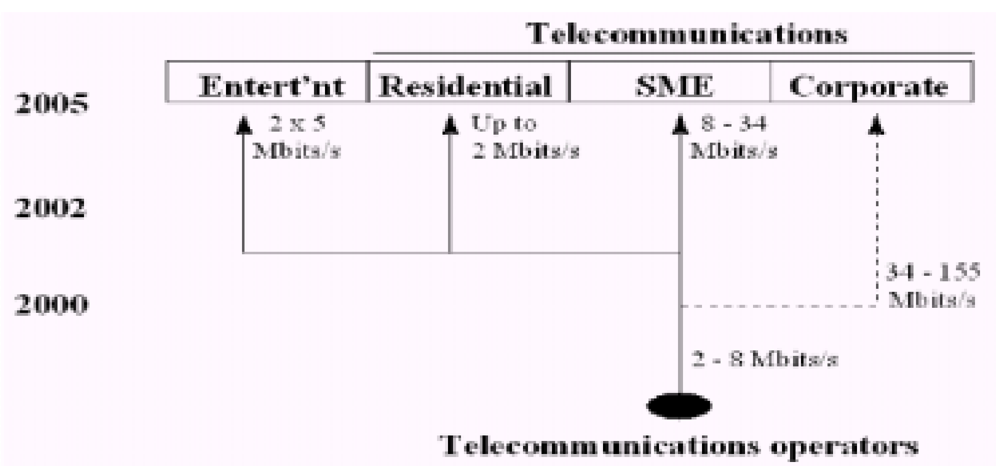

Figure 1.1: Evolution of the Broadband Market [1]

The dotted lines in the figure imply a smaller market servicing the corporate sector since its needs will be far more than broadband wireless can handle (and they would be better off leasing dedicated wired lines). “SME” in the figure refers to Small- and Medium-sized Enterprises. As can be seen by Figure 1, the need for higher data rates will become the common place and will drive the need for fixed broadband wireless access.

1.3 Key Feature of Broadband Wireless

Wireless broadband is not a single technology, but rather a collection of technologies, each with slightly different properties. The spectral allocations for wireless broadband communications range from MMDS (Multichannel Multipoint Distribution Service), through ISM (Industrial, Scientific, and Medical band), U-NII (Unlicensed band), and up to LMDS (Local Multipoint Distribution Service).

Nevertheless, the operation principle for all these broadband wireless technologies is almost identical. The digital hub is installed on the highest building or mountain so it can serve the greatest radius (up to 35 miles depending on the choice of broadband wireless technology) without too many obstructions. The user’s house or small business has either a digital transceiver on the roof or a smart antenna inside the house, which transfers signal to a wireless modem that communicates with the computer or LAN. This is a point-to-multipoint design, but other configurations (such as point-to-point) are possible.

Wireless technologies use individual radio frequencies over and over again by dividing a service area into separate geographic zones called cells. Cells can be as small as an individual building (pico-cells) or as big as 35 miles across (macro-cells). Figure 1.2 from [2] illustrates the different types of cells.

Figure 1.2: Dividing Geographic Regions into Cells [2]

Each cell is equipped with its own base station operating at a particular frequency. Because the system operates at such a low power, a frequency being used to carry a signal in one cell can be used to carry another signal in a nearby cell without interference [3]. All wireless operators are limited by allocated spectrum bandwidth, which without frequency-reuse, would be used very ineffectively (and would be very expensive). In order to increase broadband capacity, these low power facilities “reuse” frequencies on the radio spectrum.

Exactly what frequency band is used to carry the radio signal is a key parameter in the design of the system. The frequency chosen will determine cell size, frequency reuse pattern, transmitter power, and interference issues. The suitable frequencies for fixed broadband wireless access are summarized in Table 1.1 below.

Table 1.1: Suitable Frequencies for Broadband Wireless Access [4]

Band	Center Frequencies / Bandwidth	Description
ISM	2.4, 5.6, 29 GHz / 83.5 MHz	Industrial, Scientific, and Medical Band (unlicensed)
MMDS (Old)	2.100 – 2.300 GHz / 200 MHz	Multichannel Multipoint Distribution Service (licensed)
WCS	2.3 GHz / two 15 MHz blocks	Wireless Communications Service (licensed)
MMDS (New)	2.500 – 2.700 GHz / 200 MHz	Multichannel Multipoint Distribution Service (licensed)
U-NII	5.150 – 5.350 / 200 MHz	Unlicensed band in USA
U-NII	5.725 – 5.825 / 100 MHz	Unlicensed band in USA
GWCS	4. 9 GHz / five 10 MHz blocks	General Wireless Communications Service (licensed)
5 GHz	5.150 – 5.350 GHz / 200 MHz	Unlicensed band in Europe
5 GHz	5.470 – 5.725 / 255 MHz	Unlicensed band in Europe
LMDS	28 – 31 GHz / one 300 MHz block, 1150 MHz A-band, 150 MHz B-band	Local Multipoint Distribution Service (licensed)
DEMS	24 GHz	Digital Electronic Messaging Service

This paper will only focus on fixed wireless broadband services operating in the ISM and MMDS frequency bands.

1.4 Challenges of Fixed Broadband Wireless

The quality of service and data rate requirements in the fixed case are significantly higher than in the mobile case. Meanwhile, most of the problems that dominate in the mobile case still apply in the fixed case.

1.4.1 Attenuation

Attenuation is a drop in the signal power (in excess of that observed in free space) when transmitting from one point to another. It can be caused by losses and obstructions in the signal path and by multipath effects. Shadowing of the signal can occur whenever there is an obstruction between the transmitter and the receiver. It is generally caused by buildings and hills and is the most important environmental attenuation factor. For example, in the MMDS band, a path through relatively heavy foliage can incur an excess (in addition to free space) attenuation of more than 12 dB [5]. To overcome the problem of shadowing, hub units are usually placed as high as possible (on a mountain or a tall building) to minimize the number of obstructions.

1.4.2 Multipath

In a radio link, the RF signal from the transmitter may be reflected from objects such as hills, buildings, or vehicles. This gives rise to multiple incoming signals arriving over multiple transmission paths at the receiver. The relative phase of multiple reflected signals can cause constructive or destructive interference at the receiver. The Rayleigh distribution is commonly used to describe such a statistical time-varying received signal power. It describes the probability that the signal level will equal or exceed a stated value.

In any radio link, the channel power spectral density (PSD) is not flat. It has dips or fades in the response where reflections cause cancellation of certain frequencies at the receiver. Reflections off near-by objects, such as buildings or trees, can lead to multipath signals of similar signal power as the direct signal. This can result in deep nulls in the received signal power due to destructive interference. For narrow bandwidth transmissions, if the null in the frequency response occurs at the transmission frequency, then the entire signal might be lost. This can be overcome by moving the antenna a little bit to avoid the deep nulls, but that is inefficient. So, a better way to overcome this problem is by transmitting a wide bandwidth signal as in Code Division Multiple Access (CDMA) or by splitting up the transmission into many small bandwidth carriers as in Orthogonal Frequency Division Multiplexing (OFDM). These topics will be elaborated upon in other chapters.

1.4.3 Delay Spread

The received signal consists typically of a direct signal plus reflections off buildings and other objects. The reflected signals arrive at a later time than the direct signals because of the extra path length. This interval spreads the received energy. Delay spread is the time spread between the arrival of the first and last multipath signals seen by the receiver. In a digital system, the delay spread can lead to inter-symbol interference (ISI). This is due to the delayed multipath signal overlapping with the wanted symbols received later.

As the transmitted bit rate is increased, the amount of ISI also increases. The effect starts to become very significant when the delay spread is greater than half of the bit period. The amount of delay spread in fixed wireless channels depends strongly on the frequency of transmission and the antenna characteristics. For example, in [6], median root mean square (RMS) delay spreads for directional antennas in suburban environments of approximately 75 ns have been reported; with omni-directional antennas in the same terrain, a delay spread of 175 ns has been found. The reason for the difference in delay spreads is that echoes at longer delays tend to arrive at angles farther from the direct path and are thus more attenuated in the case of directional antennas [6].

For the MMDS band, delay characteristics under line-of-sight and non-line-of-sight conditions were gathered in [7]. The delay-spread information was obtained using a commercially available channel sounder operating from 2.455 to 2.495 GHz. Table 1.2 summarizes those results.

Table 1.2: Summary of Delay Characteristics for MMDS [7]

Visibility	**Receiving Antenna Type**	**RMS Delay Spread, μs**		
		Min	**Max**	**Mean**
LOS	Directional	0.02	0.04	0.03
	Omni-directional	0.02	2.39	0.13
NLOS	Directional	0.02	5.26	0.14
	Omni-directional	0.02	7.06	0.37

In the above experiment, the receiver used two antennas: a high-gain directional (non-isotropic radiation pattern) antenna and a medium-gain horizontally omni-directional antenna. The directional antenna had a gain of +21 dBi and a 10° beamwidth, and the omni-directional antenna had a +9 dBi gain with a 17° elevation beamwidth.

For the ISM band, most of the delay spreads that were observed in [8] were fewer than 100 ns, with a median value under 50 ns. Delay spreads show only a small increase in magnitude as a function of path length [8]. In [9], RMS delay spread measurements (average) were observed to be 37 ns for urban environments, 24 ns for suburban environments, and 19 ns for rural zones.

1.4.4 K-Factor (Ricean factor)

The path loss of a fixed broadband wireless channel can be represented as having a fixed component plus a scatter component. The ratio of the average energy in the fixed component to the average energy in the scatter component is called the K-factor or the Ricean factor. Generally the K-factor in fixed wireless applications can be very low, if the base transmit station (BTS) and customer premise equipment (CPE) antenna heights are kept relatively low [6]. Experiments undertaken in [6] can be concluded to state that in a fixed broadband wireless system design, very low K-factors (almost purely Rayleigh fading conditions) are necessary to provide large cell coverage and reliable operation at the edge of the cell. Experiments in [10] show that most found (average) Ricean factors are in the range –8 to 5 dB (a Ricean factor of $-\infty$ is purely Rayleigh fading).

1.4.5 Spectral Efficiency

The spectral efficiency of a wireless network is measured in bits per second per Hertz per cell (BHC). Spectral efficiency can be increased through aggressive frequency reuse and higher-order modulation. However, frequency reuse results in co-channel interference (CCI) in a multicell environment. Treating CCI as additive white Gaussian noise (AWGN), the Shannon formula for the theoretical limit on BHC can be written as

$$BHC = (L/mP)\log_2(1 + [C / (N+I)]),$$

where P is the spatial reuse factor, L is the angle reuse factor, m is the overhead factor accounting for excess bandwidth and frequency guard bands/slots, and C/(N+I) is the carrier-to-interference-plus-noise ratio [6]. Reducing P in macro/microcell systems or increasing L in single cell systems would increase BHC. However, this results in an increase of CCI and therefore a reduction of the modulation order that can be sustained. Typical values for BHC for current mobile cellular systems are 0.2 – 0.3 [6]. Fixed broadband wireless requirements are in the range of 2.0 – 2.5 [6], which implies that fixed wireless needs a significant increase in spectral efficiency.

1.4.6 Line of Sight Issues

One of the major limitations for fixed wireless services is that there should be a clear line of sight (LOS) between the antennas transmitting and receiving the signal. When there is not a clear LOS path (i.e., signals have to penetrate buildings or other obstacles), sufficient margins need to be placed in the link budgets to overcome the penetration losses. Building penetration loss is due to attenuation or shielding of the radio signal by walls, floors, and ceilings. If we decrease the height of an outdoor receiving antenna, the received signal power will usually decrease as well – this is referred to as height loss [10]. This is partially due to shielding by buildings or other obstacles in the LOS path.

Experiments in [10] show that for non-line-of-sight (NLOS) scenarios, there is a median building penetration loss of 12 dB and a height loss of 6 dB (when the receiver is much lower than the transmitting antenna). The standard deviation of delay spread for the NLOS paths ranges from 80 to 200 ns, which is an order of magnitude larger than that of the LOS case [11]. The most significant difference between LOS and NLOS is seen in the mean value of the weighted mean delays [12]. In the LOS case, the delays decrease with distance between the transmitter and receiver (independent of the base station height), while increasing for the NLOS case. This implies the dominance of the guiding effect along the streets for below rooftop base station heights [12].

1.5 Multiple Access Techniques

Multiple access schemes are used to allow many simultaneous users to use the same fixed bandwidth radio spectrum. Sharing of the spectrum is required in order to increase the user capacity of any wireless network. Frequency Division Multiple Access (FDMA), Time Division Multiple Access (TDMA), and Code Division Multiple Access (CDMA) are three of the most common methods for multiple access. There are many extensions and hybrid techniques using these methods, such as Synchronous Code Division Multiple Access (SCDMA) and Orthogonal Frequency Division Multiplexing (OFDM). However, an understanding of the three basic methods is required for understanding any hybrid techniques.

1.5.1 Frequency Division Multiple Access

In Frequency Division Multiple Access (FDMA), the available bandwidth is subdivided into a number of narrower band channels. Each user is allocated a unique frequency band in which to transmit and receive signals. The bandwidths of FDMA channels are generally small since each channel only supports one user. FDMA is used as the primary breakup of large allocated frequency bands and in most multichannel systems. Figure 1.3 shows the basic principle behind FDMA. (Usually guard bands are needed between each channel.)

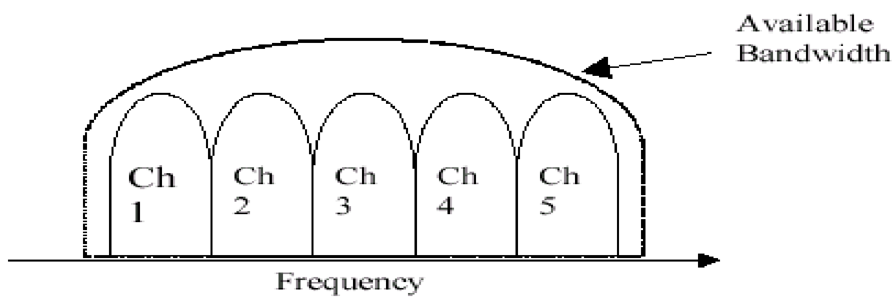

Figure 1.3: FDMA Spectrum

1.5.2 Time Division Multiple Access

In Time Division Multiple Access (TDMA), the available spectrum is subdivided into multiple time slots. Each user is given a time slot in which to transmit or receive signals. The time slots are provided to users in a round robin fashion, with each user being allotted one time slot per frame. TDMA systems transmit data in a buffer and burst method, thus the transmission of each channel is non-continuous. Due to the manner of data transmission, TDMA can only handle digital data or sampled analog signals. Figure 1.4 shows the basic principle behind TDMA (again, guard times are missing from the diagram).

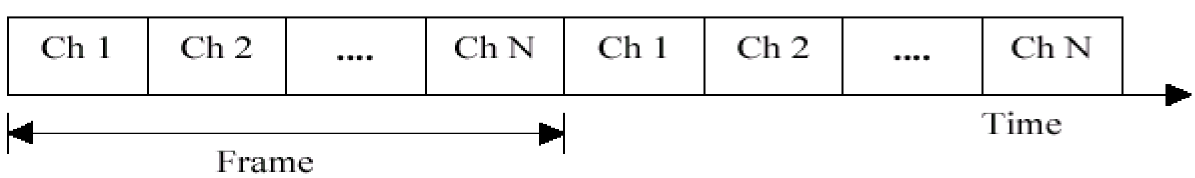

Figure 1.4: TDMA Framing Scheme

1.5.3 Code Division Multiple Access

Code Division Multiple Access (CDMA) is a spread spectrum technique that uses neither frequency nor time slots. In CDMA, the narrow band digitized message is multiplied by a large bandwidth signal that is a pseudo random noise code (PN code). All users in a CDMA system use the same frequency band and transmit simultaneously. The transmitted signal is recovered by correlating the received signal with the PN code used by the particular transmitter. Some of the major advantages of CDMA are signal hiding, non-interference with existing systems, anti-jam and interference rejection, information security, large processing gain, and multipath tolerance. The fundamental premise is that, in channels with narrowband noise, increasing the transmitted signal bandwidth results in an increased probability that the received information will be correct. If total signal power is interpreted as the area under the spectral density curve, then signals with equivalent total power may have either a large signal power concentrated in a small bandwidth or a small signal power spread over a large bandwidth. Figure 1.5 shows the general principle behind CDMA.

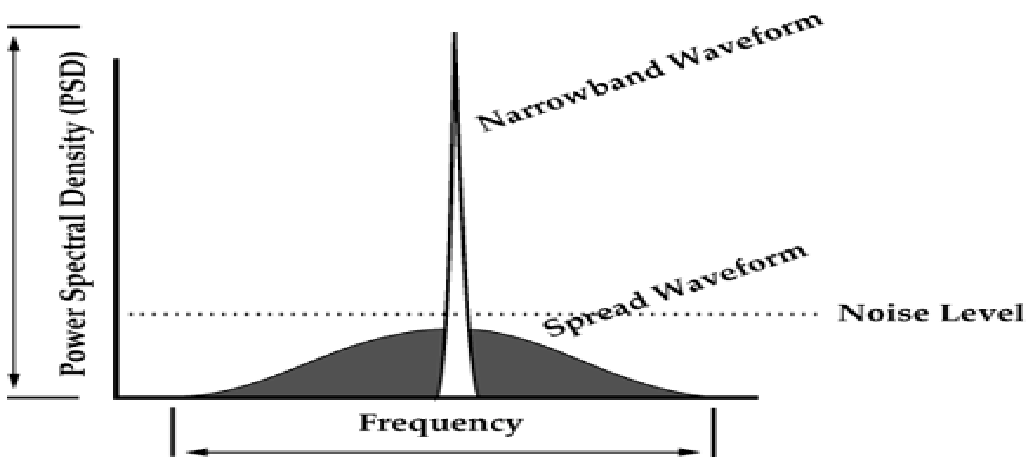

Figure 1.5: CDMA Spectrum

As can be seen in Figure 1.5, the narrowband signal is spread out to the RF bandwidth over the channel. The performance increase for very wideband systems is referred to as "processing gain." Signal spreading works well in situations with strong narrowband interference signals, since the spread spectrum signal has a unique form of frequency diversity. The actual signal can be spread by one of three basic techniques: direct sequence, frequency hopped, or hybrid forms.

1.6 Emergence of 3G

The goal for the next generation of mobile and fixed broadband communications systems is providing a variety of communication services to everyone at any time. The technology needed to tackle the challenges to make these services available is known as third generation (3G) cellular systems. The first generation systems are represented by the analog mobile systems designed to carry voice traffic. Their subsequent digital counterparts are known as second generation (2G) cellular systems. Third generation systems will constitute a significant leap, both in applications and capacity, from the current second generation systems. Third generation cellular systems are being designed to support wideband services like high-speed Internet access, video teleconferencing, and high quality image transmission with the same quality as in fixed networks. The primary requirements of the next generation cellular systems are [13]:

- Voice quality comparable to the Public Switched Telephone Network (PSTN).
- Support of high data rates: 144 kbps under high-speed moving environments, 384 kbps under outdoor-to-indoor and pedestrian, and 2 Mbps under indoor conditions [14].
- Support of packet-switched and circuit-switched applications.
- More efficient usage of the available spectrum.
- Backwards compatibility with pre-existing networks and flexible introduction of new services and technologies.
- An adaptive radio interface suited to highly asymmetric nature of most Internet communications (more bandwidth for the downlink).

Research efforts have been underway for more than a decade to standardize the air interfaces for third generation communications systems. The 3G mobile standards can be extended to the case of fixed broadband access since those are what the broadband standards are going to be based upon and since those are the current available specifications.

1.7 Third Generation (3G) Systems Proposals

Two of the most prominent bodies working on integrating the wide variety of proposals for third generation systems are the International Telecommunication Union (ITU) and the European Telecommunications Standards Institute (ETSI). Table 1.3 presents the proposals developed for the ITU in the International Mobile Telecommunications – 2000 (IMT-2000).

Table 1.3: Radio Transmission Technology Proposals for IMT-2000 [15]

Proposal	Description	Source
DECT	Digital Enhanced Cordless Telecommunications	ETSI Project DECT
UWC-136	Universal Wireless Communications	USA TIA TR45.3
WIMS W-CDMA	Wireless Multimedia and Messaging Services Wideband CDMA	USA TIA TR46.1
TD-SCDMA	Time-Division Synchronous CDMA	China CATT
W-CDMA	Wideband CDMA	Japan ARIB
CDMA II	Asynchronous DS-CDMA	S. Korea TTA
UTRA	Universal Mobile Telecommunications System (UMTS) Terrestrial Radio Access	ETSI SMG2
NA: W-CDMA	North American: Wideband CDMA	USA T1P1-ATIS
CDMA2000	Wideband CDMA (IS-95)	USA TIA TR45.5
CDMA I	Multiband synchronous DS-CDMA	S. Korea TTA

Table 1.4 presents the UTRA air interface technology proposals developed by the ETSI.

Table 1.4: ETSI UTRA Air Interface Technology Proposals [16]

Concept Group	Multiple-Access Scheme
Alpha	Wideband Code Division Multiple Access (W-CDMA)
Beta	Orthogonal Frequency Division Multiplexing (OFDM)
Gamma	Wideband Time Division Multiple Access (W-TDMA)
Delta	Time Division / Code Division Multiple Access (TD-SCDMA)
Epsilon	Opportunity Driven Multiple Access (ODMA)

This paper will only focus on two of the proposed air interfaces for third generation communication systems: Time-Division Synchronous Code Division Multiple Access (TD-SCDMA) and Orthogonal Frequency Division Multiplexing (OFDM).

1.8 Contributions and Scope

This thesis will present the key features of TD-SCDMA and OFDM for broadband fixed wireless access. Chapter 2 will present the basic features and background of TD-SCDMA. Then, in Chapter 3, the Navini Networks Ripwave system, which uses TD-SCDMA, will be analyzed and compared to theory. Chapter 4 will present the key features and background of OFDM. Finally, Chapter 5 will present a numerical and theoretical comparison between TD-SCDMA and OFDM. From this work, we will draw general conclusions about the suitability of synchronous CDMA and OFDM for broadband fixed wireless systems.

Chapter 2

Synchronous CDMA

TD-SCDMA was proposed by the Chinese Wireless Telecommunications Standards group (CWTS) to ITU, and was accepted as a candidate for third generation systems. This chapter gives an overview of the basics, the implementations, and the benefits of TD-SCDMA (Time Division – Synchronous CDMA) for optimized spectral efficiency in a TDD (Time Division Duplexed) operation for symmetric and asymmetric services. The support of asymmetric services (e.g., high-speed Internet access) in a highly efficient manner is one of the key differences of 3G services over the current 2G systems. The scheme of TD-SCDMA uses the existing GSM infrastructure with 3G-service availability.

2.1 TD-SCDMA Basic Principles

A basic system in TD-SCDMA includes a Wireless Base Station (WBS) and multiple User Terminals (UTs) or Customer Premise Equipments (CPEs). The combination of FDMA, TDMA, CDMA, and Spatial Division Multiple Access (SDMA) gives TD-SCDMA a high flexibility of minimizing intercell interference (ICI). The FDMA component allows the use of different carriers to minimize ICI by frequency domain dynamic channel allocation (DCA). The TDMA component ensures that only a relatively small number of users are operating simultaneously within a given timeslot. Therefore, only a small group of users within a cell is causing ICI. The CDMA component allows multiple access in each timeslot. The SDMA component, through the use of smart antennas and space domain DCA, ensures a very effective directional decoupling of users, thus, minimizing ICI.

The basic difference between TD-SCDMA and the current IS-95 CDMA standard is that in synchronous CDMA, the spreading sequences of the multiple CPEs' CDMA signals are synchronized at the base station (so the reverse link, as well as the forward link, is synchronized). This means that all the CPE signals arrive at the base station at the same tiem. This feature is important in a CDMA system to guarantee the orthogonality of the spreading codes, thus virtually removing the co-channel interference from other code channels.

Each system uses a carrier RF frequency channel and can handle up to 64 combined TDMA and SCDMA code channels that can be aggregated to provide a 2 Mbps data rate in the indoor environment. Specifically, each RF channel includes 8 TDMA time slots and 16 CDMA code channels in each TDMA time slot. Figure 2.1 shows the basic principle of TD-SCDMA.

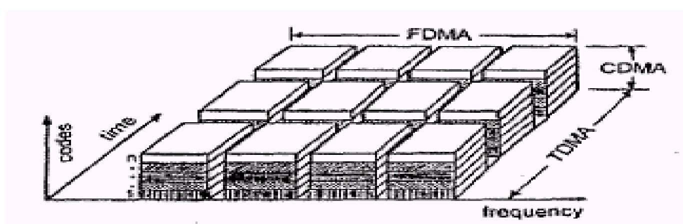

Figure 2.1: Basic Principle of TD-SCDMA [17]

These slots and code channels share the same RF bandwidth by using the well-known direct-sequence CDMA (DS-CDMA) method. Each code channel is identified by a specific Walsh code exclusive-ORed with a common pseudo-random (PN) spreading code. The transmitted code channels are transmitted mutually orthogonal in a mathematical sense. Mutually orthogonal means that the cross correlations between the signals are small (ideally zero). This is established by "covering" the forward error corrected (FEC) code symbols with one of the 64 Walsh codes. Since only whole periods of the Walsh functions occur in each code symbol, the effect of the Walsh cover is to make the channels separable at the receiver in the absence of multipath [18]. The orthogonality means that there is no interference between users in the same cell as well as meaning there is no intermingling of the channels. This has a substantial beneficial effect on the capacity – yielding theoretically twice as much as IS-95 when multipath is negligible [19]. In an asynchronous CDMA system, whenever a new user enters a particular cell site, the power level of all users within that cell must be increased. In other words, when each new user joins the network, the noise floor increases so all users on the system must increase their power output to be "heard." After a certain point, the asynchronous CDMA system hits a pole capacity – the point where the power requirements are so high that the terminals hit their power output limits. In a synchronous CDMA system, the code channels are orthogonal, which minimizes interference and increases capacity.

The basic scheme of TD-SCDMA also incorporates TDMA operation in TDD mode. For parallel transmission of multiple lower bit rate signals (e.g., speech), CDMA transmission is applied. However, for serial transmission of high bit rate signals (e.g., high-speed Internet), TDMA transmission without spreading is applied [20]. For multiple-signal CDMA transmission, the timeslots of the basic TDMA frame are filled with a maximum number of 16 coded and spread CDMA signals per time slot (as explained above). For high bit rate TDMA transmissions, the timeslots are filled with one serial wideband signal representing a sequence of information packets for different users and varying sizes depending on demand. This concept is illustrated in Figure 2.2 below.

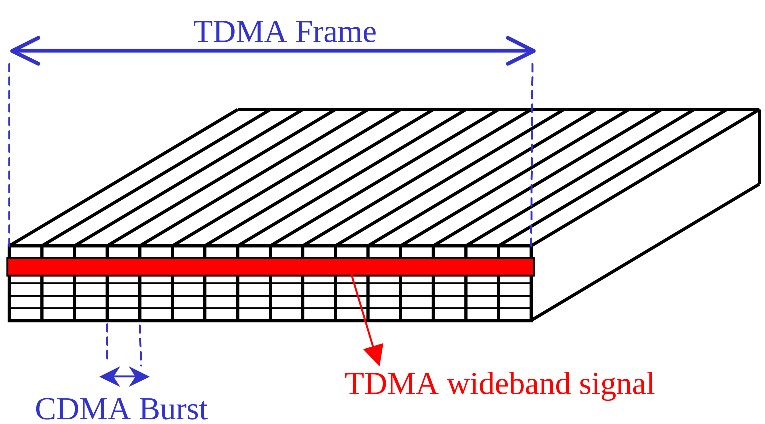

Figure 2.2: TD-SCDMA Frame

For lower bit rate transmissions, the basic TDMA frame in Figure 2.2 would be filled with a maximum of CDMA bursts. For higher bit rate transmissions, a wideband signal takes up the entire TDMA frame. The system internal switching from parallel CDMA to serial TDMA transmissions is accomplished by changing the filing modes of the basic TDMA timeslot and frame structure in the digital signal processor (DSP) [20].

A smart antenna and baseband DSP are also key features of the TD-SCDMA system. A smart antenna system is formed by an array of multiple antennas and coherent transceivers. Instead of just a fixed beam pattern, the smart antenna system can generate multiple beam patterns, each of which is specific for a particular CPE. Smart antennas and spatial diversity will be expanded upon later in the chapter.

These basic descriptions of TD-SCDMA leads to the block diagram presented in Figure 2.3.

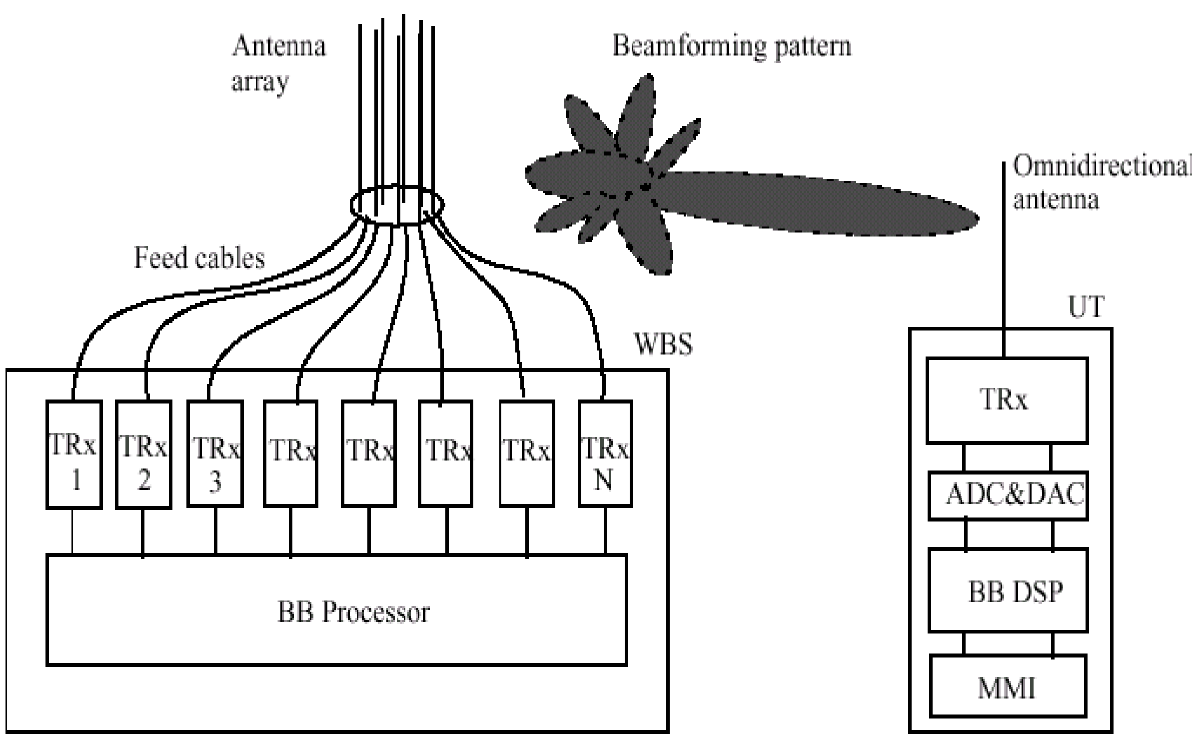

Figure 2.3: Block Diagram of TD-SCDMA System [21]

The block diagram shown above leads into the generic link level transmission models of TD-SCDMA shown in Figures 2.4 and 2.5 for the uplink and downlink respectively.

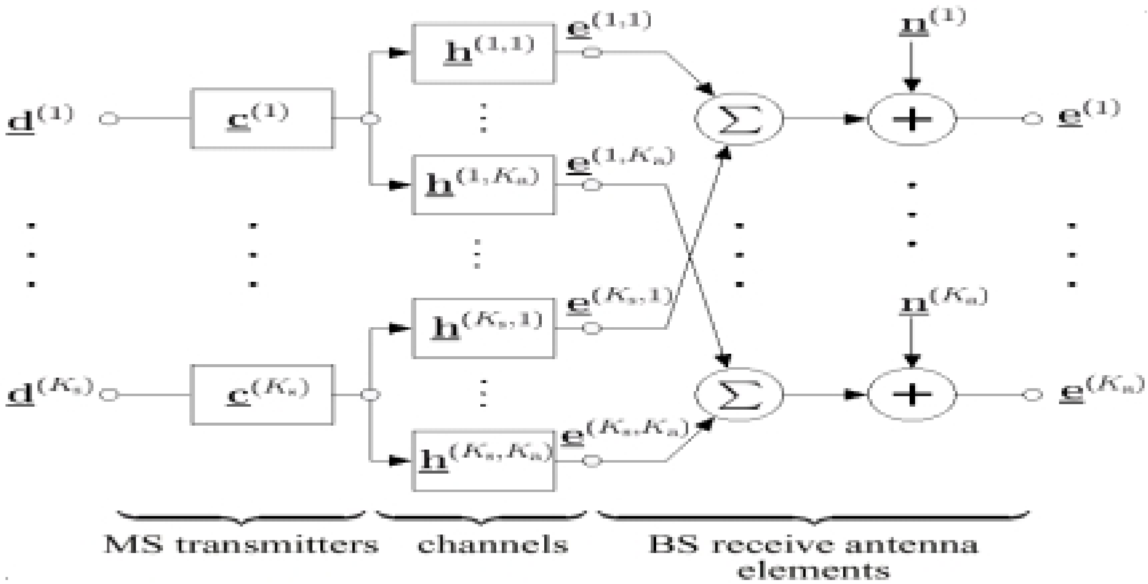

Figure 2.4: Link level Uplink Transmission Model [22]

In Figure 2.4, the time discrete equivalent low-pass representation of the signals and impulse responses are shown. In these models, $\underline{\mathbf{d}}$ represents the data block vectors, $\underline{\mathbf{c}}$ represents the CDMA code vectors, $\underline{\mathbf{h}}$ represents the impulse response vectors, $\underline{\mathbf{n}}$ represents the noise vectors, and $\underline{\mathbf{e}}$ represents the receiver input vector.

Let us consider one of the two data blocks (Figure 2.12 will show that there are two data blocks in each burst) of the simultaneously transmitted burst signals. Then, Ks data blocks consisting of N data symbols $\underline{d}_n^{(k_s)}$, $n = 1 \ldots N$, each are simultaneously transmitted. Each of these data blocks can be written as the partial data vector

$$\underline{\mathbf{d}}^{(k_s)} = [d_1^{(k_s)} \ldots d_N^{(k_s)}]^T, \; k_s = 1 \ldots K_s.$$

The N data symbols $\underline{d}_n^{(k_s)}$ in $\underline{\mathbf{d}}^{(k_s)}$ take on values from a finite data symbol set

$$V_d = \{\underline{V}_{d,1} \ldots \underline{V}_{d,M_d}\}$$

of cardinality Md. By stacking the Ks partial data vectors $\underline{\mathbf{d}}^{(k_s)}$, the total data vector

$$\underline{\mathbf{d}} = [\underline{\mathbf{d}}^{(1)T} \ldots \underline{\mathbf{d}}^{(K_s)T}]^T$$

of dimension NK_s can be obtained. Prior to transmission, each data symbol $\underline{d}_n^{(k_s)}$ is spectrally spread by a CDMA code

$$\underline{\mathbf{c}}^{(k_s)} = [\underline{c}_1^{(k_s)} \ldots \underline{c}_Q^{(k_s)}]^T, \; k_s = 1 \ldots K_s,$$

of dimension Q assigned to the partial data vector $\underline{\mathbf{d}}^{(k_s)}$. Then, the N spectrally spread data symbols $\underline{d}_n^{(k_s)}\underline{\mathbf{c}}^{(k_s)}$ are inputted into a radio channel each with impulse response

$$\underline{\mathbf{h}}^{(k_s)} = [\underline{h}_1^{(k_s)} \ldots \underline{h}_W^{(k_s)}]^T, \; k_s = 1 \ldots K_s,$$

of dimension W. Next the output signals of the K_s radio channels are superposed by the receive antennas and noise (symbolized by the noise vector $\underline{\mathbf{n}}$) is added. Now, the final receiver input signal symbolized by $\underline{\mathbf{e}}$ in Figure 2.4 is obtained. Both $\underline{\mathbf{n}}$ and $\underline{\mathbf{e}}$ have dimensions NQ+W-1.

Figure 2.5 shows the downlink link-level transmission model and is displayed below.

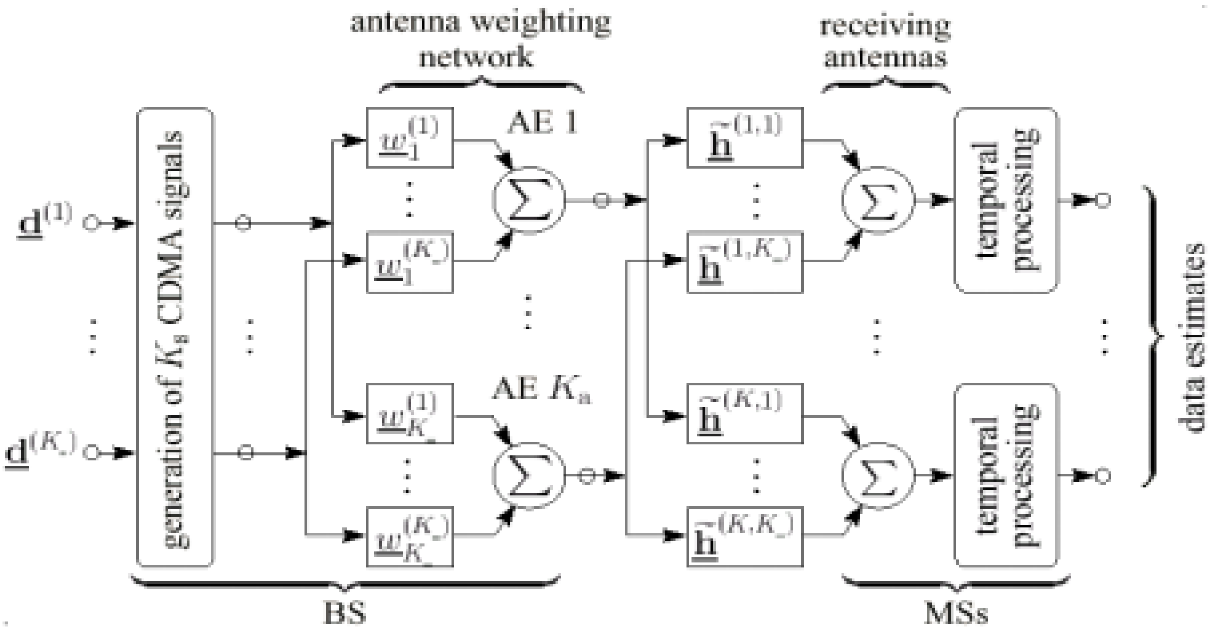

Figure 2.5: Link Level Downlink Transmission Model [23]

In Figure 2.5, once again the time discrete equivalent low-pass representation of the signals and impulse responses are shown. In these models, **d** represents the data block vectors, **w** represents the antenna weight vector, **h** represents the impulse response vectors, and **AE** represents the antenna element. A similar description of the downlink model to that of the uplink model is explained in [23].

2.2 RF Channel Parameters

The RF interface for the TD-SCDMA system in the proposal to the ITU specified the following RF requirements for both the Wireless Base Station (WBS) and User Terminal (UT) [21].

1. Operation Frequency Band: IMT-2000 band (1900 MHz – 1920 MHz, 2010 MHz – 2025 MHz).
2. Carrier Frequency: f_c = F1 + 0.8 + (N*1.4 MHz), where N = 0,1, …N (see Figure 2.6).

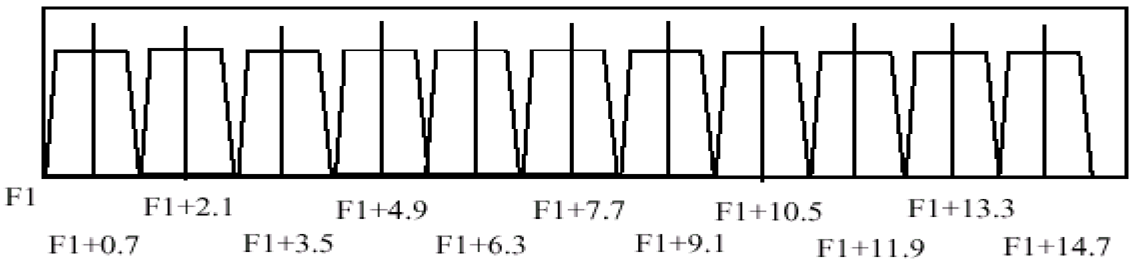

Figure 2.6: Carrier Frequency Allocation

3. Bandwidth: 1.12 MHz (3-dB), 1.4 MHz (99% energy).
4. Duplex Scheme: Time Division Duplex (TDD) with a frame size of 5 ms.
5. Baseband Modulation: DQPSK or 16-QAM.
6. Multiplex Scheme: TD-SCDMA.
7. Spreading Factor: 16 down to 1.
8. Chip Rate: 1.28 Mchip/s.
9. Maximum Transmit Power: WBS: 30 – 36 dBm, UT: 20 – 33 dBm.
10. Receiver Noise Figure (NF): 5 dB.
11. Receiver Dynamic Range: WBS: 30 dB, UT: 80 dB.
12. Receiver Sensitivity: -110 dBm (BER < 10^{-3} for DQPSK).

However, the CWTS and vendors (such as Navini) are constantly changing these parameters as the TD-SCDMA standard matures.

2.3 Frame and Multiplexing Structure

In TD-SCDMA, a maximum of up to 16 differently coded bursts are transmitted in parallel in each timeslot of the TDMA frame. Each data symbol is made up of a code word with chip sequences of up to 16 chips. A “midamble” for channel state measurement is placed in the center of each burst. Channel estimation can therefore be performed by a cyclic correlation and this training sequence. (TD-SCDMA is intrinsically protected against co-channel interference since orthogonal spreading codes are used. However, in the presence of multipath, the signals lose their orthogonality, leading to increased cross correlation. In these cases, channel estimation may be needed to improve the detection of the desired symbols [24].) Figure 2.7 shows an example of the frame, burst, and symbol structure of TD-SCDMA.

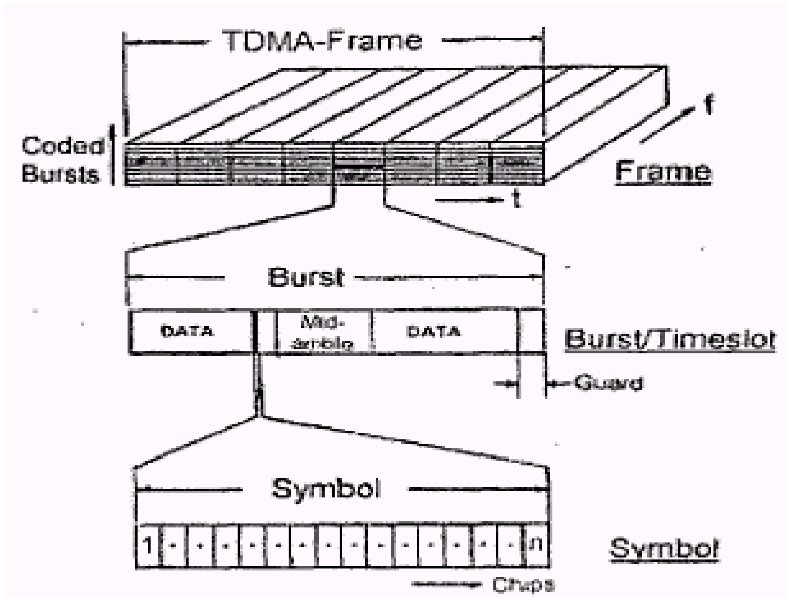

Figure 2.7: Frame, Burst, and Symbol Structure of TD-SCDMA [17]

2.3.1 Frame Structure

The radio frame has a duration of 10 ms and is subdivided into two subframes of 5 ms each. Each subframe is then subdivided into seven main time slots (TS) of 675 μs each and three special time slots: DwPTS (downlink pilot), G (guard period), and UpPTS (uplink pilot). Figure 2.8 describes the division mechanism for a TD-SCDMA frame.

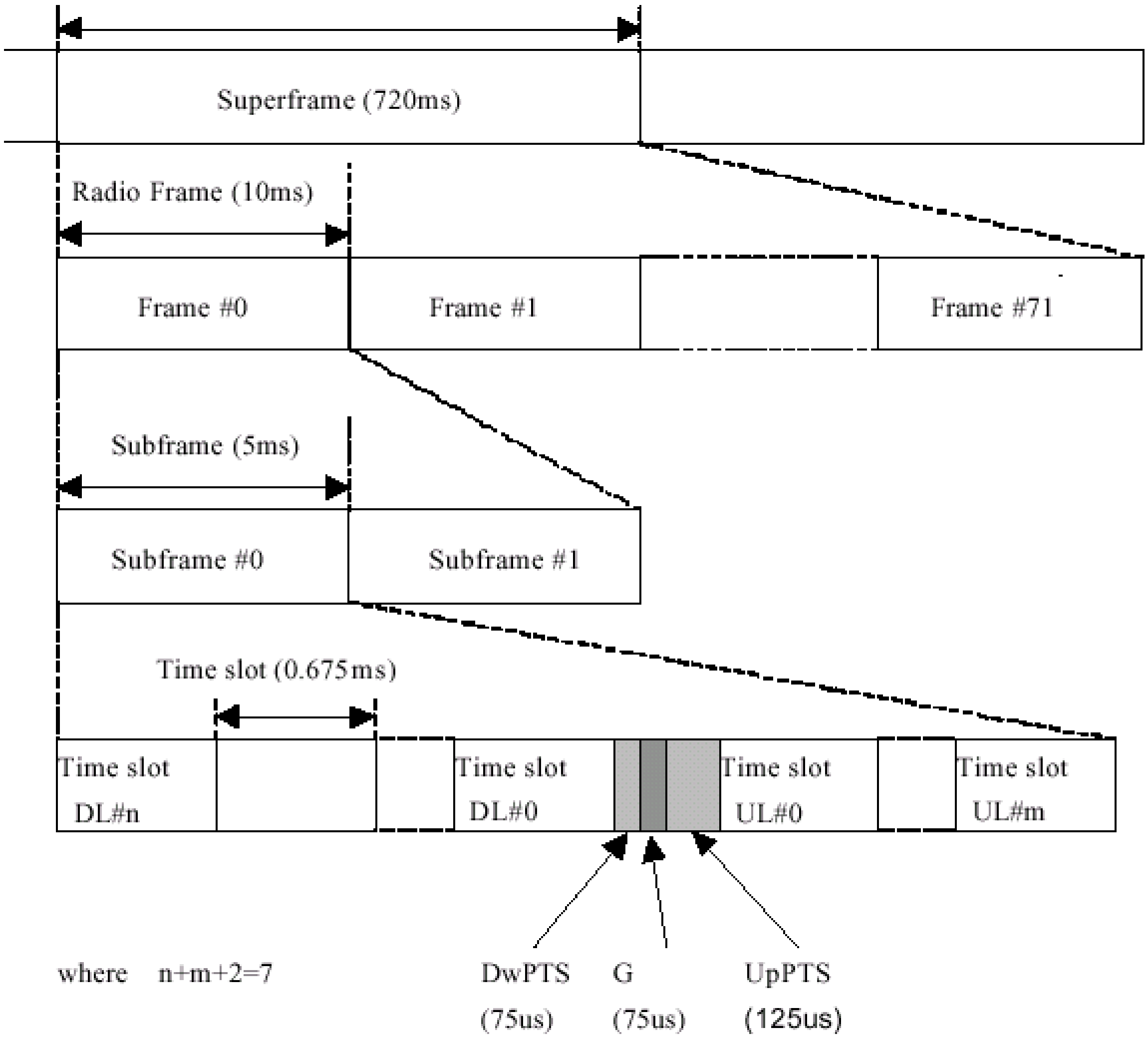

Figure 2.8: Frame Structure for TD-SCDMA [25]

A single switching point separates the uplink and the downlink slots (the switching point is thought of another time slot to make 8 total). All the main time slots (at least one main time slot) before the single switching point are allocated as downlink, and all the main time slots (at least one main time slot) after the single switching point are allocated as uplink. Figure 2.9 shows the timeslot assignments in one subframe.

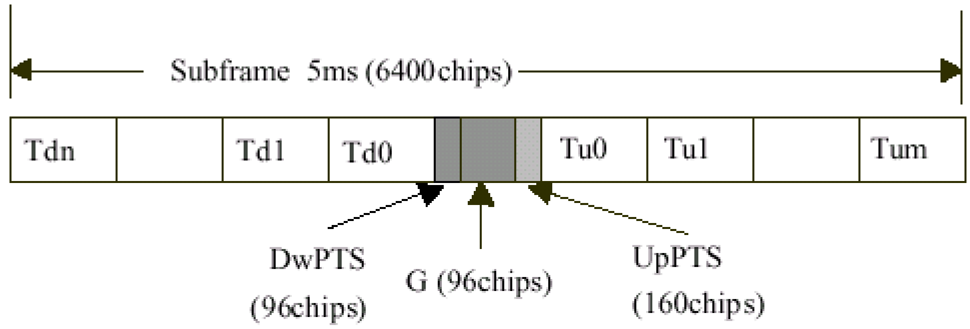

Figure 2.9: Time-Slot Structure for the TDD Frame [25]

The location of the TDD switching point may be varied dynamically depending upon the uplink and downlink transmission rate, but there is only one switching point in a subframe [19]. Figure 2.10 below shows a symmetric and an asymmetric frame allocation.

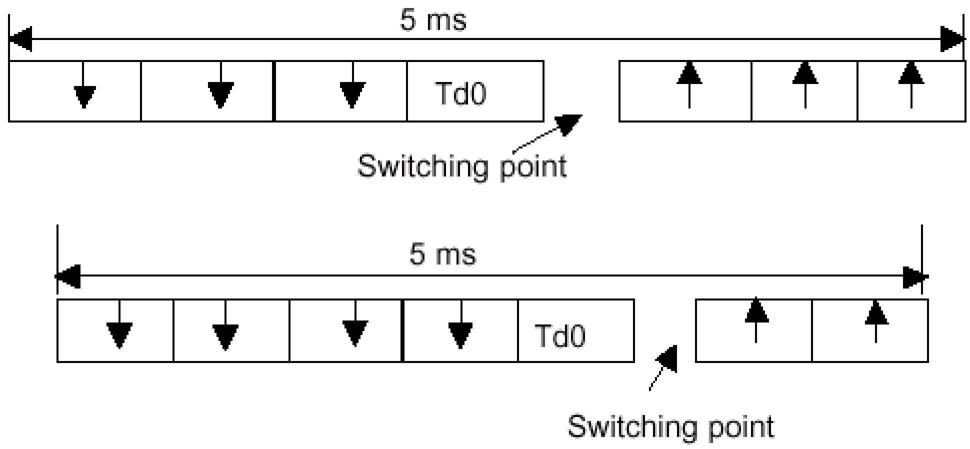

Figure 2.10: Symmetric and Asymmetric TDD Slot Assignments

The top frame in Figure 2.10 represents a symmetric transmission and the bottom frame represents asymmetric transmissions. The uplink and downlink frames can be adjusted dynamically – this feature is important to maximize the system throughput and spectral efficiency of data applications. Figure 2.11 shows the two possible arrangements for uplink and downlink frames in a 5 ms TDD frame.

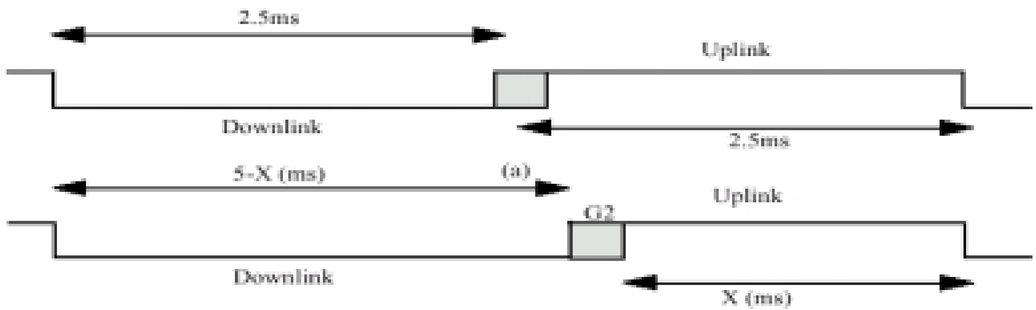

Figure 2.11: TDD Scheme for TD-SCDMA [21]

In Figure 2.11, 'G2' is the switching point and 'X' has exactly 6 possible values as shown below:
X = N * 0.675 + 0.275 ms, where N = 1,2…6

2.3.2 Burst Structure

Each 675 μs subframe (or burst) consists of two data symbol fields, a midamble of 144 chips and a guard period of 16 chips. The burst structure is illustrated in Figure 2.12 below.

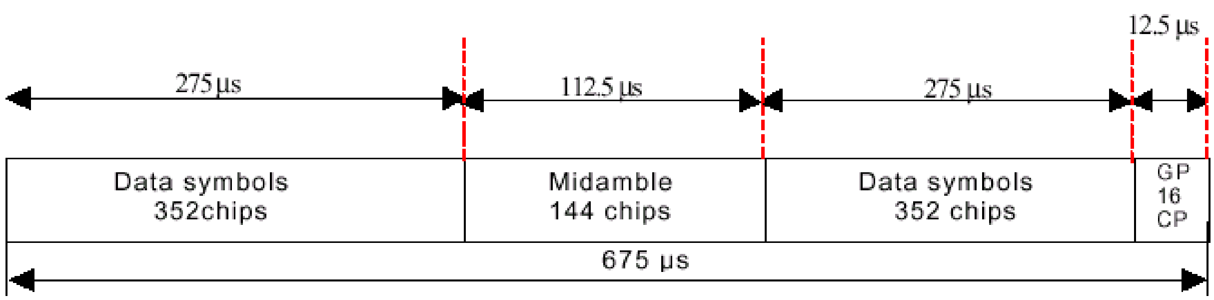

Figure 2.12: Burst Structure

In the burst structure of Figure 2.12, each data field contains one chip per symbol (and since QPSK modulation is used, one symbol = 2 bits). It is clear that the data symbols total 704 chips (two data fields of 352 chips each), but the corresponding number of symbols depends on the spreading factor as indicated in Table 2.1.

Table 2.1: Number of Symbols per Data Field

Spreading Factor	Number of Symbols per Data Field	Timeslot Information Rate (bps)
1	352	281,600
2	176	140,800
4	88	70,400
8	44	35,200
16	22	17,600

The Timeslot Information Rate (bps) is calculated by

Timeslot Information Rate = (Symbols/Burst) * (bits / symbol) / (Subframe length)

= (352 + 352) * (2) / (5E-03) = 281,600 bps.

The data part of the burst is spread with a combination of channelization code and scrambling code. The channelization code is an Orthogonal Variable Spreading Factor (OVSF) code that can have a spreading factor of 1, 2, 4, 8, or 16. The data rate of the physical channel is depending on the used spreading factor of the used OVSF code.

2.4 Modulation

For voice and data services with data rates less than 384 kbps, the basic RF modulation method is DQPSK. However, for data services up to 2 Mbps (as in fixed broadband wireless), the primary RF modulation method is 16-QAM. The other method of providing 2 Mbps is the multi-carrier technology, where the RF modulation on each carrier is DQPSK. Figure 2.13 shows the spreading and 16-QAM modulation for the dedicated physical data channel (DPDCH) and the dedicated physical control channel (DPCCH).

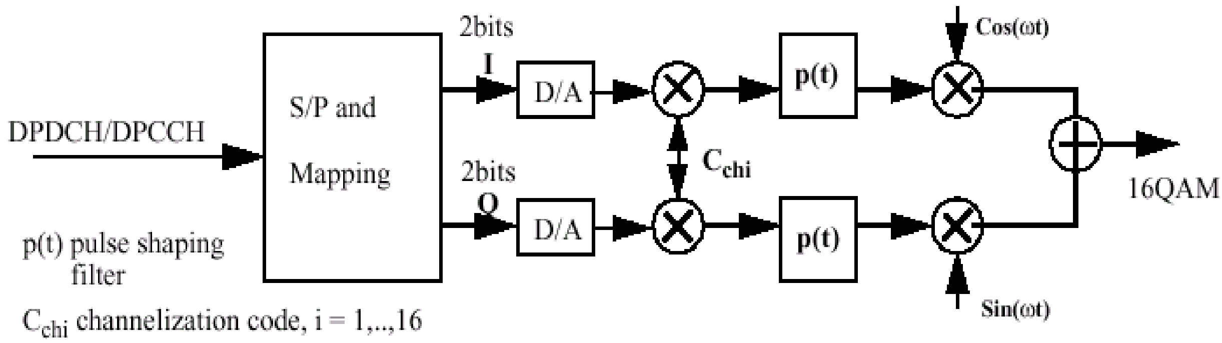

Figure 2.13: Spreading & 16-QAM Modulation Block Diagram [21]

The lowpass filter for pulse shaping, p(t), is a root raised cosine (RRC) filter with $\alpha = 0.25$, making the 3 dB bandwidth 556.8 kHz.

2.5 Coding

As with any digital wireless channel, forward error correction (FEC) coding is used to lower the bit error rate (BER) on that channel. Only convolutional coding is applied in the case where a BER of 10^{-3} is needed. The convolutional coding rates change according to the different services. Rates from ¼ to 1 can be chosen such that the entire system will be able to reuse as much of the decoding hardware as possible. Normally, the inner convolutional coding rate of ¾ is chosen. Parameters of the code polynomials for ¾-rate coding are given in Table 2.2.

Table 2.2: Parameters for ¾ Rate Convolutional Coding

Rate	Constraint Length	Generator Polynomial 1	Generator Polynomial 2	Generator Polynomial 3	Generator Polynomial 4	Free Distance
3/4	9	472	215	113	764	6

After convolutional coding, interleaving is used. For services requiring a BER = 10^{-6}, a concatenated code scheme such as Reed-Solomon (RS) or outer interleaving and convolutional coding could be used. Figure 2.14 shows such a possible FEC coding scheme.

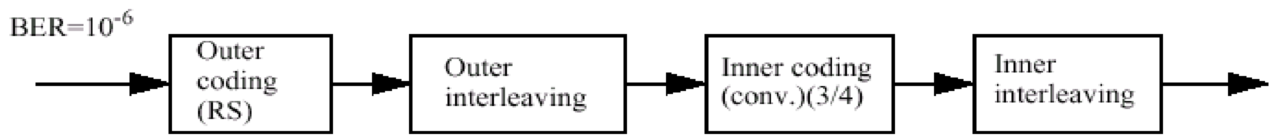

Figure 2.14: FEC Coding for BER $\leq 10^{-6}$

The outer interleaver is necessary to break the error burst at the output of the Viterbi decoder. This is needed in addition to the inner interleaver for breaking the error bursts due to fading [21]. Alternatively, for services requiring a BER of 10^{-6} and high data rates, Turbo coding could be used. The proposed turbo code encoder and decoder (by the Chinese Academy of Telecommunications Technology to the ITU) for TD-SCDMA is shown in Figure 2.15 below.

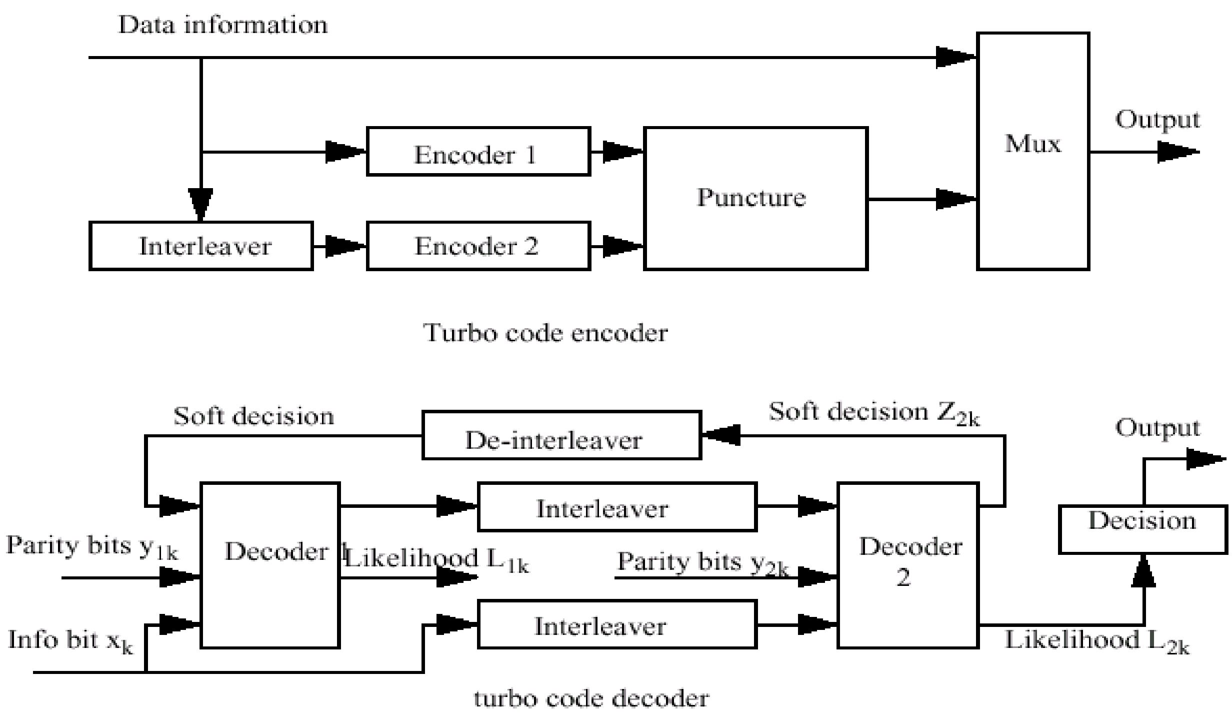

Figure 2.15: Turbo Code Encoder and Decoder [21]

2.6 Synchronization

One of the requirements of 3G systems is the high system capacity. SCDMA implies that the uplink channels always work synchronously, which can increase capacity by 3 dB and simplify the demodulator [26]. The downlink channel is synchronized on all CDMA systems; therefore this paper will not explore the topic any further. However, uplink synchronicity is unique to SCDMA and involves two stages: synchronization establishment and synchronization maintenance. Figure 2.16 illustrates in greater depth the stages that the CPE has to follow.

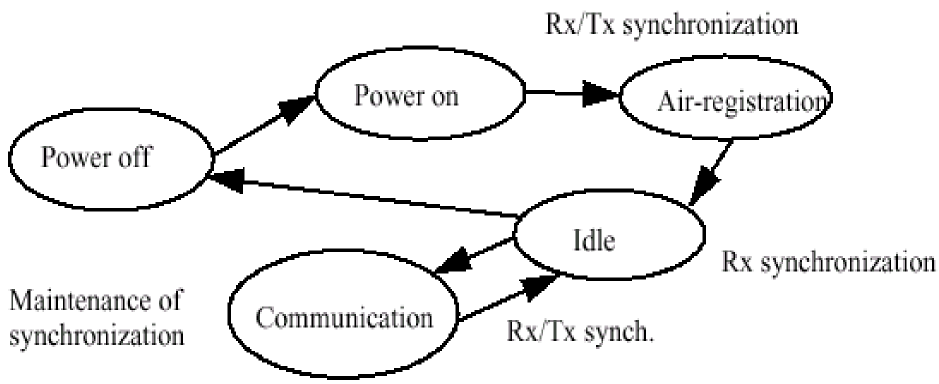

Figure 2.16: CPE Status Flow Diagram

The CPE starts off in the powered down stage. After the CPE is powered on, it will establish synchronization with the base station and start the procedure of *Air Registration*. Afterwards, it goes into the idle stage to conserve battery power. The CPE may establish link and communication with the base station only from the idle stage. These operations are explained in greater detail in the following two subsections.

2.6.1 Uplink Synchronization Establishment

The main guard time slot at the switching point (from uplink to downlink) is an empty period sufficient to establish uplink synchronization. Theoretically the guard time should be larger than the sum of the signal processing time plus 2D/C, where *D* is the largest transmission distance and *C* is the speed of light [19]. The guard time is usually kept constant at the side of the base station and is adjusted at the CPE side based on the distance. In the physical layer signaling, the synchronization shift (SS) and power control (PC) fields are assigned in the main downlink time slot. These fields are used to calculate the distance between the CPE and the base station based on the transmission time.

When a CPE is turned on, it will receive the strongest signal from the nearby base stations (for the case of fixed wireless access, the same base station will always provide the strongest signal). When it receives the strongest signal, it will obtain receiving synchronization, and then demodulate the received signal in the common control physical channel (CCPCH) to obtain the necessary information (the SS and PC fields). After the receiving synchronization and the information from the downlink are obtained, the CPE will begin the *Air Registration* procedure by using the open loop synchronization algorithm. The open loop synchronization algorithm is used by the CPE to find its transmission time and send the Air Registration information to the base station through a physical random access channel (PRACH). The base station then receives the Air Registration information and will find the tolerances in the transmitter power and in the arriving time. Afterwards, it will send the response on the SS and PC (located in the CCPCH) fields described above. Consequently, the CPE will adjust its transmission power and transmission time to establish uplink synchronization. Figure 2.17 shows the open loop synchronization procedure.

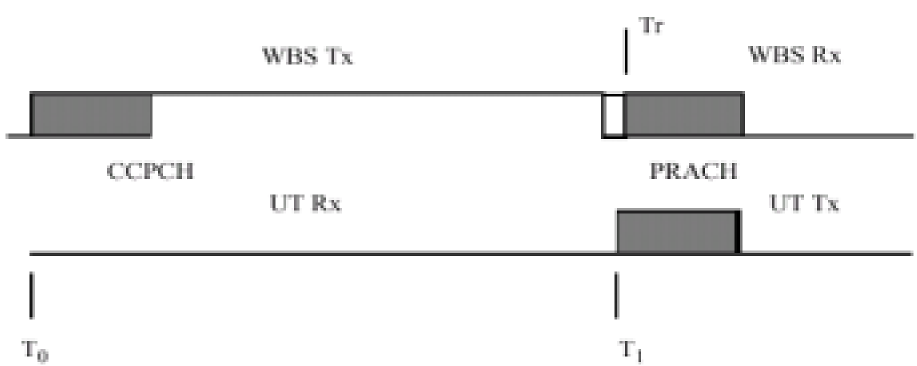

Figure 2.17: Open Loop Synchronization [21]

In Figure 2.17, T_0 and T_r represent the point at which receiving synchronization is established and T_1 represents uplink synchronization being obtained. The time between the two can be calculated by:

$$T_1 - T_r = R / C,$$

where *R* is the cell radius, *C* is the speed of light, $T_r = T_0 + 611 + (N*582) + 230\ \mu s$, and N is the number of the current downlink time slot [21].

2.6.2 Uplink Synchronization Maintenance

In the “idle” status (refer to Figure 2.16), the CPE will be in sleep mode to conserve its battery for most of the time. However, it will come out of sleep mode when the frame number (FN) is matched with the last four digits of its PID. Then, the CPE will adjust its receiver synchronization and receive the information in the CCPCH. This way, the Rx synchronization is always maintained (even under movement or clock drift) [21].

In the “communication” status (refer to Figure 2.16), uplink synchronization is maintained through the framing. There is a synchronization field (E/SYNC2) in the control channel multiplexed frame and only the CPE, in which the distributed Walsh number matches the present frame number (FN), may send the SYNC2 data. Other CPEs operating in this time slot, but with a different channel code, will be in the EMPTY status. Once this data is received, the following downlink frame will have the necessary SS and PC field data to perform both close loop power control and synchronization control. The close loop synchronization control will be executed once every 80 ms, which is equivalent to 16 TDD intervals, for each CPE [19].

2.7 Smart Antennas

As seen in Figure 2.3, smart antennas are one of the key features of TD-SCDMA. Smart antennas are dual-function antennas (are able to transmit and receive) installed at the base station. Directivity is achieved by an array of fixed antenna elements with programmable electronic phase relations. Using this, each link from a base station to a CPE has a unique directivity. Since the duplexing scheme is TDD, the transmission and reception of user signals take place at the same frequency. Therefore, the directive smart antennas show the same two-way antenna pattern and thus, reciprocity of propagation conditions in both directions is given. Reciprocity allows the full utilization of ICI and intracell interference reduction. Therefore, smart antennas can lead to a remarkable improvement of spectral efficiency.

2.7.1 Smart Antenna Basics

In the basic system, smart antennas are composed of a concentric array of eight antenna elements having a diameter of 25 cm. This configuration allows a directivity of 8 dB in either the transmit or receive direction as compared to an omnidirectional antenna. Based on such a layout, the angle of directivity (beamwidth) amounts to 40 degrees [27].

If a base station had N antenna elements and N coherent RF transceivers, the smart antenna system would have the following advantages:

- Rx sensitivity could increase N times,
- Tx EIRP could increase N^2 times (with coherent transmitters), and
- Inter- and intra- cell interference could decrease by a factor of N.

Thus, the Tx power can be kept lower at both the base station and the CPE, yet the received SINR is higher. Experiments in [28] show the range, capacity, and data rate increases a smart antenna system can achieve. These experiments also show that a smart antenna system exhibits greater resistance to multipath, delay spread, and CCI.

The main problem with smart antennas in sectorial applications is the limited beamwidth, which is directly determined by the number of antenna elements. Transmitter or receiver antenna diversity is one alternative to directional smart antennas. Diversity and beamforming will be investigated when exploring the TD-SCDMA and Vector OFDM systems.

2.7.2 Joint Detection

Joint detection is primarily a multi user detection scheme, which refers to the highly effective detection procedure for multiple parallel signals transmitted in the CDMA mode of TD-SCDMA. Consequently, joint detection is applied for multiple transmissions of bit rates of 8 kbps to 384 kbps. Joint detection minimizes multiple access interference (MAI) of all users and as a consequence, the user load per carrier can be increased by a factor of three [29].

In CDMA, a very high number of user signals are transmitted in parallel per RF channel respective to a particular transceiver. Each of the signals transmitted in parallel is differently coded from others and separated by code correlation in the receivers. The power of all the signals transmitted from the CPEs to the base stations (multipoint-to-point) are summed at the base station's receiver input. A precondition for successful detection of all signals is a balanced mutual signal level with a mutual level deviation of $\pm$1.5 dB [29]. Different path lengths, different delay spreads, and different path attenuations uniquely affect each signal. Therefore, in order to mutually balance all the received signals at the receiver of the base station, a multi loop fast power control (FPC) is required [30]. The balanced multiple signals cause a Gaussian distributed sum level at the base station receiver, which leads to a strong interference to each detected (by code correlation) signal. This MAI directly limits the traffic load of each carrier and therefore limits the entire spectrum utilization.

Minimized MAI extends the signal detection range for each signal to a permissible level difference of 20 dB [29]. Thus, fast signal fluctuations caused by Rayleigh fading does not affect the signal detection. Therefore, the complexity of the power control is greatly reduced. However, joint detection cannot be applied without limitations. By increasing the number of parallel users, joint detection leads to a square law increase of computing power. Also, by an increase in the number of users, a "more than proportional noise enhancement" occurs, which degrades the range of the system [29]. Thus, joint detection is only effective if the number of parallel users is already semi-low.

There are many different joint detection techniques and a lot of research is devoted to the subject. Powerful joint detection algorithms are given in [30] and a number of other sources, but that is beyond the scope of this paper.

2.8 Summary

In conclusion, this chapter described the basic concepts of synchronous CDMA. The key principle that differentiates SCDMA from IS-95 CDMA is that all signals in the uplink channels are synchronous at the input of the base station demodulator with high accuracy. A complete block diagram of a synchronous CDMA system was given in Figure 2.3 above. Next, the framing, modulation, coding, and synchronization details were given. Finally, details on the smart antenna system were described. Since the scope of this paper is limited to fixed broadband wireless, there has been no description of the Baton handover or any other mobile-related topics specific to TD-SCDMA. The next chapter will describe and characterize an example TD-SCDMA system: Navini Network's Ripwave system.

Chapter 3

Navini Ripwave

Navini Networks has developed a broadband wireless system based on time division synchronous CDMA (TD-SCDMA) as described in the previous chapter. The Navini Ripwave system is advertised to provide high-speed data rates on par with cable modems and DSL, does not require any installation of hardware at the customer premise, allows for non-line-of-sight deployment, and allows end-users to have freedom of movement. This chapter will first describe the Navini Ripwave system as a whole. Then, descriptions of the Base Transceiver Station (BTS), the Radio Frequency Subsystem (RFS), and the Customer Premise Equipment (CPE) will be given. Next, data from the field trials will be analyzed in terms of beamforming gain, Carrier-to-Interference (C/I) ratio, and data rates. Afterwards, uplink and downlink power and noise budgets will be formulated based on some of the experiment results.

3.1 System Specifications

Developed to support operation in the unlicensed frequency spectrum at 2.4 GHz, Navini Networks' Ripwave 2400 is a broadband wireless access solution. Although intended to work in unlicensed bands, the Ripwave has been extended to MMDS, WCS, WLL, and PCS bands as well. The Ripwave solution supports a downstream channel size of 5 MHz (ten 500 kHz sub-channels), with QPSK, 8PSK, 16-QAM, and 64-QAM modulation schemes. The upstream channel size is 2 MHz (four 500 kHz sub-channels) and also supports QPSK, 8PSK, 16-QAM, and 64-QAM. With a 3:1 TDD, this leads to a maximum downstream rate of 18 Mbps and a maximum upstream rate of 6 Mbps under ideal conditions. The asymmetric time slot assignment of 3:1 refers to three downlink slots per every uplink time slot in each frame.

3.1.1 Forward Link

On the forward link, when a signal intended for a certain CPE is transmitted from an antenna array at the BTS, the amplitude and phase of the signal at each antenna can be adjusted so that they combine coherently at the CPE. The signal is radiated from the BTS antennas in such a way that it forms a beam of energy directed at the particular CPE. Suppose that the average transmitter power at each antenna is P and the number of antennas is N. Then, the received signal strength at the CPE is $P * N^2$ on average. In the current version, $N = 8$.

The CPE does not use beamforming; instead it uses two internal patch antennas and a single omni antenna. During the forward link, the CPE will switch between the three antennas and automatically select the best signal. Once that antenna is selected on the forward link, the same antenna is used on the reverse link. The CPE will switch between the three antennas every 10 ms [31].

3.1.2 Reverse Link

On the reverse link, the CPE will send the signal to the BTS on the same antenna that was selected for the forward link. When a signal from a specific CPE is received, the base-station receiver can adjust the weight and phase for the signal from each antenna so that the intended signal can be combined coherently and the interference suppressed. Since the desired signal is combined coherently and noise is combined incoherently, the SNR of the received signal can be increased on average by a factor of *N* after uplink beamforming (under idealized conditions). Therefore, *N* times less transmission power is needed for both uplink and downlink, which translates into a longer battery run-time on the CPE units [31].

Another key feature of the adaptive beamforming on the reverse link is that the system can be configured to avoid radiating energy in any specific direction. If an interference source is detected in a particular direction, the system can create a null in that direction. This is especially critical in the ISM band where there are sure to be cordless phones, WLANs, or microwave ovens radiating energy towards the CPE and base station.

3.1.3 Bandwidth Allocation

The Ripwave 2400 system can allocate channels in increments as small as 25 Kbps, which provides the BTS with the flexibility of allowing variable bandwidth from 25 Kbps to 9.6 Mbps (using 64-QAM) per CPE. Channels are allocated on a per-user burst basis, thus allowing for up to one thousand subscribers per BTS [31]. The BTS can dynamically assign symmetric and asymmetric uplink and downlink bandwidths to maximize the bandwidth utilization. The system runs on a 10 ms TDD cycle that consists of an uplink / downlink time. During normal allocation, the send and receive times are equal (same forward and reverse link speeds). The system is also capable of changing to a 3:1 asymmetric TDD cycle based upon loading conditions where the forward link is allocated 3 times the number of slots as the reverse link. The entire BTS and all CPEs connected to it must be set to the same symmetric or asymmetric level.

The Ripwave BTS can run up to a 5 MHz contiguous bandwidth spectrum. This spectrum is divided into 500 kHz sub-carriers (3-dB bandwidth of 400 kHz) with each using 32 code channels (sub-carrier spacing and number of code channels are both different from the CWTS TD-SCDMA specifications of Chapter 2). A CPE can occupy up to a maximum of 4 sub-carriers or 128 code channels. This matches the CPE contiguous bandwidth of 2 MHz (4 * 500 kHz = 2 MHz). A CPE does not have to necessarily occupy all 32-code channels in a sub-carrier. The

CPE allocation of code channels and subcarriers is controlled by the BTS. This allocation can be dynamic and on a burst-by-burst basis.

If each CPE uses all 32-code channels and the maximum 4 sub-carriers (for a higher data rate), then the BTS can only support 2.5 CPEs. So, when more CPEs need to be supported, the subcarrier will divide its code channels between different users. The maximum number of users that can be supported with one base station is 320, each at a maximum total data rate of 25 kbps using QPSK. The reason for this is that with the FCC limitations on transmitted power in the ISM band, a high spreading gain is always required. The Ripwave system uses 32-length Walsh codes to achieve a 15 dB spreading gain for all users. The highest downlink data rate that can be supported by one CPE is 7.2 Mbps using 64-QAM and asymmetric 3:1 TDD timing. If using this mode, the uplink data rate will be 2.4 Mbps. In this mode, one CPE has been assigned the maximum of 4 subcarriers and all 32 code-channels within each subcarrier. (These calculations are shown in Appendix A).

3.1.4 Modulation

The system is capable of using four modulation schemes: QPSK, 8-PSK, 16-QAM, and 64-QAM. The modulation is selected by the BTS based upon the SNR at the CPE. The modulation is dynamic and can change with each 10 ms TDD cycle. Each code channel can also have different modulation schemes based upon traffic and needs [32].

3.1.5 Frequency Selection

In order to avoid interference, the CPE will select the “quietest” subcarriers (one of ten) with which to communicate with the BTS. If the level of noise on a subcarrier increases, the CPE can move to a quieter subcarrier. In extreme cases when interference changes drastically, the CPE can switch to another BTS entirely. If this is not possible, then the BTS may move the entire system to another 5 MHz bandwidth and request all CPEs to reinitialize to the new frequency [31].

3.2 Base Station

The Ripwave base station consists of two units, the Base Transceiver Station (BTS) and the Radio Frequency Subsystem (RFS).

3.2.1 Base Transceiver Station

The BTS shown in Figure 3.1 below consists of a digital shelf and an RF shelf, and performs all transmit, receive, and signal processing functions.

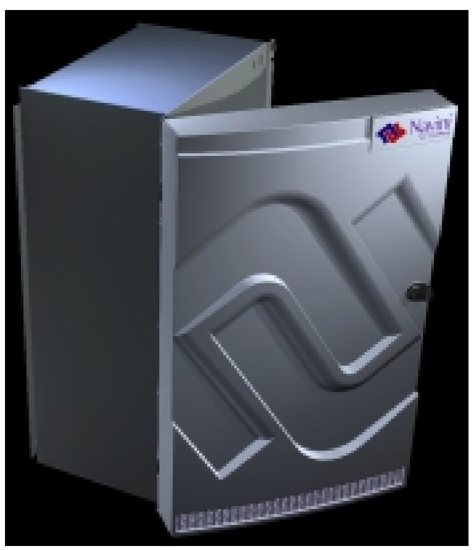

Figure 3.1: Ripwave Base Transceiver Station (BTS) [32]

The digital shelf consists of an IF card, synthesizer card, channel processor card, modem card, and communications controller card. The IF card is a 4-channel IF-to-baseband converter. The synthesizer card is a local oscillator (LO) generation card with a single calibration transceiver incorporated. The channel processor card contains the DACs and ADCs that interface to the IF card. The modem card monitors the physical layer functions and periodically performs system calibrations. Finally, the communications controller card is the master controller in the BTS that provides all the WAN interfaces (T1/IMA, and Ethernet).

The RF shelf is the upper portion of the BTS chassis and contains the digital and power amplifier (PA) modules. The PA card provides the forward link high power amplification, the RF to IF conversion, and the TX/RX time division circuitry. All elements are fully redundant and function in a load-sharing manner.

3.2.2 Radio Frequency Subsystem

A key component of the Ripwave solution is its cost-effective use of digital beamforming. The digital beamforming function is provided by the adaptive phased array smart antenna subsystem of Navini's wireless broadband base station, also known as the RFS. The RFS, seen in Figure 3.2 below, houses an antenna array, passive calibration circuits, filtering, low noise amplifiers, and lightning protection [31].

Figure 3.2: Radio Frequency Subsystem (RFS) [32]

The RFS is typically deployed on a transmission tower or a building rooftop. The current Ripwave system contains an array of eight antenna elements.

3.2.3 Base Station Data Sheet

The data sheet of the base station, which includes both the BTS and RFS, is given in [33] and the key parameters are summarized in Table 3.1 below.

Table 3.1: Key Base Station Data

Operational Frequency Band	MMDS, ISM, WCS, WLL, PCS, UNII bands Frequency agnostic, programmable platform
Multiple Access Scheme	Multi-carrier synchronous CDMA
Duplex Format	Time Division Duplexing (TDD)
Carrier Bandwidth	500 kHz
Total Signal Bandwidth	5 MHz contiguous
Number of Code Channels	320 (Access / Data Channels)
Antennas	Omni or 3-sectored Adaptive phased-array antenna with beamforming
Total Sectors	Up to 3
Uplink/Downlink Duplex	TDD with a maximum 3:1 ratio for down/up time slots
Spreading Spectrum Scheme	Direct Sequence Spreading (DSS)
Baseband Modulation	QPSK, 8PSK, 16-QAM, 64-QAM
System Throughput	Up to 24 Mbps per sector (fully loaded max raw data rate)
Output Power	49 dBm EIRP 36 dBm EIRP (2.4 GHz ISM band)
Average Coverage	Up to 80 sq. km (5 km radius) Up to 29 sq. km (3 km radius) – 2.4 GHz ISM band
Forward Error Correction	Reed Solomon (RS)
Redundancy	99.999% high availability (three-nines availability)
WAN Interfaces	T1, ATM, IMA, DS-3, OC-3, 10/100 Ethernet
Packet Format	IEEE 802.3, Ethernet II
Temperature	-40 to +50 ° C (operational) -40 to +70 ° C (storage)

3.3 Customer Premise Equipment

The Ripwave CPE is the customer premise modem that communicates with the BTS to provide high-speed wireless access. The CPE unit, shown in Figure 3.3 below, consists of an analog (RF) side and a digital (DSP) side, which are both packaged in a 4.5” x 2” x 4” part that weighs 9 ounces with the optional battery installed.

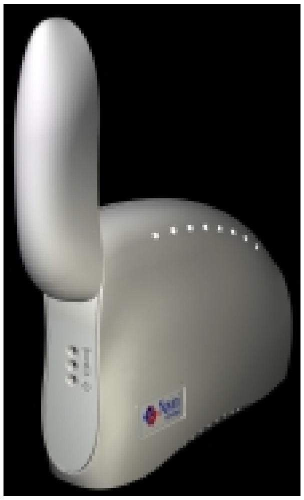

Figure 3.3: Customer Premise Equipment (CPE) [32]

The CPE comes with an optional 1800-mAh Li-Ion battery that allows the end user to be nomadic, connected to the Internet anywhere there is sufficient RF coverage. But the Navini CPE is not mobile, since there is no soft handoff from cell to cell [31].

The data sheet of the CPE is given in [33] and the key parameters are summarized in Table 3.2 below.

Table 3.2: Key CPE Data

Operational Frequency Band	MMDS, ISM, WCS, WLL, PCS, UNII bands
Multiple Access Scheme	Multi-carrier synchronous CDMA
Duplex Format	Time Division Duplexing (TDD)
Total Signal Bandwidth	2 MHz contiguous
Number of Carriers	4
Antennas	Single Omni and 2 patch directional antennas
Uplink/Downlink Duplex	TDD with a maximum 3:1 ratio for down/up time slots
Spreading Spectrum Scheme	Direct Sequence Spreading (DSS)
Baseband Modulation	QPSK, 8PSK, 16-QAM, 64-QAM
Data Rates	Up to 9.6 Mbps (max raw data rate)
Output Power	32 dBm EIRP 31 dBm EIRP (2.4 GHz ISM band)
Average Coverage	Up to 80 sq. km (5 km radius) Up to 29 sq. km (3 km radius) – 2.4 GHz ISM band
Forward Error Correction	Reed Solomon (RS)
LAN Interfaces	Ethernet or USB
Temperature	+5 to +40 ° C (operational) -40 to +70 ° C (storage)

3.4 Field Trials

The system under test, depicted in Figure 3.4 below, was tested in Dallas by Navini Networks in July 2001 in the 2.4 GHz unlicensed band. This section presents a summary of the experiment results.

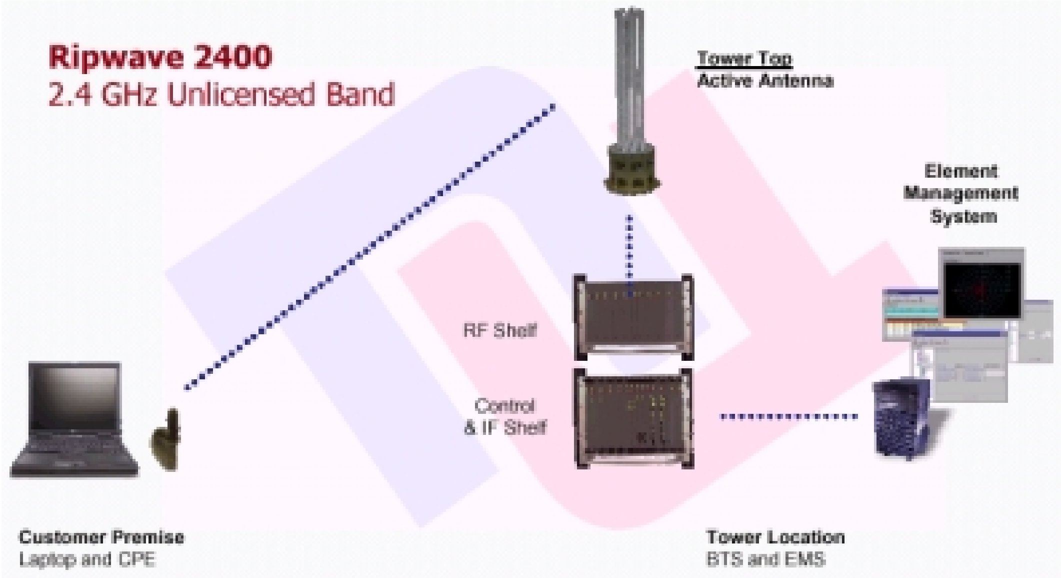

Figure 3.4: Ripwave System Under Test [34]

In Figure 3.4, EMS refers to the Element Management System that is responsible for monitoring and configuring the CPEs and BTS. The RFS is located on a 64 ft. transmission tower.

3.4.1 Downlink Beamforming

For the downlink beamforming test, the objective was to test the gain of using all eight RFS smart antennas versus any single one on the forward link. The test method was to compare the receiver power at the CPE when the BTS transmitted with only one antenna and then with all eight antennas. This technique is only applicable for locations that were within the coverage range of one antenna with no beamforming gain. The locations of tests, along with sample beamforming gains, are illustrated in Figure 3.5 below.

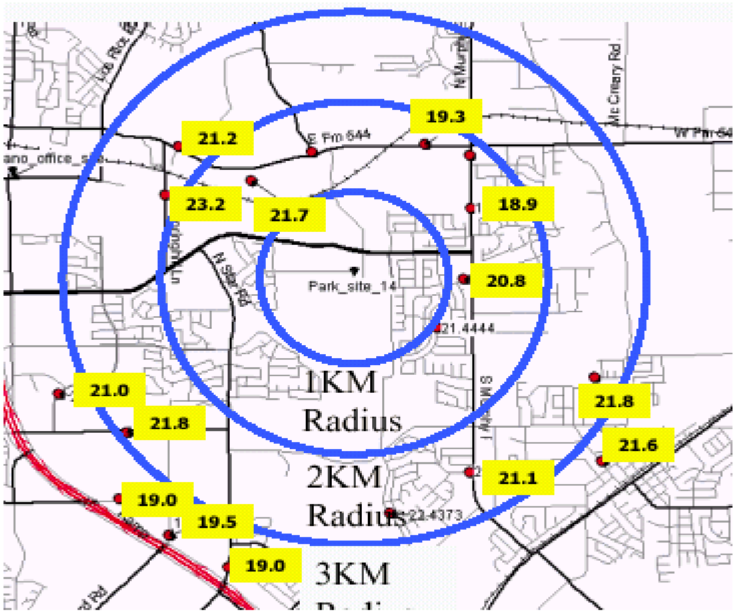

Figure 3.5: Locations for Downlink Beamforming Test [34]

Figure 3.6 summarizes the distribution of the CPE results during the drive testing. In the figure, the percentage of the data samples that fall within a certain beamforming gain are showng.

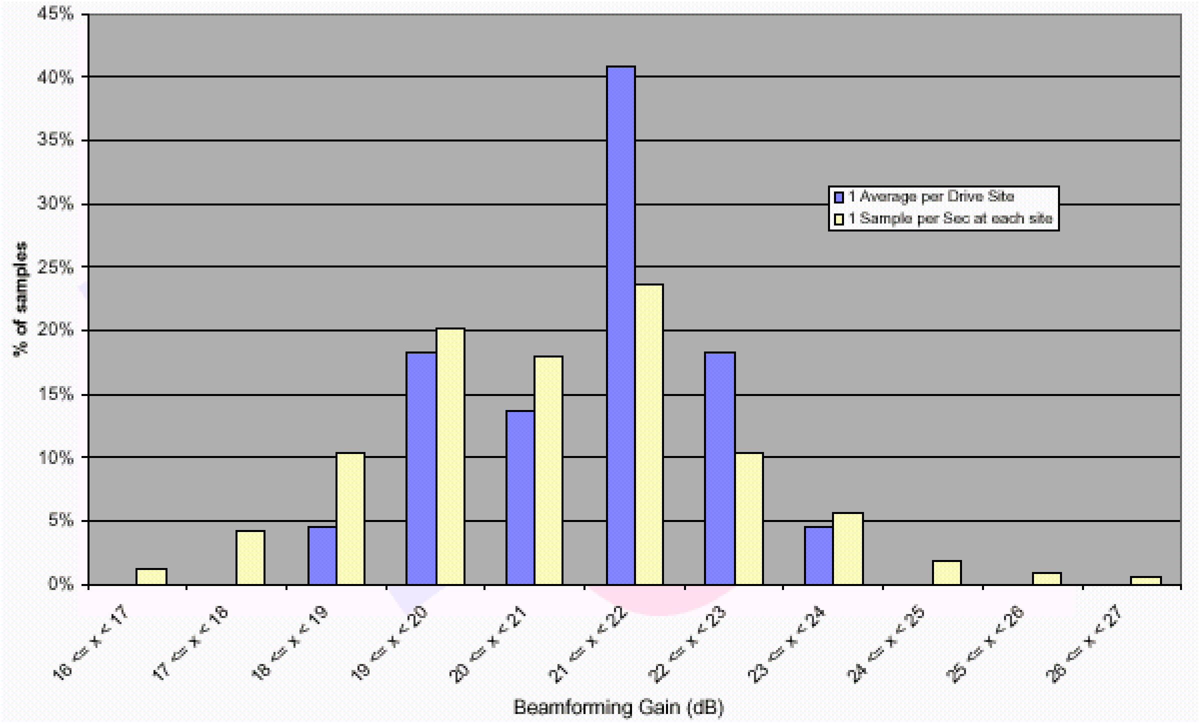

Figure 3.6: Distribution of Downlink Beamforming Gains [34]

In Figure 3.6, the beamforming gain (x-axis) refers to the gain of using eight transmitting antennas versus one. Both the average and instantaneous beamforming gains are shown in the figure. It can be observed that the average downlink beamforming gain was roughly 21 dB and the minimum gain was 18 dB. The raw data (not shown) also reveal that 92% of the non-line-of-sight (NLOS) locations had a downlink beamforming gain of 18 dB or better [34].

These results are consistent with what theory predicts. If the average transmission power at each antenna is P and the number of antennas is N, the received signal strength at the CPE is $P \times N^2$ on average. So with eight transmitting antennas, the received signal power should be 64 times (or 18 dB) higher on average than with one antenna. The CPE receiver uses a selection diversity antenna system with three branches. This results in an additional 2.6 dB of gain [35]. So, that gives an average total theoretical gain of 20.6 dB. This is consistent with the 18 dB average gain seen with Navini's adaptive beamforming algorithms in the experiment above.

3.4.2 Uplink Beamforming

For the uplink beamforming test, the objective was to test the gain of using all eight RFS smart antennas versus any single one on the reverse link. The test method was to compare the CPE transmitter power required at the CPE when the BTS received signals with only one antenna and then with all eight antennas. This technique is only applicable for locations that were within the coverage range of one receiving antenna with no beamforming gain. The following graph illustrates the uplink beamforming gain results.

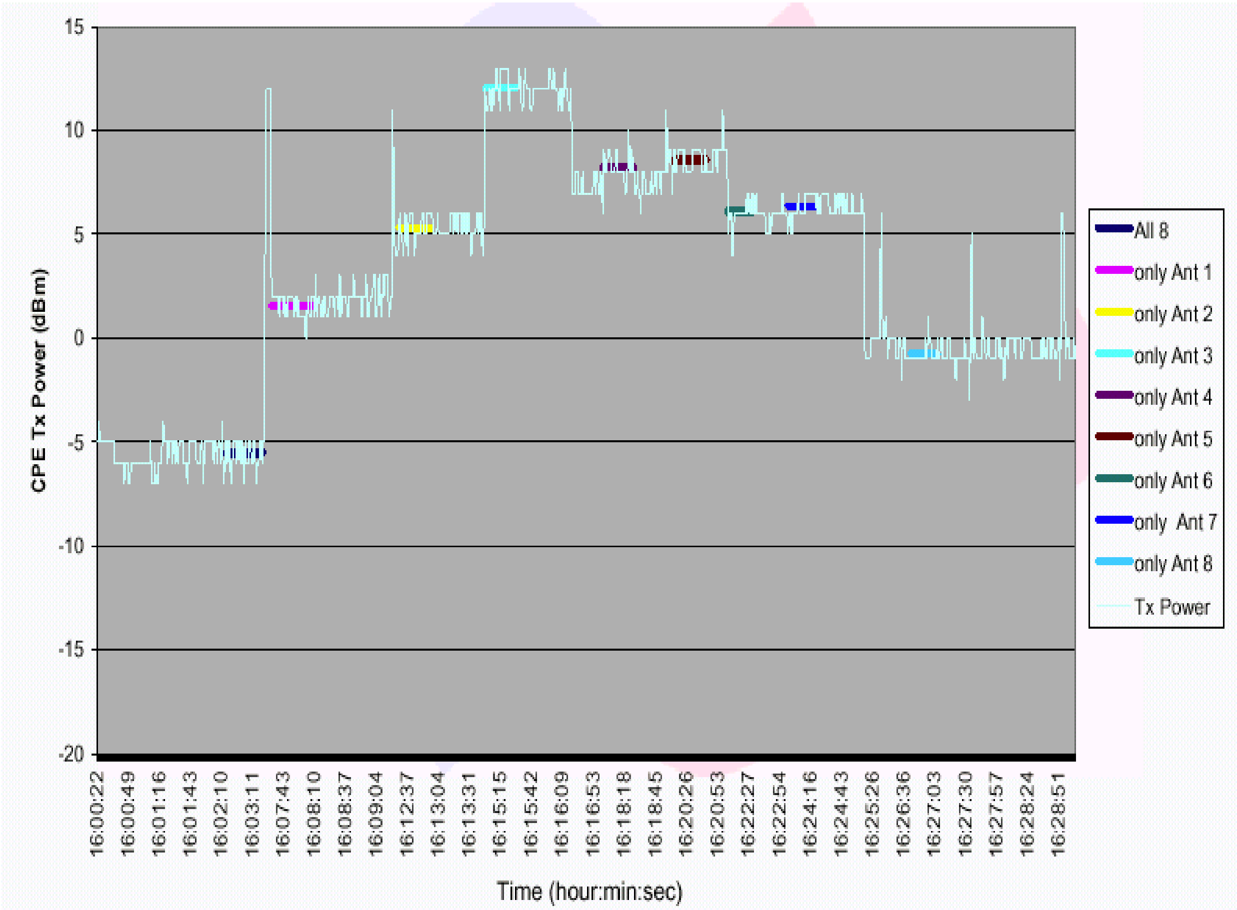

Figure 3.7: Uplink Beamforming Gain [34]

Figure 3.7 shows the CPE transmission power needed when different antenna elements are switched on. The following table summarizes the results seen in Figure 3.7.

Table 3.3: Summary of Uplink Beamforming Gains

	Only Ant. 1	**Only Ant. 2**	**Only Ant. 3**	**Only Ant. 4**	**Only Ant. 5**	**Only Ant. 6**	**Only Ant. 7**	**Only Ant. 8**	**All 8 Ants.**
CPE Tx Power (dBm)	1.6	5.3	12.0	8.2	8.6	6.1	6.3	-0.8	-5.5
All 8 Gain over Single Ant. (dB)	7.1	10.8	17.5	13.7	14.1	11.6	11.8	4.7	N/A

As can be determined from Table 3.3, the average uplink beamforming gain was 11.4 dB, with the highest gain being 17.5 dB. The average CPE transmit power is proportional to the BTS receiver sensitivity, which increases proportionally to the log of the number of antennas. So with eight receiving antenna elements, the theoretical average gain should be 9 dB over a single antenna. There is a 2.4 dB discrepancy between the 9 dB theoretical gain and the 11.45 dB observed gain because the theoretical gain has not taken into account the diversity gain at the BTS due to multiple antennas.

3.4.3 Uplink Carrier-to-Interference Ratio (CIR)

For the uplink carrier-to-interference ratio test, the objective was to test the amount of interference a CPE could tolerate while still being able to send a strong enough signal to the BTS. The test method was to first establish a link between the BTS and CPE. Then, interference was generated through the use of a second CPE. The interference level was slowly increased and the degradation of the primary CPE (in terms of received signal-to-noise ratio (SNR) at the BTS was recorded. The following graph illustrates the degradation of the received SNR for four independent tests.

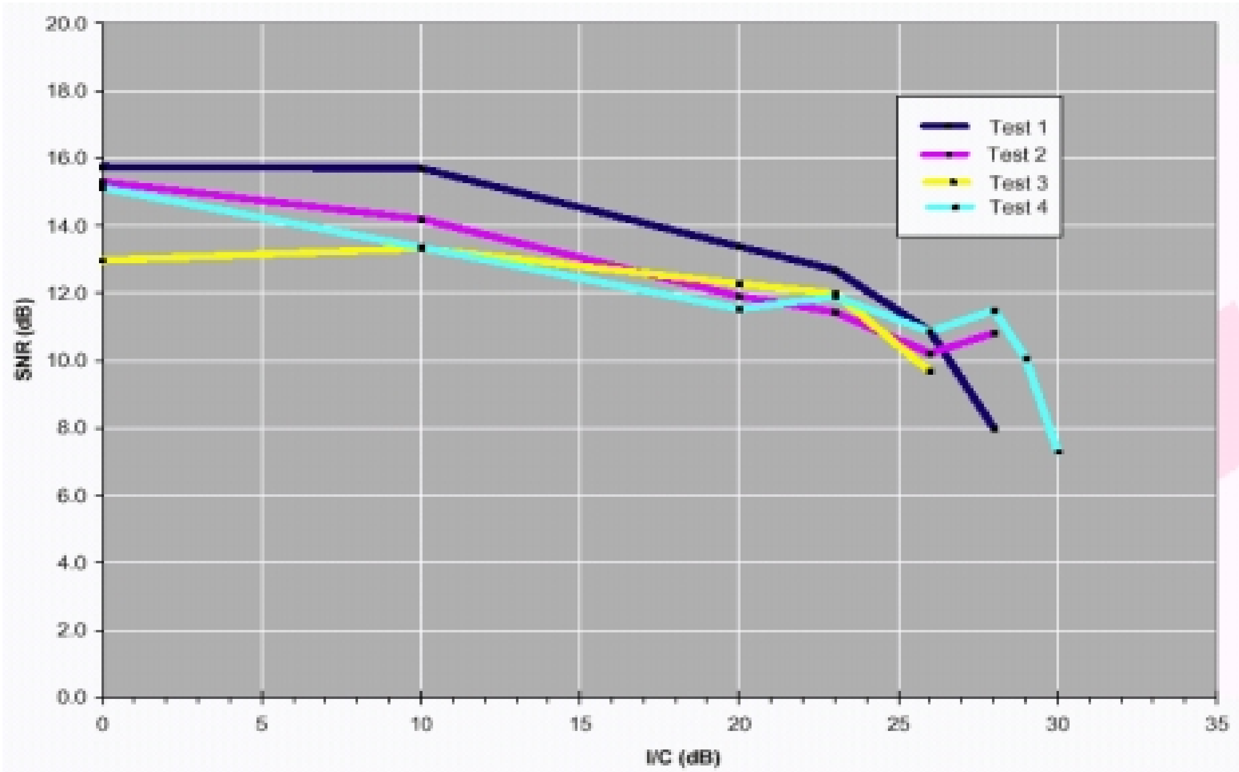

Figure 3.8: Uplink SNR vs. I/C [34]

As can be seen by Figure 3.8, an interference level of over 25 dB still results in a S/N of greater than 10.5 dB at the BTS (a 10.5 dB S/N is needed to demodulate a QPSK signal at an uncorrected BER of 1 x 10^{-3} for the Ripwave system [36]). The interfering CPE can output 25 dB more power before the system stops responding. This is directly due to the synchronicity of the uplink signals and thus being able to take advantage of the smart antennas. It should also be noted that this test is highly sensitive to the placing of the units.

3.4.4 Downlink Carrier-to-Interference Ratio (CIR)

For the downlink carrier-to-interference ratio test, the objective was to test the amount of interference a CPE could tolerate from another base station (other than the one it is linked with) while still being able to demodulate the signal. The test method was to first place the primary CPE at a location with equal path loss to both the base stations. Then a link was established between the CPE and the primary BTS. Afterwards, a link was established between the secondary CPE (at another location) and the secondary BTS. Then, the power of the secondary BTS was raised and the SNR of the primary CPE was observed. This was repeated at multiple locations. Figure 3.9 shows the locations of the base stations and the test sites.

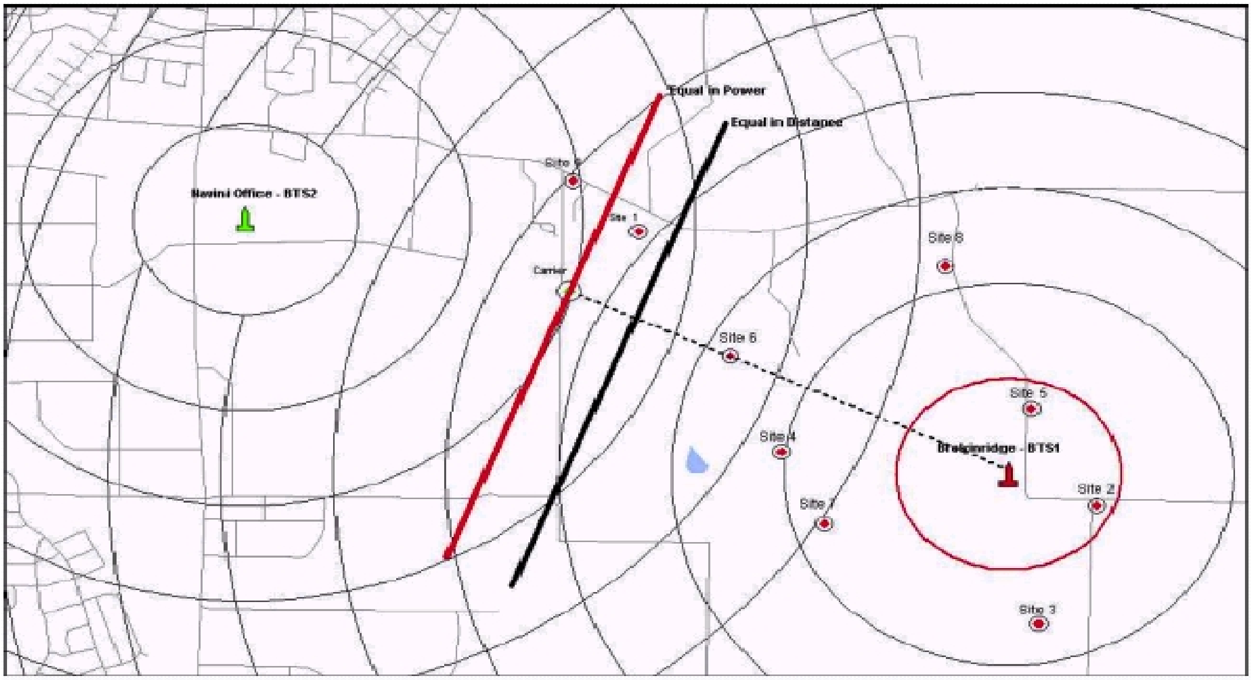

Figure 3.9: Location of Test Sites for Downlink CIR Test [34]

The following graph illustrates the degradation of the received SNR at the primary CPE versus the level of interference caused by the secondary BTS (at seven different locations).

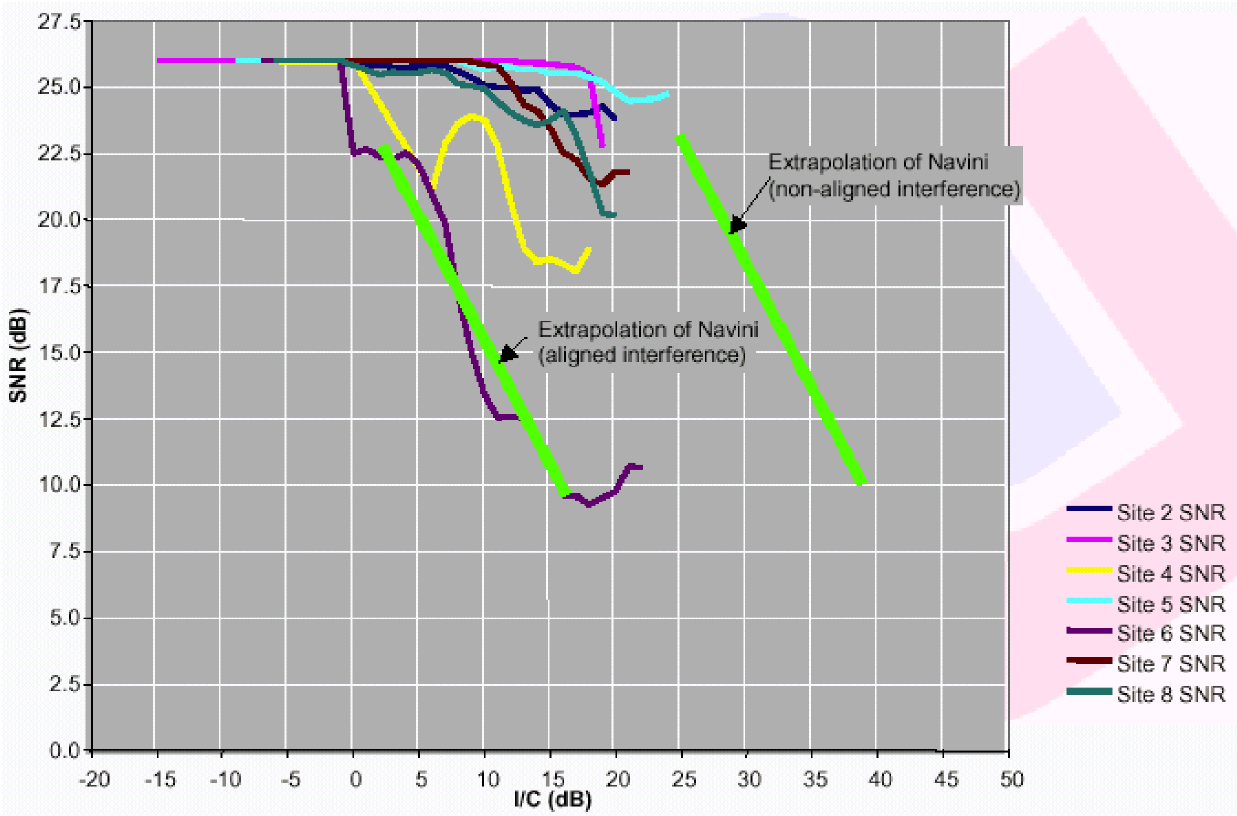

Figure 3.10: Downlink SNR vs. I/C [34]

In the figure above, the aligned interference locations are sites 6 and 4, and the non-aligned interference locations are sites 2, 3, 5, 7, and 8 (see Figure 3.9). As can be seen by Figure 3.10, the aligned interference sites can tolerate an I/C of 15 dB while maintaining an SNR of 10.5 dB. Meanwhile, the non-aligned interference sites can tolerate an I/C of 38 dB while maintaining an SNR of 10.5 dB. Aligned interference sites refer to those where the interfering carriers, modulation schemes, etc., are phase coherent with the desired signal. Non-aligned interference sites are those where there is no coherence between the interferer CPE and the local CPE.

3.4.5 Download Data Rates

For the download data rate tests, the system was operated in the asymmetric 3:1 TDD timing mode using QPSK. With this modulation scheme and TDD assignment, the peak download data rate per CPE is 2.4 Mbps (calculation shown in Appendix A). However, only 2.5 CPEs can be accommodated per base station per time at this data rate if using the full bandwidth allowed per CPE and the full spreading factor of 32. Figure 3.11 below shows the data from the download test results.

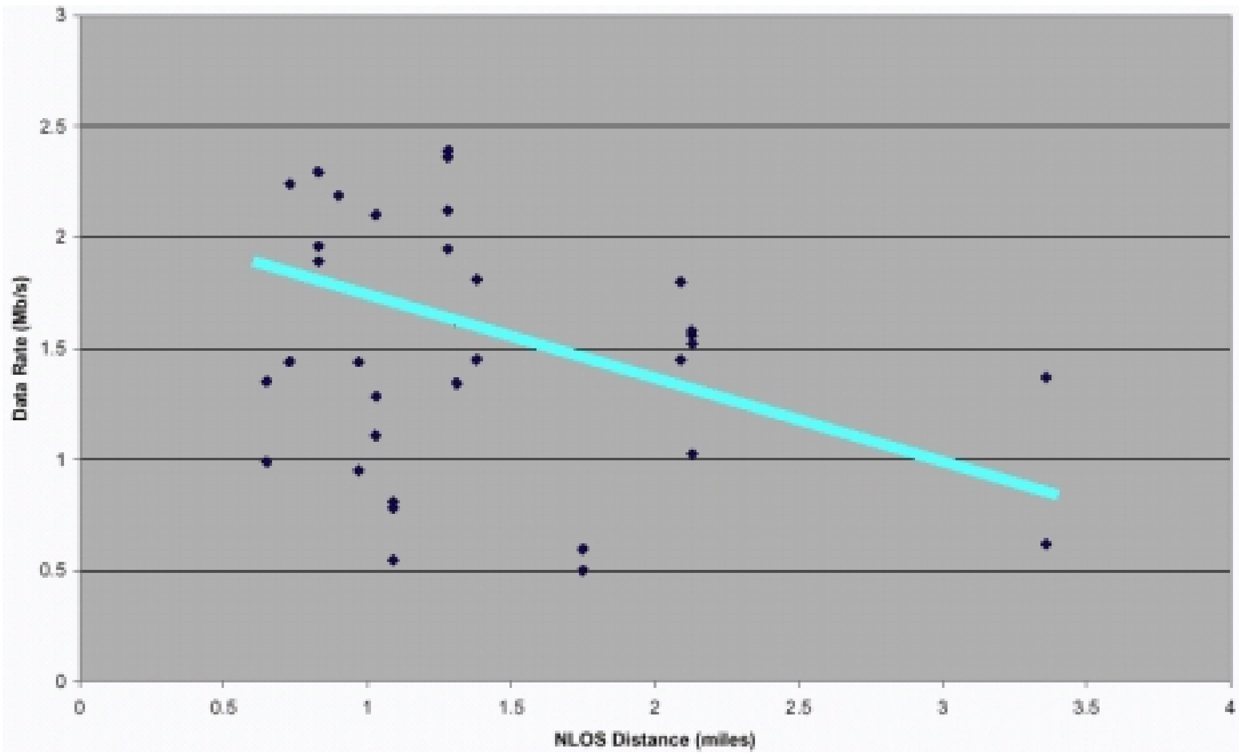

Figure 3.11: Download Data Rates [34]

As can be seen by Figure 3.11, the peak data rates are exactly 2.4 Mbps as calculated above. The lower data rates arise due to greater path losses with increasing distance. When there is more path loss, the signal strength drops and so a reduction in noise bandwidth is needed to offset the path loss. Therefore, the data rate has to be lowered to still produce a signal that can be demodulated with a BER of 10^{-3}. Since we are more concerned with path loss over distance (since different places within the cell radius and within the home itself will cause different losses), we can take an average data rate of 1 Mbps and create a downlink power budget. This power budget is shown in Table 3.4 below.

Table 3.4: Link Budget for 1 Mbps QPSK Downlink Signal

Parameters	Value	Comments
BTS Parameters		
Output power (avg.) from one RF port of a BTS for 5MHz (dBm)	34.0	PA output power for each RF port. Product is capable of 37.0dBm. 34.0 dBm is to meet FCC limit of 36.0dBm peak EIRP.
Antenna gain (dBi)	8.0	Gain of omni-directional antenna.
Antenna array beamforming gain (dB)	18.0	Beamforming gain of 8 antennas without adding any additional diversity gain due to multiple antennas
RFS Loss (dB)	-3	
Cable /connector loss (dB)	-9	Assuming 130-ft LMR400 cable
Adjustment for One Code Channel (dB)	-25.1	10*log(1/320); there are 320 total code channels in the 5 MHz BTS
Effective total power for one code channel (dBm)	**22.9**	Assuming the worst-case scenario, i.e., all the active users on the edge of the cell.
CPE Parameters		
Antenna gain (dB)	4.0	Average Gain of CPE antennas
Diversity gain (dB)	2.6	Gain due to selection diversity operation
Receiver noise figure (dB)	8.0	Noise figure of CPE
Thermal noise density (dBm/Hz)	-174.3	Thermal noise density at room temperature
Rx thermal noise power for 500kHz (dBHz)	57.0	500kHz Noise Bandwidth
CDMA spreading gain (dB)	15.1	Spreading gain of 32-chip code
Required SNR for QPSK (dB)	10.5	Required for 10^{-3} BER for QPSK before Reed-Solomon encoding
Required signal level at Rx (dBm)	**-120.5**	Required signal strength at the CPE antenna
Margins & Factors		
Log Normal Shadow/Penetration (dB)	6.0	Blocking of neighboring trees and houses
In-building penetration (dB)	12.0	For a typical residence home
Total Margins & Factors (dB)	**18.0**	
Maximum downlink path loss with margins (dB)	**125.4**	Total Power per code channel - Required Signal Level - Margins

As can be seen from Table 3.4, the maximum downlink path loss allowed is 125.4 dB for a 1 Mbps QPSK signal. Since this signal is going from outdoors to indoors (and possibly through different walls/floors within the house), the path loss exponent can vary between 2 and 6 [37]. Therefore, there is no clear relationship between the 125.4 dB allowed path loss and distance. If it were just free space, then at 2.4 GHz, this path loss would be more than enough to traverse the entire 3 km cell radius.

3.4.6 Upload Data Rates

For the upload data rate tests, the system was operated in the symmetric 1:1 TDD timing mode using QPSK. With this modulation scheme and TDD assignment, the peak upload data rate per CPE is 1.6 Mbps (calculation shown in Appendix A). Figure 3.12 below shows the data from the upload test results.

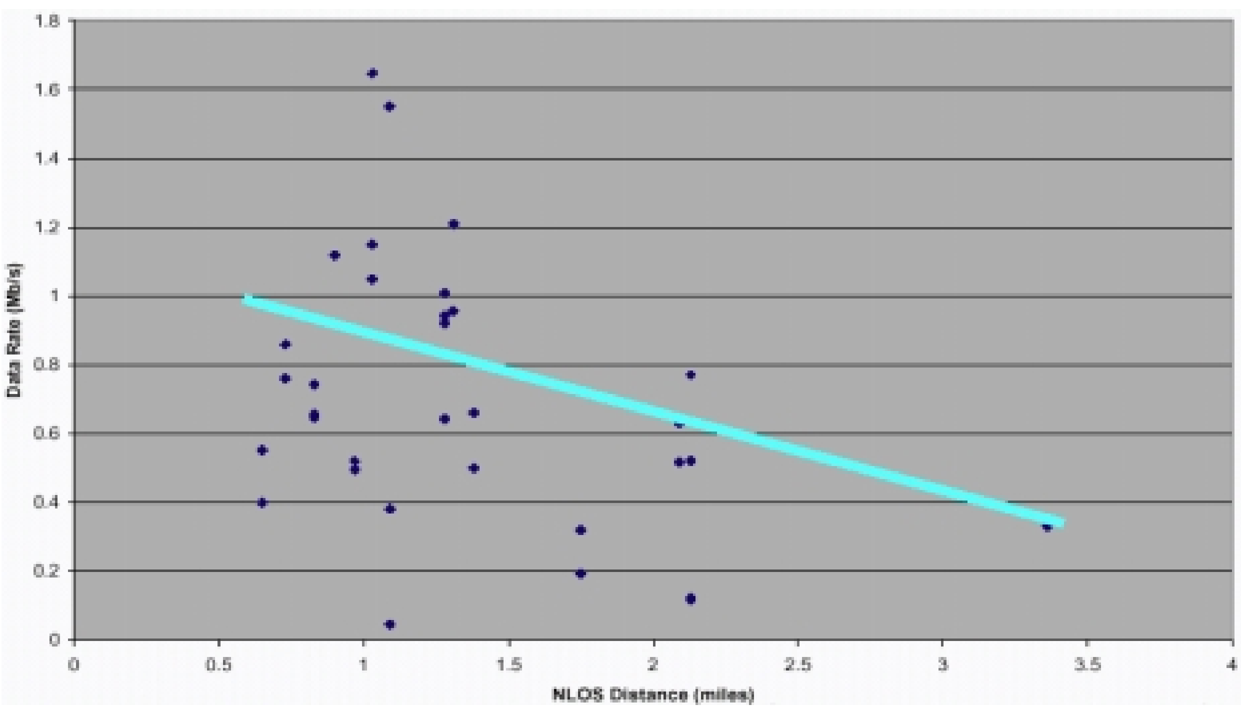

Figure 3.12: Upload Data Rates [34]

As can be seen by Figure 3.12, the peak data rates are exactly 1.6 Mbps as calculated above. When there is more path loss, the signal strength drops and so a reduction in noise bandwidth is needed to offset the path loss. Therefore, the data rate has to be lowered to still produce a signal that can be demodulated with a BER of 10^{-3}. Since we are more concerned with path loss over distance (since different places within the cell radius and within the home itself will cause different losses), we can take an average data rate of 700 kbps and create a downlink power budget. This power budget is shown in Table 3.5 below.

Table 3.5: Link Budget for 1 Mbps QPSK Uplink Signal

Parameters	Value	Comments
CPE Parameters		
CPE Tx power (dBm)	31.0	Output power to the CPE antenna
Antenna gain (dBi)	4.0	Average Gain of CPE antennas (omni)
Diversity gain (dB)	2.6	Gain due to diversity operation
Adjustment for One Code-Channel (dB)	-18.1	10*log(1/64); there are 64 total code channels in the 2 MHz CPE
Effective TX power per code channel (dBm)	**19.5**	
BTS Parameters		
Antenna gain (dBi)	8.0	Gain of omni-directional antenna
RFS/Cable loss (dB)	0.0	Due to tower top LNA
Beamforming gain (dB)	9.0	Beamforming gain of 8 antennas without adding any additional diversity gain due to multiple antennas
Receiver noise figure (dB)	5.0	Noise figure of the BTS tower top LNA and Rcvr. Includes loss to LNA.
Thermal noise density (dBm/Hz)	-174.3	Thermal noise density at room temperature
Rx noise bandwidth (dBHz)	57.0	Thermal noise density + noise figure
CDMA spreading gain (dB)	15.1	Spreading gain of 32-chip code
SNR for QPSK (dB)	10.5	Required for 10^{-3} BER for QPSK before Reed-Solomon decoding
Required average signal level at the BTS antennas (dBm)	**-133.9**	Required average signal strength at the BTS antennas
Margins & Factors		
Log Normal Shadow/Penetration (dB)	6.0	Blocking of neighboring trees and houses
In-building penetration (dB)	12.0	For a typical residence home
Total Margins & Factors (dB)	**18.0**	
Maximum uplink path loss with margins and factors (dB)	**135.4**	Total Power per code channel - Required Signal Level - Margins

As can be seen by Table 3.5, the maximum uplink path loss allowed is 135.4 dB for a 750 kbps QPSK signal.

3.5 Summary

In conclusion, this chapter described Navini's Ripwave system. The system operates in the 2.4 GHz ISM band and can function in either the symmetric or asymmetric TDD mode. The maximum downstream channel size is 5 MHz (ten 500 kHz subcarriers) and the maximum upstream channel size is 2 MHz (four 500 kHz subcarriers). Each subcarrier contains 32 Walsh code channels and only one CPE is assigned per code channel in order to take advantage of the 32-chip spreading factor (for a processing gain of 15 dB). The maximum number of CPEs that can be accommodated by one BTS is 320, with each having a total data rate of 25 kbps using QPSK. The maximum download rate than can be achieved by a CPE is 7.2 Mbps using 64-QAM and 3:1 asymmetric TDD timing.

The downlink beamforming test was consistent with theory and proved that with eight BTS antennas, an 18 dB downlink beamforming gain was possible. The uplink beamforming test was also consistent with theory and proved that with eight BTS antennas, a 9 dB uplink gain was possible. The uplink CIR test showed that an interference level of over 25 dB still resulted in a S/N of greater than 10.5 dB at the BTS. This was due to the synchronicity of the uplink signals and thus being able to take advantage of the smart antennas. The downlink CIR test showed that an aligned interference level of 15 dB and a non-aligned interference level of 38 dB resulted in a S/N of greater than 10.5 dB at the BTS. The download data rate test proved the maximum bit rate of 2.4 Mbps (using QPSK and 3:1 TDD) and the upload data rate test proved the maximum bit rate of 1.6 Mbps (using QPSK and 1:1 TDD). The maximum allowed path loss for the downlink is 125.4 dB and 135.4 dB for the uplink.

Chapter 4

Orthogonal Frequency Division Multiplexing (OFDM)

Orthogonal Frequency Division Multiplexing (OFDM) was proposed as a possible air interface standard for 3G communications by the Beta group of the ETSI. OFDM is a special case of multicarrier transmission, where a single datastream is transmitted over a number of lower rate subcarriers. In actuality, OFDM can be seen as either a modulation technique or a multiplexing technique. OFDM is conceptually very simple, but the implementation relies on very high speed digital signal processing (DSP) that has only recently become available at a price that makes OFDM a competitive technology. In practice, some of the carriers in OFDM are used for channel estimation and extra bits exist for error detection and correction. Doing this is called Coded Orthogonal Frequency Division Multiplexing (COFDM). However, doing this is so fundamentally common that most sources (including this one) drop the ‘C’ and just assume coding is used.

4.1 OFDM Basic Principles

A basic idea of OFDM is to divide the available spectrum into many narrowband, lower-data-rate carriers (subcarriers). To obtain high spectral efficiency, spectra are overlapping and the time domain waveforms are orthogonal. Each narrowband subcarrier is modulated using various modulation formats such as quadrature phase shift keying (QPSK) or quadrature amplitude modulation (QAM). Figure 4.1 displays the difference between the conventional nonoverlapping multicarrier technique and the overlapping multicarrier modulation technique used in OFDM.

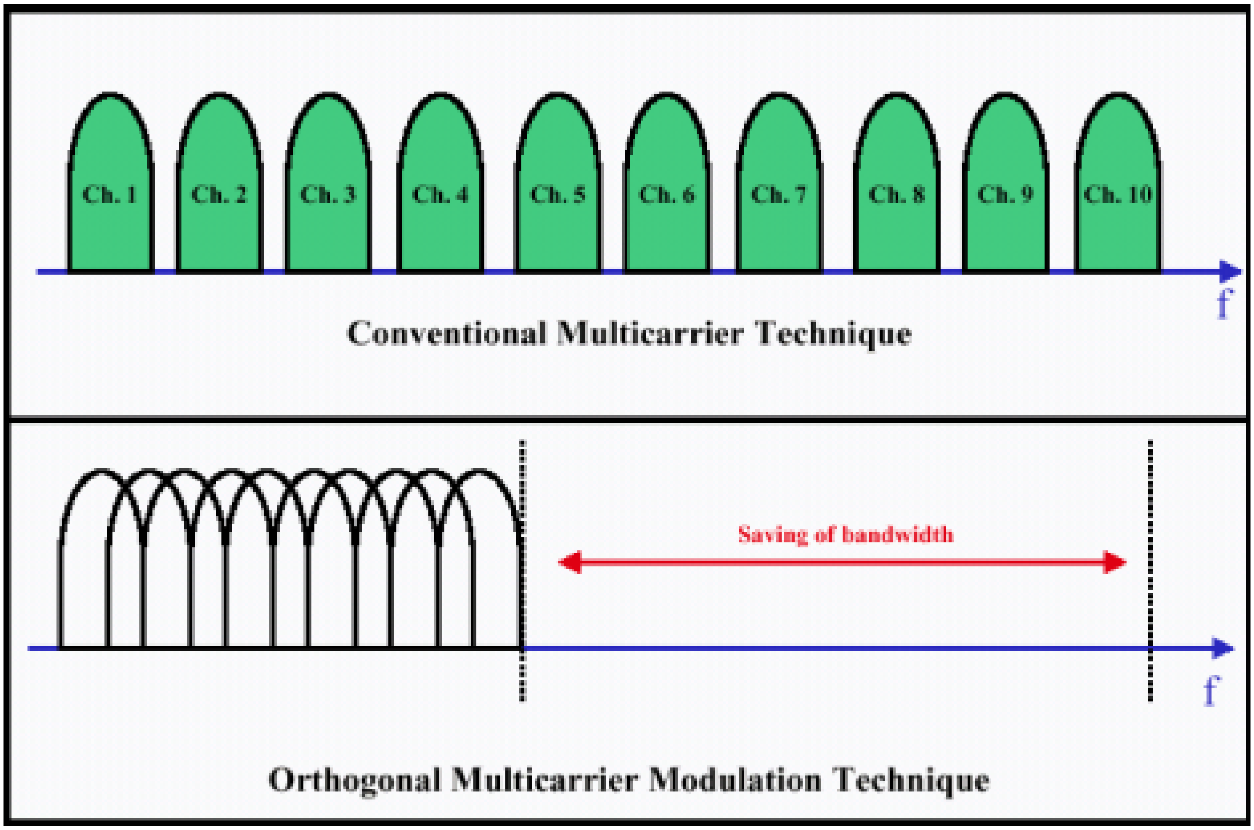

Figure 4.1: Concept of Multicarrier Modulation Techniques

As can be seen in Figure 4.1, by using the overlapping multicarrier modulation technique, half of the bandwidth is conserved. However, to realize the overlapping technique, crosstalk between the subcarriers needs to be reduced and, thus, orthogonality preserved. The orthogonality of the carriers means that each carrier has an integer number of cycles in a symbol period. This implies that the carriers are all synchronized in time and that their frequencies are integer multiples of a common factor. Consequently, the spectrum of each carrier has a null at the center frequency of each of the other carriers in the system. An example of OFDM spectra is shown in Figure 4.2 below.

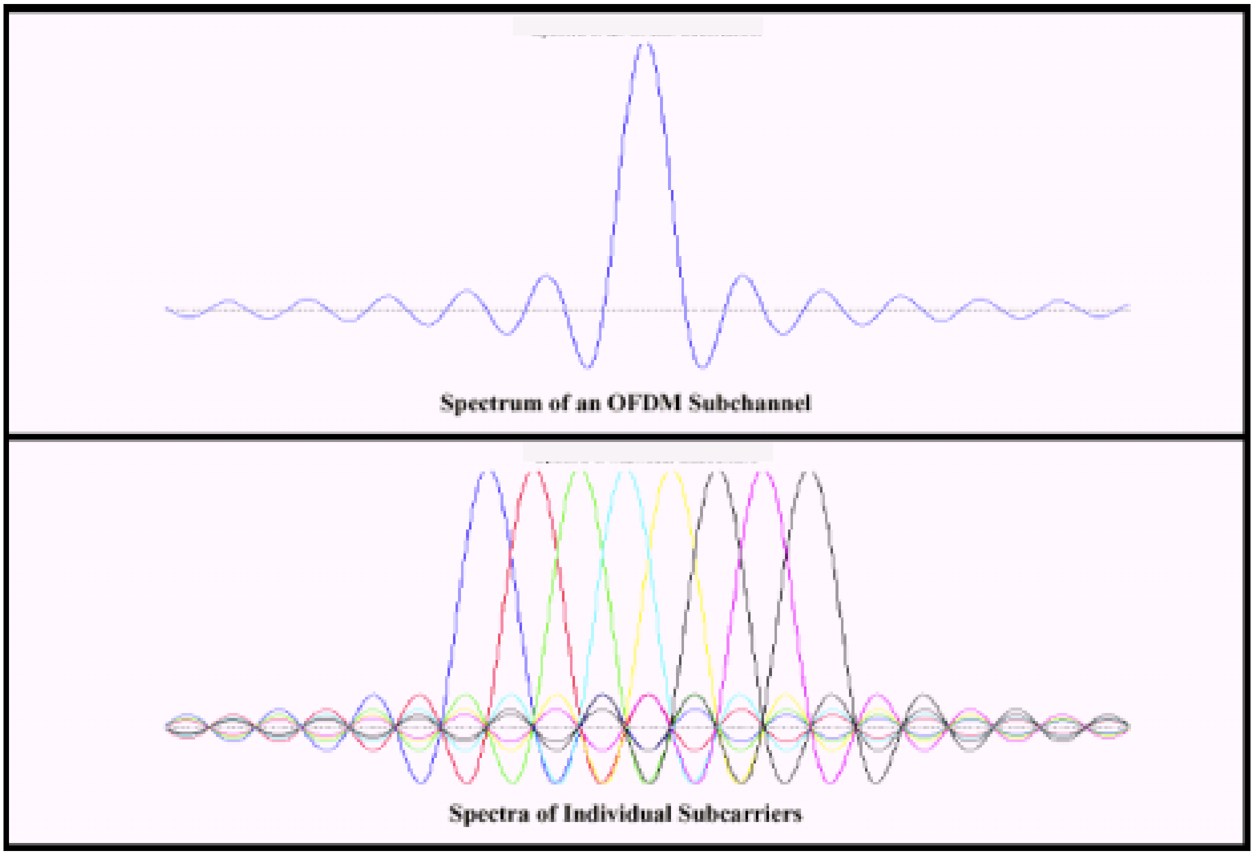

Figure 4.2: OFDM Spectra

Orthogonality eliminates interference between the carriers (crosstalk) and allows the carriers in an OFDM signal to be arranged in a manner where the sidebands of the individual carriers overlap (as shown above). This overcomes the problem of overhead carrier spacing (and guard bands) required in FDMA (see Chapter 1). Therefore, if a discrete Fourier transform (DFT) is used at the receiver and correlation values with the center frequency of each subcarrier are calculated, the transmitted data can be recovered with no crosstalk. In addition, using the DFT, frequency division multiplexing (FDM) is achieved by baseband processing instead of bandpass filtering. This is a huge advantage in the number of complex DSP operations and processing time. In actuality, the fast Fourier transform (FFT), an efficient implementation of the DFT, is used at the transmitter and receiver to reduce the number of operations from N^2 in DFT to $N\log N$ [38].

4.2 OFDM Generation

An OFDM signal consists of a sum of subcarriers that are modulated using PSK or QAM. If using complex QAM symbols, the equivalent complex baseband notation of an OFDM symbol can be written as:

$$s(t) = \sum_{i=-Ns/2}^{(Ns/2)-1} (d_{i+Ns/2})\exp(j2\pi(i/t)[t-t_s]),\ t_s \leq t \leq t_s + T$$

$$s(t) = 0,\ t < t_s \ \wedge\ t > t_s + T$$

where Ns is the number of subcarriers, T the symbol duration, d_i the complex QAM symbols, t the time, and t_s the OFDM symbol starting time.

Figure 4.3 shows the operation of an OFDM modulator in a block diagram.

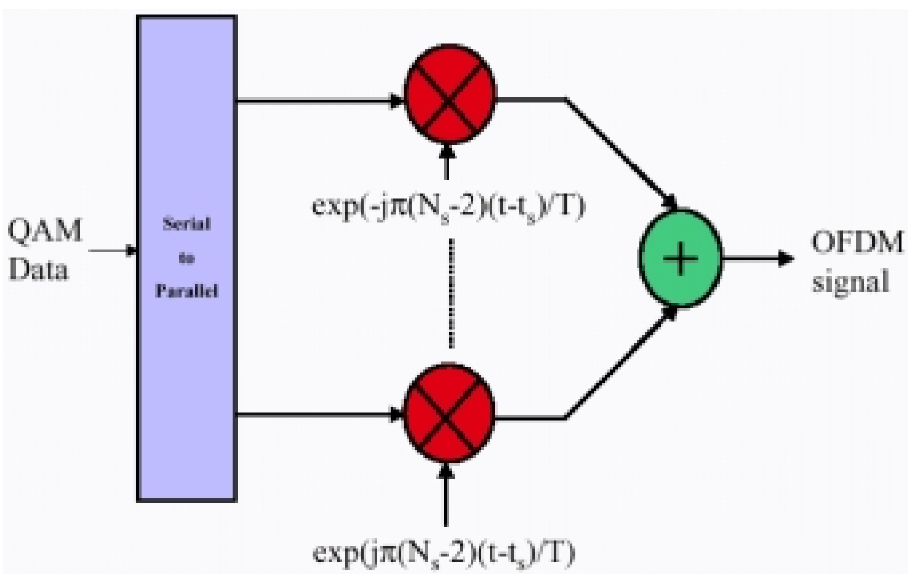

Figure 4.3: OFDM Modulator [38]

As an example, Figure 4.4 shows the generation of five subcarriers into an OFDM signal. In this example, all subcarriers have the same amplitude and phase, but this does not have to be the case (and usually is not).

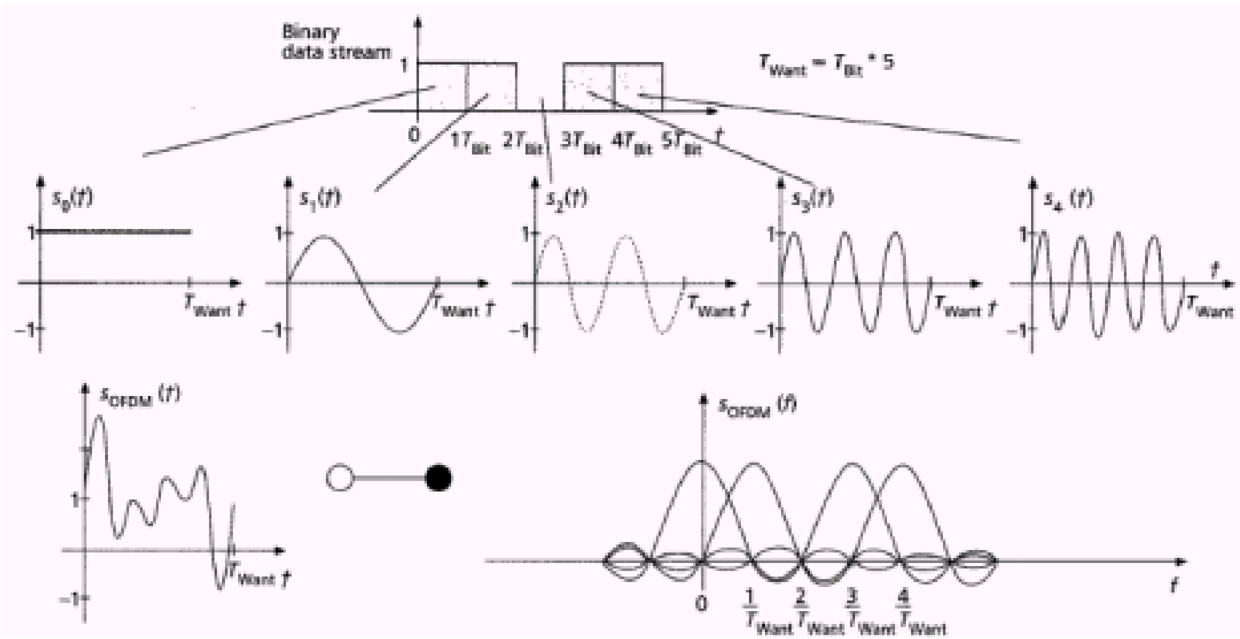

Figure 4.4: Simplified Presentation of an OFDM Signal [39]

Each subcarrier in Figure 4.4 has an exact integer number of cycles in the interval T and the number of cycles between adjacent subcarriers differs by exactly one. This property accounts for the orthogonality between the subcarriers.

In actuality, OFDM is generated by choosing the spectrum required, based on the input data, and the modulation scheme used. Each carrier to be produced is then assigned data to transmit and the required amplitude and phase of the carrier are calculated based on the type of modulation. The required spectrum is then converted back to the time domain using an inverse FFT (IFFT). In the receiver, the opposite is done – the FFT transforms a cyclic time domain signal into its equivalent frequency domain spectrum.   This is done by finding the equivalent waveform, which is generated as a sum of orthogonal sinusoidal components. The amplitudes and phases of the components constitute the frequency spectrum. Therefore, a simplified block diagram of an OFDM transceiver may look like the one in Figure 4.5.

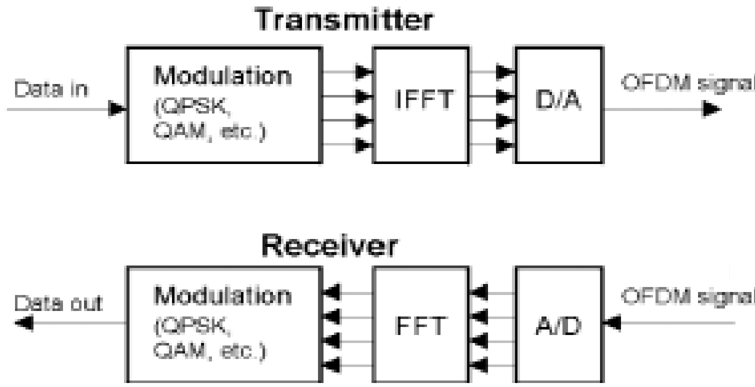

Figure 4.5: Simplified OFDM Transceiver

4.2.1 Cyclic Extension

One of the most important properties of OFDM transmissions is the robustness against multipath delay spread. Dividing the input data stream into N subcarriers makes the symbol duration N times longer, which reduces the relative multipath delay spread, relative to symbol time, by the same amount [38]. The level of robustness can be increased even more (to eliminate ISI almost completely) by adding a guard period between the transmitted symbols. The guard period allows time for multipath signals from the pervious symbol to die out before the information from the current symbol is gathered. Therefore, the guard time is chosen larger than the expected delay spread. To eliminate ICI, the guard period is chosen to be a cyclic extension of the symbol. This ensures that delayed versions of the OFDM symbol still have an integer number of cycles in the FFT interval. Therefore, multipath signals with smaller delays (smaller than the guard time) cannot cause ICI. Using the cyclic extended symbol, the samples required for the FFT can be taken anywhere over the length of the symbol. This provides symbol time synchronization tolerance as well as multipath immunity.

4.2.2 Coding

As with any digital wireless channel, forward error correction (FEC) coding is used to lower the bit error rate (BER). Only convolutional coding is applied in the case of BER = 10^{-3}. The convolutional coding rates change according to the different services. Rates from ¼ to 1 can be chosen so that the entire system will be able to reuse as much of the decoding hardware as possible. After convolutional coding, interleaving is used. Because of the frequency selective fading of typical radio channels, the OFDM subcarriers usually have different amplitudes. Deep fades in the frequency spectrum may cause groups of subcarriers to be less reliable than others – thereby causing bit errors in bursts. Most FEC codes are not designed to deal with error bursts and so interleaving is applied to randomize the occurrence of bit errors prior to decoding.

For services requiring a BER = 10^{-6}, a concatenated code scheme such as Reed-Solomon (RS) or outer interleaving and convolutional coding could be used. The outer interleaver is necessary to break the error burst at the output of the Viterbi decoder. This is needed in addition to the inner interleaver for breaking the error bursts due to fading [21]. Alternatively, turbo coding could be applied.

4.2.3 Synchronization

Before an OFDM receiver can demodulate the subcarriers, it has to find out where the symbol boundaries are and what the optimal timing instants (sampling points) are to reduce the effects of ICI. Also, the receiver has to estimate and correct for any offset on the carrier frequency of the received signal (also to reduce ICI). In an OFDM link, the subcarriers are orthogonal only if the transmitter and receiver operate at the same frequencies. Any frequency offset immediately leads to ICI in the receiver. Phase noise also causes a similar problem – a practical oscillator does not produce a carrier at exactly one frequency, but rather a carrier that is phase modulated by random phase jitter. As a result, the frequency (since it is the derivative of phase) is never constant and leads to ICI. OFDM is more robust to timing errors, but to achieve the best possible multipath robustness, there exists an optimal timing instant. Any deviation from this optimal sampling point leads to an increase of sensitivity due to delay spread, which, in turn, leads to a less robust system. Therefore, synchronization issues are more important in OFDM and must be dealt with. There are many methods to achieve synchronization in an OFDM system, such as via the cyclic prefix or through special training sequences, but that is beyond the scope of this paper. Specifically, [38], [40], [41], [43], [44], and [45] talk about the effects of frequency, phase, and timing errors and how to deal with them effectively (and reduce their effects).

4.2.4 Signal Detection

Knowledge about the reference phase and amplitude of the constellation on each subcarrier is needed to estimate the bits at the receiver. In general, frequency offset, timing offset, and frequency selective fading can cause random phase shifts and amplitude changes in the constellation of each subcarrier. Coherent detection and differential detection are two methods to compensate for the random phase shift and amplitude change.

Coherent detection uses estimates of the reference amplitudes and phases to determine the best possible decision boundaries for the constellation of each subcarrier. The main concern with coherent detection is determining a method to find the reference values without introducing too much overhead with respect to training symbols. Differential detection looks at the phase and amplitude differences between two symbols. It can be done both in the time domain and in the frequency domain. In the time domain, differential detection compares each subsymbol with the subsymbol on the same subcarrier of the previous OFDM symbol, as depicted in Figure 4.6 below. In the frequency domain, each subcarrier is compared with the adjacent subcarrier within the same OFDM symbol [38]. Several estimation and detection techniques exist and are covered in numerous papers such as [38], [40], and [45] among others.

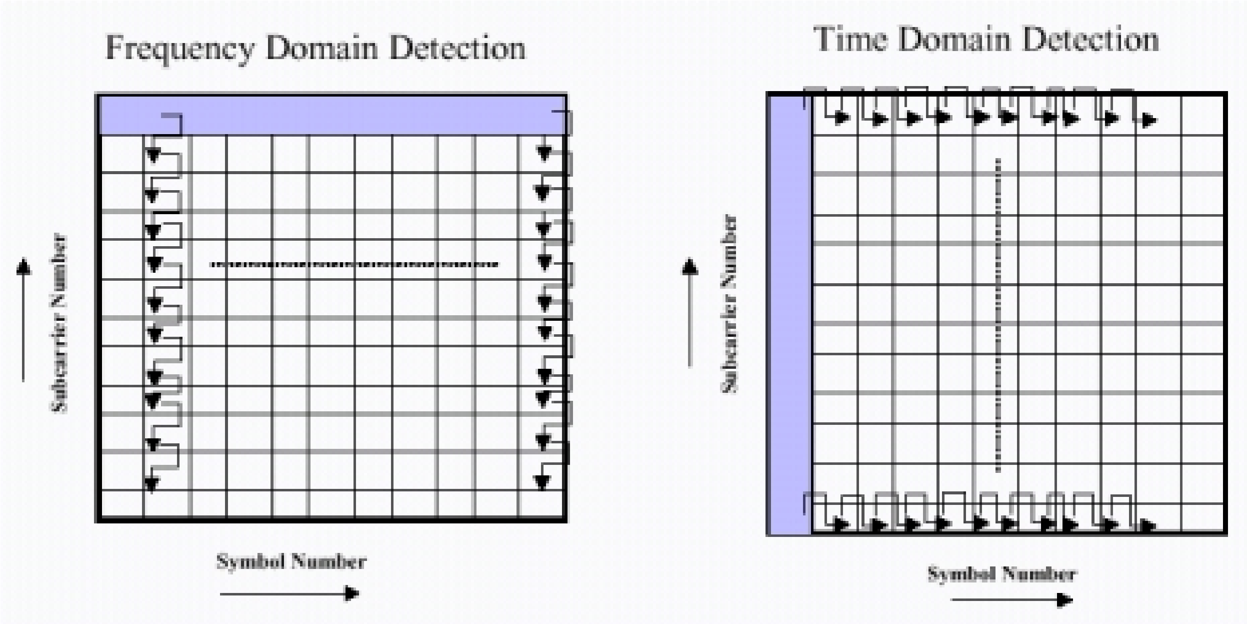

Figure 4.6: Differential Detection in the Frequency and Time Domains [38]

4.2.5 OFDM System

Figure 4.7 shows the basic block diagram of a complete OFDM modem, where the upper path is the transmitter course and the lower path is the receiver chain.

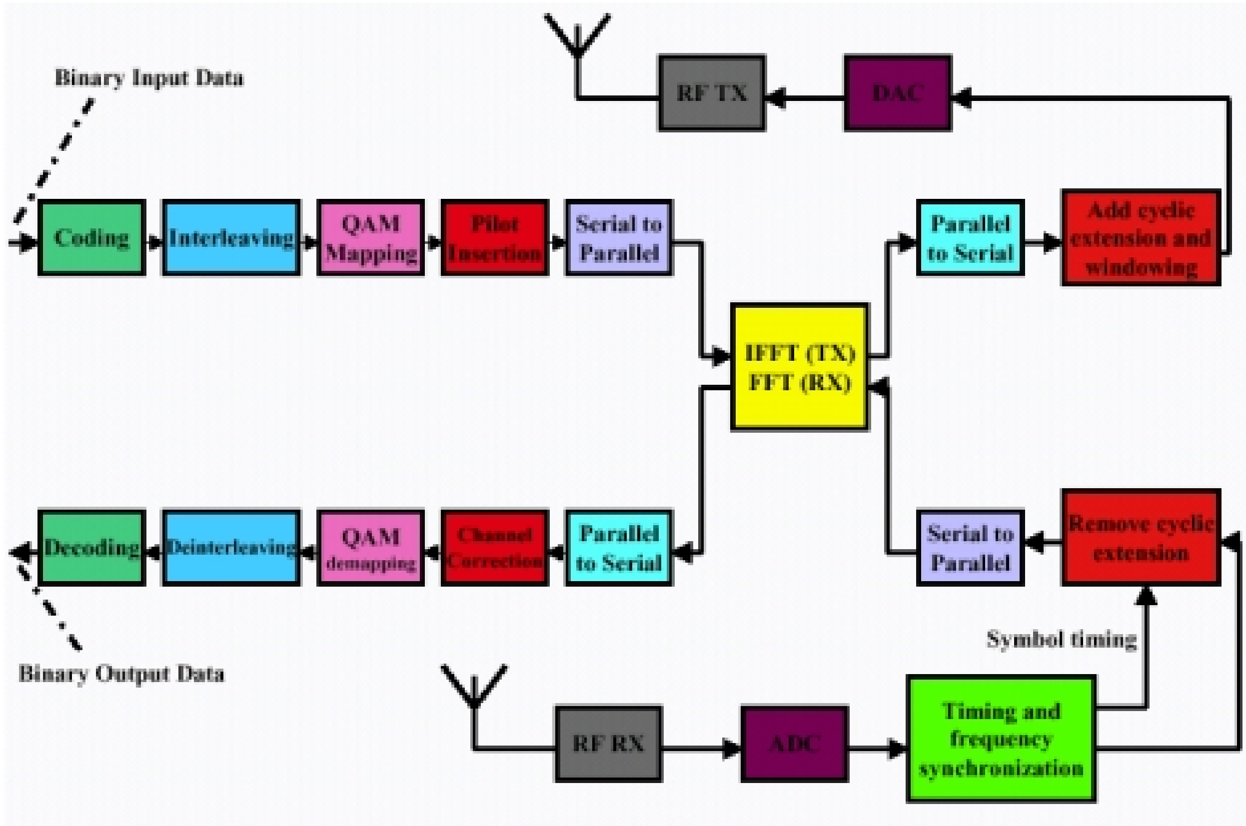

Figure 4.7: OFDM Transceiver [38]

Due to the different types of media that are going to be sent over 3G communication systems, the upstream and downstream block diagrams can be application specific. Figures 4.8 and 4.9 show the downstream block diagrams and Figures 4.10 and 4.11 show the upstream block diagrams.

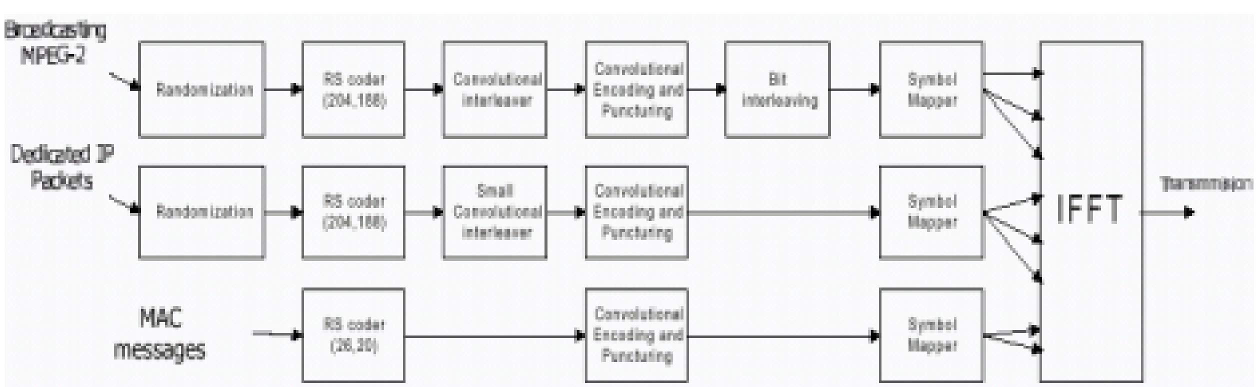

Figure 4.8: Downstream Encoding and Modulation [46]

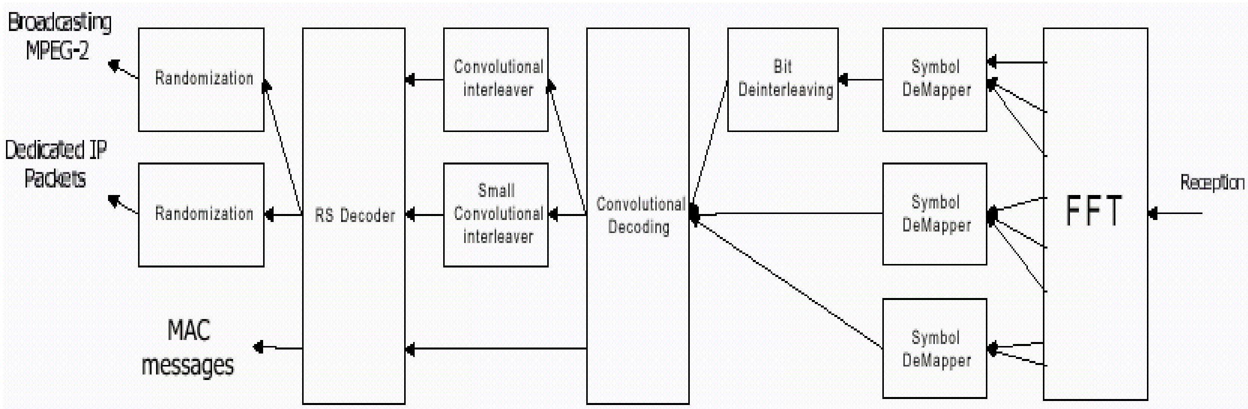

Figure 4.9: Downstream Demodulation and Decoding [46]

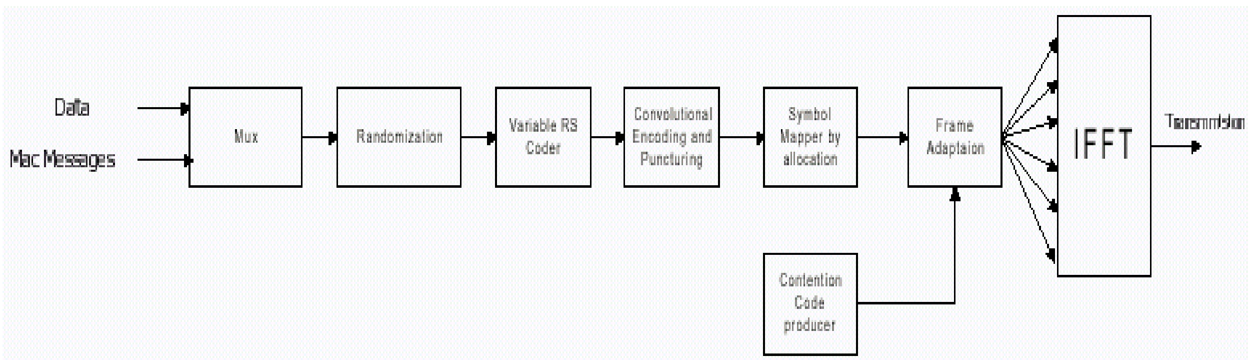

Figure 4.10: Uplink Encoding and Modulation [46]

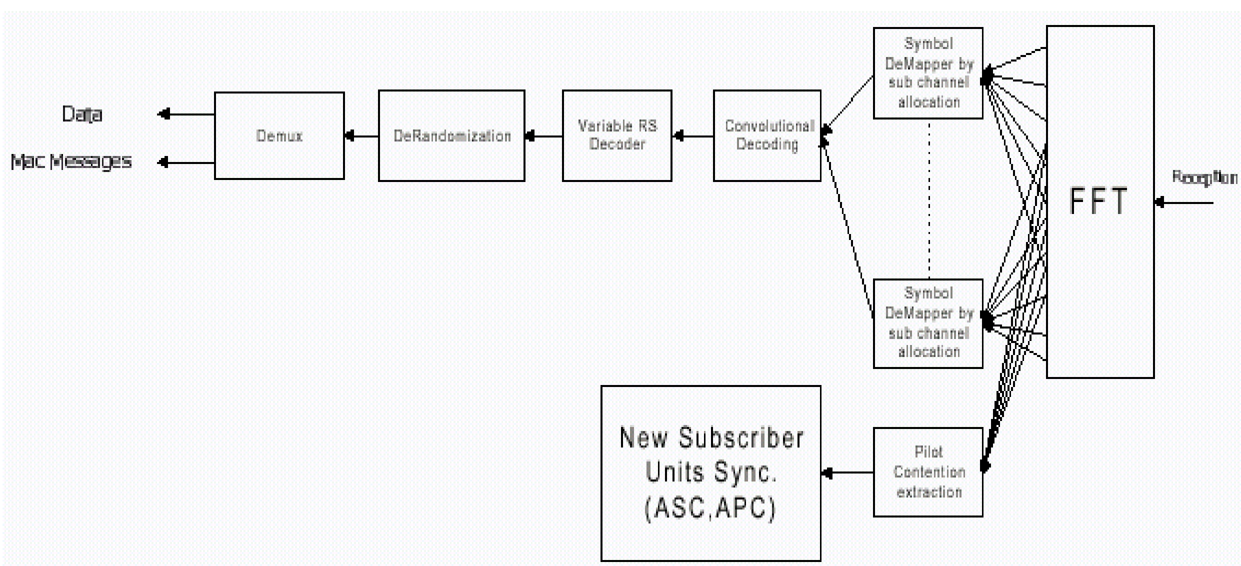

Figure 4.11: Uplink Demodulation and Decoding [46]

4.3 OFDM Varieties

With a number of vendors competing for airtime, OFDM's supporters have divided into two factions: the Broadband Wireless Internet Forum (BWIF) and the OFDM forum. Led by Cisco Systems, Texas Instruments, and Broadcom, BWIF backs and has developed a specification for Vector OFDM (VOFDM). Led by Wi-LAN, the OFDM forum has developed another type of OFDM – Wideband OFDM (WOFDM). Finally, Flarion Technologies, a spin-off from Lucent, has developed a spread spectrum technology referred to as Flash OFDM [47]. This paper is primarily concerned with BWIF's VOFDM, but brief descriptions of WOFDM and Flash OFDM are listed below for completeness. Henceforth, the rest of the thesis will focus only on VOFDM.

4.3.1 Vector OFDM (VOFDM)

The key to Vector OFDM is the concept of multiple input, multiple output (MIMO). By using spatial diversity, a wireless system's tolerance to noise, interference, and multipath can be greatly increased. Vector OFDM can deliver multiple signals on a single antenna or receive them on multiple antennas. This increases the likelihood of a good signal being received. By placing two or more antennas in a wireless system with each having a different set of multipath signals, the effects of each channel will vary from one antenna to the next. Thus, channels unusable on one antenna may prove to be acceptable on another antenna. Figure 4.12 illustrates the idea of MIMO as applied to VOFDM. Antenna spacing is at least ten times the wavelength [48].

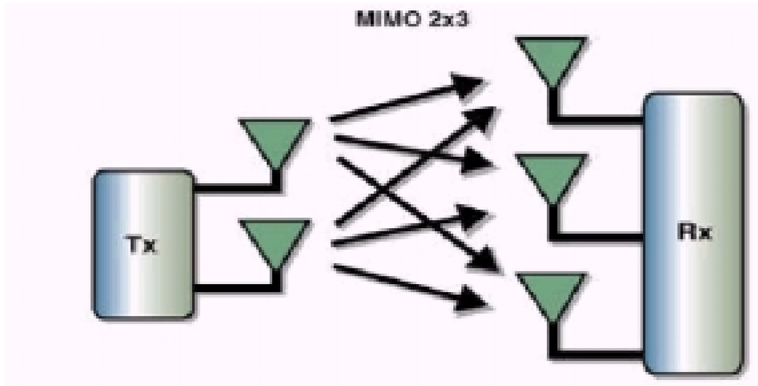

Figure 4.12: MIMO for VOFDM [47]

Vector OFDM will be discussed in much more detail in Section 4.4.

4.3.2 Wideband OFDM (WOFDM)

In Wideband OFDM, the spacing between the channels is large enough so that any frequency errors between the transmitter and receiver have no effect on the performance of the system. WOFDM allows several independent channels to operate within the same band. This creates an overlay of low-power, multipoint radio networks and point-to-point backbone systems [47]. The basic block diagram of the WOFDM transceiver can be seen in Figure 4.13 below.

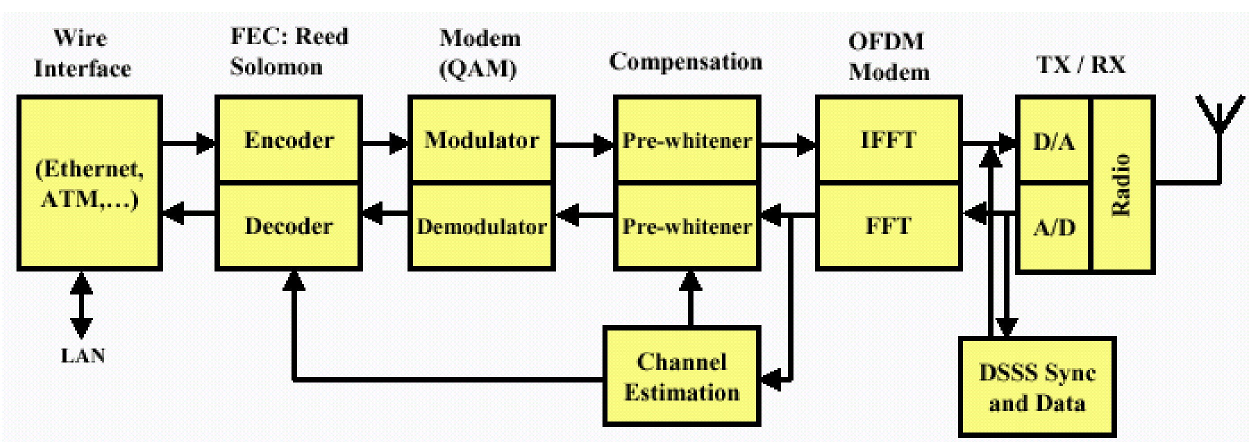

Figure 4.13: WOFDM Transceiver [49]

WOFDM overcomes the problem of multipath by sending training symbols. Specifically, six training symbols are added to the data stream. The first five symbols are used to estimate the channel transfer function, and the inverse is applied to every OFDM frame to compensate for the channel. The other key to WOFDM is the signal whitener. The signal whitener reduces the peak to average power ratio that must pass through the radio amplifiers and the A/D converters. The WOFDM symbol is pre-whitened, which means that it is multiplied by a vector of complex values, *R* that is known to the transmitter and receiver. All values in *R* have unity amplitude and phases are selected so that the average power level of the resulting transmitted signal varies less than without doing this operation [49]. There are many different vectors that can be used for *R* so this can be used to add a security feature to the system [49].

4.3.3 Flash OFDM

Flash OFDM is often referred to as a fast-hopped spread spectrum version of OFDM. It uses multiple tones and fast hopping to spread signals over a given spectrum band. Figure 4.14 shows the basic idea behind Flash OFDM.

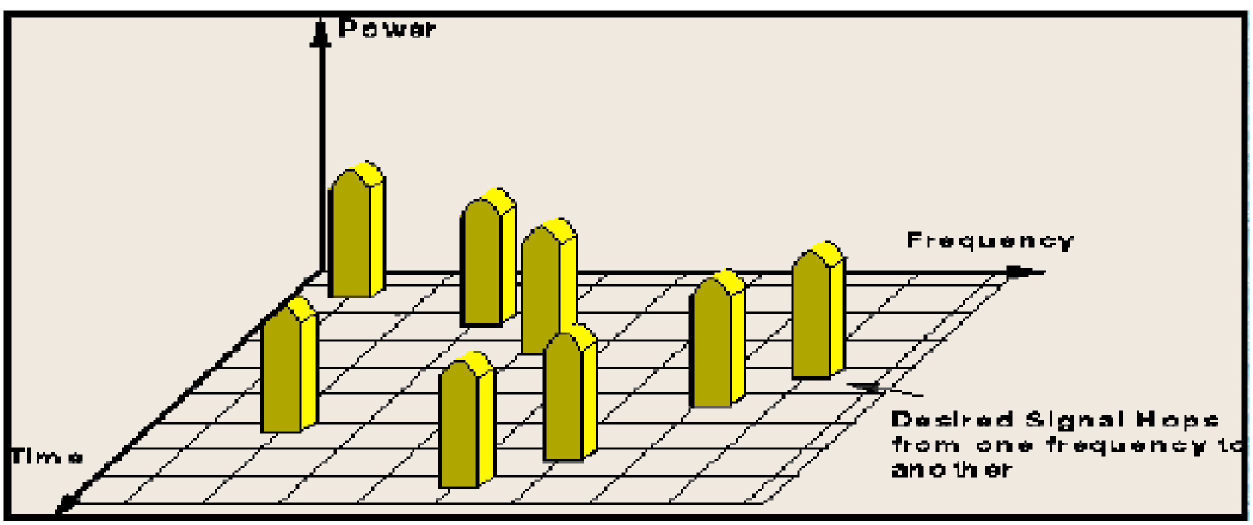

Figure 4.14: Flash OFDM Principle [50]

4.4 Vector OFDM Details

This section will go deeper into the details of BWIF's Vector OFDM (VOFDM). The basic idea behind VOFDM is to combine OFDM with spatial processing so that diversity in frequency, time, and space are all exploited. VOFDM is indeed a cost-optimized implementation of the MIMO technology. Figure 4.15 shows a high-level block diagram of a MIMO VOFDM system and Figure 4.16 shows an example of such a system at work.

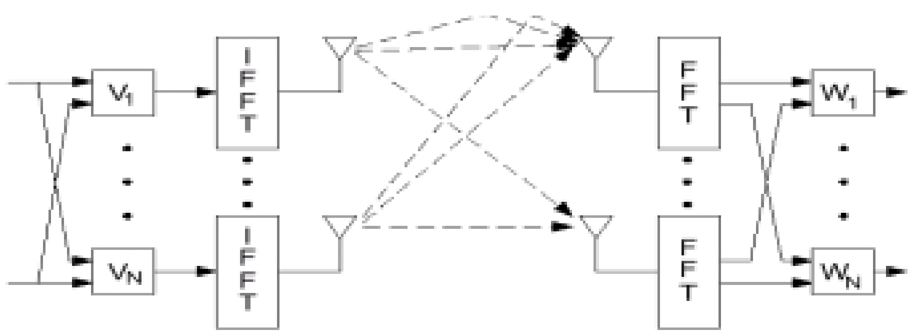

Figure 4.15: VOFDM System (showing MIMO technology) [51]

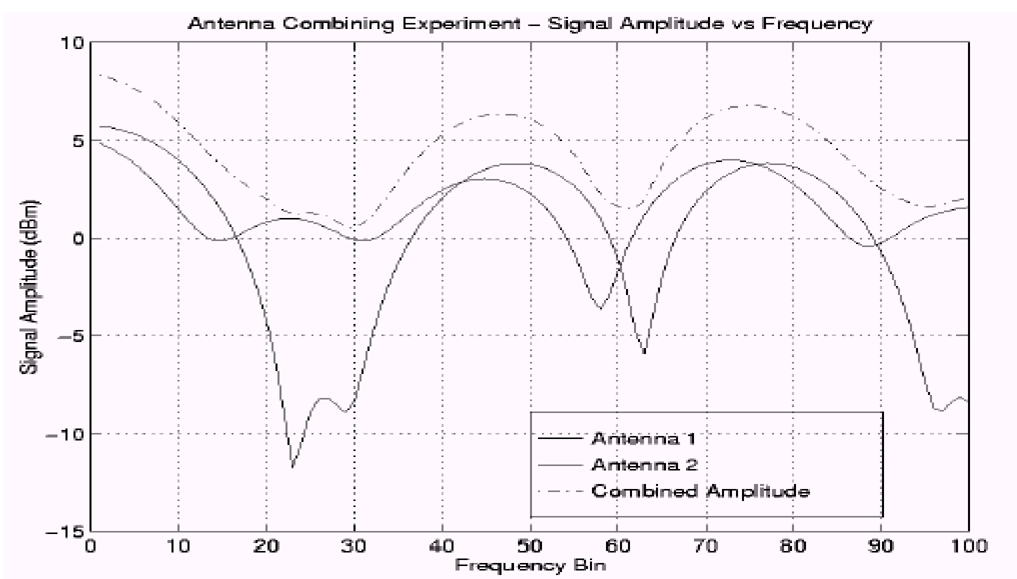

Figure 4.16: VOFDM Experiment with Two Antennas [51]

Antenna diversity will be expanded on later in this chapter. Next, Figures 4.17 and 4.18 show the specific VOFDM transmit and receive system block diagrams respectively.

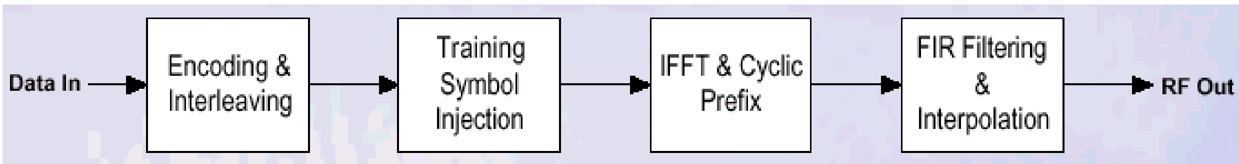

Figure 4.17: VOFDM Transmitter Block Diagram [52]

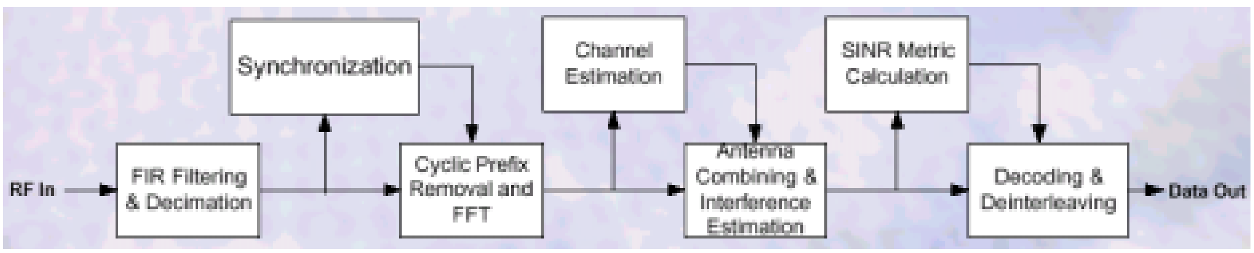

Figure 4.18: VOFDM Receiver Block Diagram [52]

All of the following features are implemented in VOFDM:

1. Dynamically programmable data rates and the delay spread tolerance.
2. Optimum burst-mode training approaches (for channel estimation).
3. Timing and frequency synchronization.
4. Spatial processing (for interference cancellation).
5. Convolutional and Reed-Solomon coding.
6. Soft Viterbi decoding.

4.4.1 Upstream

First, we will compare upstream transmissions in the burst mode in a MMDS channel using VOFDM and single carrier modulation (SCM). Experiments for such an MMDS channel using

16-QAM and a ½ μs delay spread were carried out in [51] in terms of Codeword Error Rate (CER) and are shown in Figure 4.19 below.

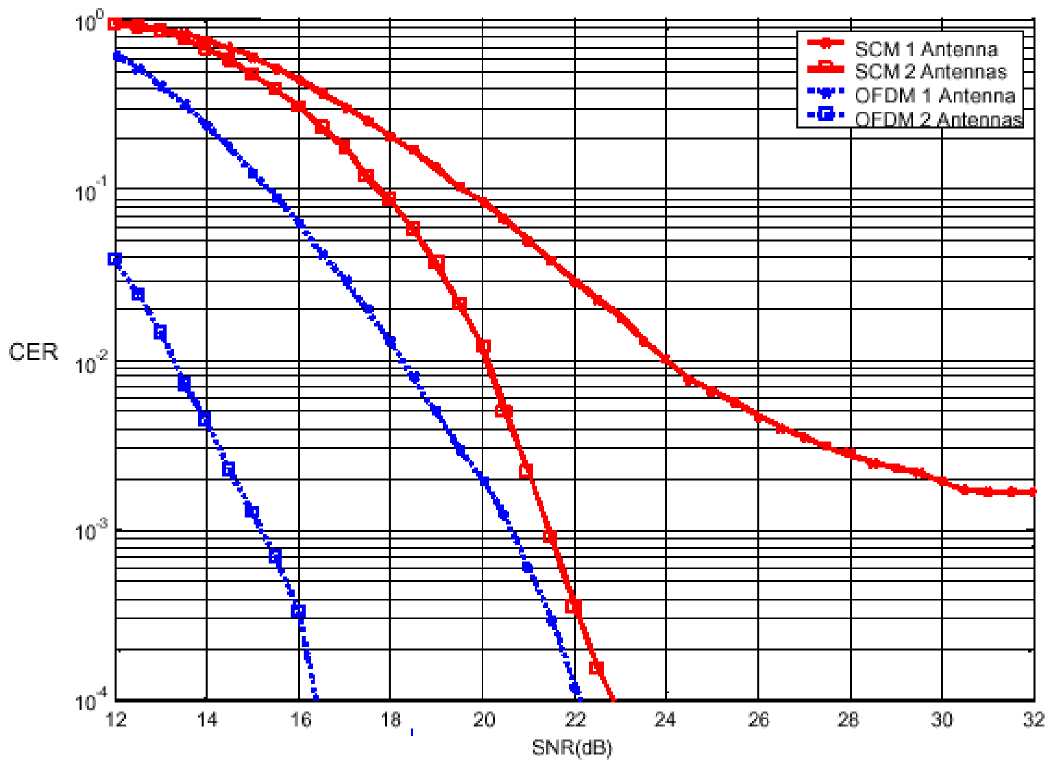

Figure 4.19: Upstream Performance Comparison of VODFM and SCM [51]

The antenna outputs are combined using Signal-to-Interference Ratio (SINR) combining for the dual antenna VOFDM system and a Decision Feedback Equalizer (DFE) is used for SCM. SINR combining refers to combining the individual S/I ratios from each antenna element. The equalizer for a single antenna system has 31 taps in its feedforward portion and five taps in its feedback portion. When dual antennas are employed, two feedforward equalizers of 31 taps each are combined to feed a 5-tap feedback equalizer with decision feedback. In general, the VOFDM system provides more capacity since, in order to operate at the same CER, single carrier modulation either needs more coding or more SNR. As can be seen by Figure 4.19, for a CER of 10^{-4}, the single antenna VOFDM system is infinitely better than the single antenna SCM system and 1 dB better than the dual antenna SCM system. For the same CER, the dual antenna VOFDM system is 6 dB better than its single antenna counter part and 7 dB better than the dual antenna SCM system.

4.4.2 Downstream

Experiments in [51] were also done for VOFDM and SCM in continuous carrier demodulation (downstream). The SCM system equalizer uses a fully adapted equalizer that utilizes the Lease Mean Squares (LMS) algorithm. The VOFDM system uses interference cancellation whereas SCM employs optimum space-time equalization. A 2/3-rate convolutional code along with a (252,232) RS code is used for both systems. Results of the simulation can be seen in [51], but again, the VOFDM system outperforms the SCM system in all regards.

4.4.3 Transmit Diversity

Transmit diversity in a VOFDM system can be used either on the uplink or on the downlink. Transmit diversity uses a second transmit antenna, and reduces the required fading margin by exploiting the lack of correlation between fast fading that each path encounters.

To employ transmit diversity, dual-receivers, a signal modifier, and a second analog chain are needed. In some scenarios, the channel will have such little delay spread that the signals from the two antennas could arrive at 180 degrees out of phase across the entire frequency band. Therefore, a signal modifier is used on one of the transmit antennas to fix this problem. Signal modifiers could constitute a pure delay element, a magnitude response modifier, and a phase response modifier. Figure 4.20 shows the simulation results carried out in [52] corresponding to transmit diversity.

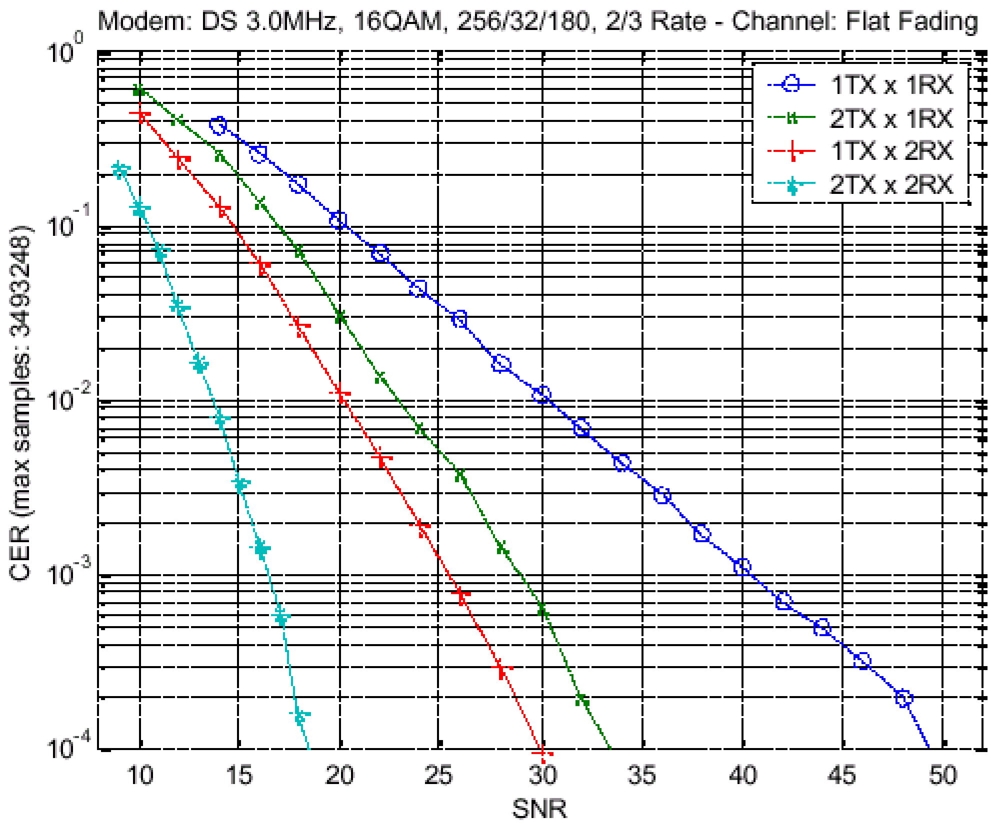

Figure 4.20: Simulation Results for Transmit Diversity [52]

As can be seen by Figure 4.20, transmit diversity results in a significant improvement in the CER for a given SNR.

4.4.4 Receive Diversity

Receive diversity in a VOFDM system also provides a significant advantage over SCM technique. A system using only one antenna must employ a larger fade margin. The effects of a larger fade margin are demonstrated in [51]. Since the channel fades on each antenna (of a MIMO system), the mean SNR is chosen to incorporate a fade margin. The fade margin is designed in [51] to accommodate fades that yield 99.99% reliability. The single antenna SCM system in [51] requires roughly a 21 dB larger mean SNR than the dual antenna OFDM system, at a CER of 10^{-4}. This translates directly to spectral efficiency.

An M cell by N sector frequency plan has a spectral efficiency per area proportional to 1/(MN). However, the smaller the MN, the lower the average carrier-to-interference (C/I) ratio the plan can deliver. Studies show that a 3-cell by 3-sector system provides 32.5 dB of C/I for a 90% availability [51]. Therefore, a dual antenna VOFDM system studied could support such a frequency reuse plan with 90% availability and an outage probability of 99.99%. Conversely, the single antenna SCM system requires 54 dB of C/I, which translates to 12-19 cells for the same outage probability and availability.

4.4.5 Complexity

In fact, VOFDM is actually less complex to employ than decision feedback equalization. Figure 4.21 shows that VOFDM exhibits a log linear computational complexity, whereas DFE exhibits a quadratic computational complexity. Computational complexity refers to the number of complex multiply-accumulate operations per second that need to be computed for a given data rate.

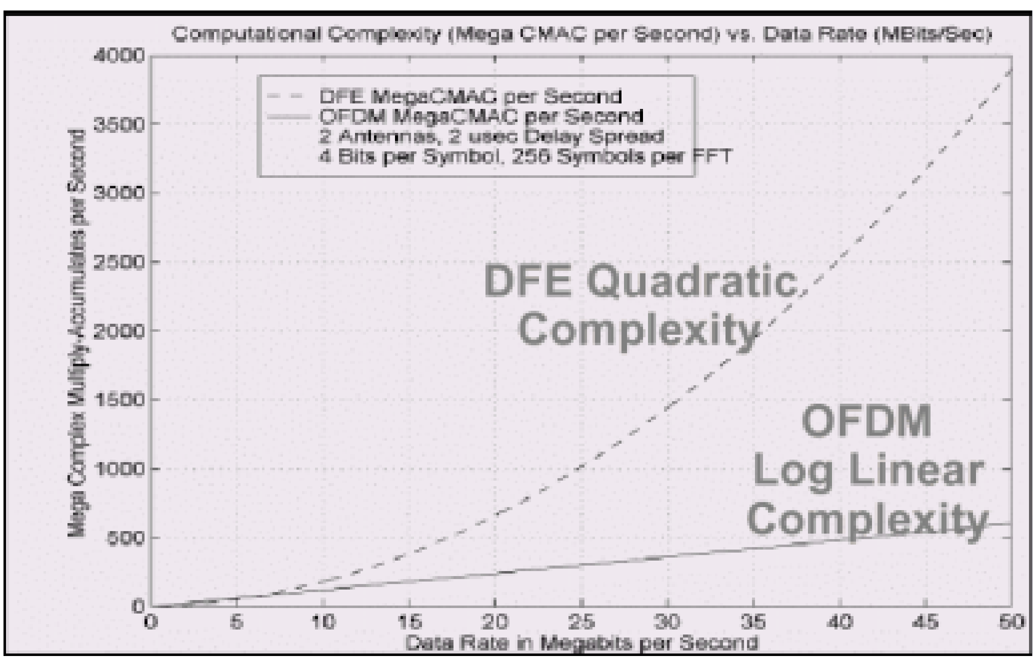

Figure 4.21: VOFDM and DFE Complexity [52]

4.5 Summary

In conclusion, the basic concepts of OFDM have been described in this chapter. Basically, OFDM is a special case of multicarrier transmission, where a single datastream is transmitted over a number of lower rate subcarriers. In actuality, OFDM can be seen as either a modulation technique or a multiplexing technique. A block diagram of a complete OFDM system was also given in Figure 4.7 above. Finally, the different varieties of OFDM – Vector, Wideband, and Flash – were described. The rest of this thesis will focus on Vector OFDM (VOFDM) and its comparison to synchronous CDMA for fixed broadband wireless systems.

Chapter 5

TD-SCDMA Versus OFDM

The previous chapters addressed the possibility of using third generation (3G) mobile cellular wireless systems as the basis for fixed broadband wireless service. In particular, this thesis has examined synchronous CDMA and OFDM. This chapter will compare and contrast the Navini TD-SCDMA and BWIF VOFDM systems as viable broadband access technologies. It will compare different Media Access Control (MAC) layer issues as well as physical layer issues like duplexing strategies, spectral efficiency, coverage, and nonlinearities. Finally, it will draw general conclusions about which system performs better.

5.1 Duplexing Strategies

At this point it should be clear that VOFDM duplexes in the frequency domain (FDD) and TD-SCDMA does so in the time domain (TDD). Both have implications that we will explore in this section. There are four basic things to consider: implementing FDD guard bands, TDD system timing, hardware implications, and frequency reuse.

5.1.1 FDD Guard Bands

In the front ends of both an FDD and a TDD transceiver, the transmitter and receiver typically share the same antenna. For an FDD system, this requires a coupled pair of RF filters known as a duplexer. The transmit portion of the duplexer suppresses transmitter spurious signals in the receive spectrum and the receive portion suppresses the high power transmit signal to prevent the LNA from being overloaded. The duplexer requires high Q (sharp RF cutoffs) filters and therefore becomes moderately expensive. Also, the transmit and receive bands cannot be contiguous and, therefore, a guard band is needed between them. Sometimes, the guard band is described as wasted spectrum. However, by employing a scheme like OFDM, the size of the guard band needed can be minimized. In a network with multiple links, separated by moderate distances, one link may use a frequency that falls in another link's guard band so that no frequencies are wasted.

A TDD system can operate anywhere since no guard bands are necessary. However, regulations like the FCC often make frequency allocations with FDD in mind. An example of this is for the WCS band shown in Figure 5.1 below.

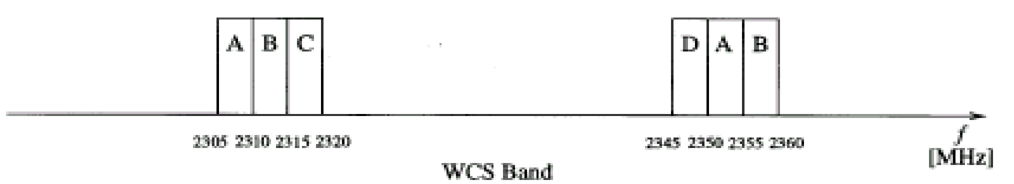

Figure 5.1: WCS Band (Blocks A and B are FDD Pairs)

In WCS, A and B are allocated as FDD frequency pairs and the presence of a guard band is no longer an issue. In this case, TDD may actually be at a disadvantage since building a TDD transceiver to operate in two noncontiguous frequency bands with significant separation is not trivial.

However this is not always the case. It is not a consideration in the MMDS band for example. The MMDS band can be broken up into four groups, and FDD can be made to operate in these bands without wasting any spectrum (explained below). The MMDS band and the partitioning into four groups are illustrated in Figure 5.2 below.

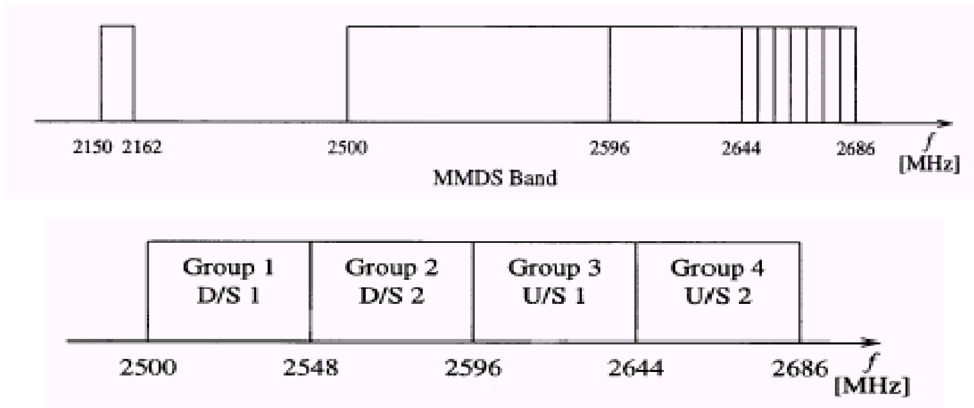

Figure 5.2: MMDS Band

Two sets of transmit and receive bands can be made from these four groups without wasting any spectrum. In the first set, Group 1 can be used for downlink and Group 3 can be used for uplink. Similarly, in the second set, Group 2 can be used for downlink and Group 4 for uplink. This makes Group 2 the guard band for the first set, and Group 3 the guard band for the second set.

Also, a TDD system may not completely avoid needing sharp cutoff filters. Since MMDS operators plan to co-locate their bands at existing Instructional Television Fixed Service (ITFS) or Multipoint Distribution Service (MDS) sites, they have limited control over adjacent channel interference and antenna configurations [53]. Due to limited antenna spacing and non-ideal filtering, a high-level of isolation between the adjacent channel transmitters and receivers is very difficult to provide without a guard band. Furthermore, a dynamic adaptive TDD system requires a guard band separating each transceiver channel unless the transceivers are operated in a fixed frame mode (coordinated mode), which significantly decreases spectral efficiency [53].

5.1.2 TDD System Timing

One important feature of TDD systems is their recognized performance advantages over FDD systems when transporting bursty data like Internet traffic. Furthermore, TDD can accommodate any asymmetric traffic dynamically, as offered by Navini's TD-SCDMA system. FDD has a static ratio between the transmit and receive data rates and cannot easily change it. A dynamic load balancing is difficult to implement in wireless networks.

In a wireless network, base station antennas are located as high above ground as possible to increase coverage. As a result, the base stations are often in line-of-sight of each other (since they are each above the tree and roof line). In a TDD system, this requires the transmit and receive cycles of different base stations to be synchronized. Otherwise, co-channel interference from a neighboring base station can interfere with the uplink transmission from CPEs in a cell. This can happen even if the two base stations do not directly face each other, since the leaked back-propagation from the same sector can engulf signals of the local CPE due to the propagation characteristics of LOS connections versus NLOS [12]. This phenomenon is illustrated in Figure 5.2.5 below.

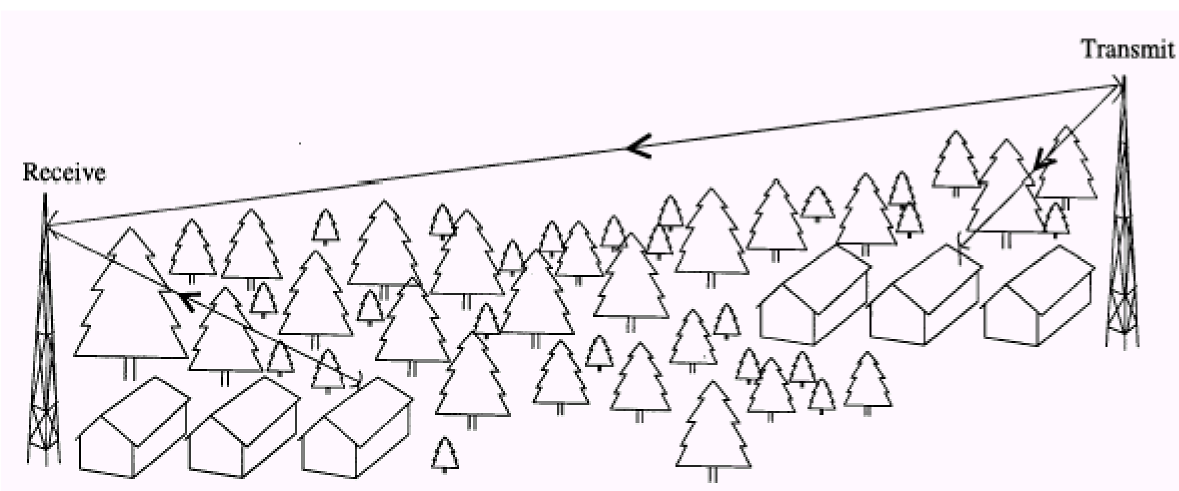

Figure 5.2.5: Back-Propagation Between LOS Base Stations [53]

This requirement for synchronization effectively cancels out the dynamic load balancing advantage of TDD. When all the transmit and receive intervals for all the LOS base stations have to be synchronous, the transmit and receive periods at a given base station can no longer be dynamically changed due to local traffic characteristics.

The synchronicity required between base stations also necessitates guard times between the transmit and receive cycles. This guard interval is necessary so that the transmit signal from a distant base station will die out before the receive period begins. This way, the base station can "listen" to the CPE units in its cell without co-channel interference. The guard time is set to be equal to the propagation time between the two LOS base stations. For a typical cellular frequency reuse plan, two base stations that employ the same frequency are usually 10 - 25 miles apart. This corresponds to a 50 – 125 μs propagation time that should be also used as the guard time. Due to delay considerations, there is a limit on the order of 1 ms on the frame size [53]. Therefore this 50 – 125 μs guard time leads to a 5 – 12.5% loss in efficiency for TDD. FDD systems have the same issue with wasted spectrum due to imperfect filters. Similarly, the CPE units can also generate CCI to force transmit and receive cycle synchronization and guard times. Even if there is no interference from other cells, there is still a guard time required to allow for upstream propagation time. If the cell radius is about 5 miles, then the guard time is an additional 25 μs.

5.1.3 Hardware Implications

A TDD system operates as either a transmitter or a receiver at a given time. This enables the sharing of the local oscillators, amplifiers, and some filters. On, the other hand, this sharing requires transfer switches, which can offset the system cost savings achieved by sharing components. Furthermore, maintaining proper timing of these switches is not trivial.

Consider a TDD system and an FDD system operating at the same data rate. Since the receiver of the TDD system is operational half of the time that the FDD system is, the TDD signal occupies twice the bandwidth (although the average occupied bandwidth is the same). Therefore, the noise power at the TDD receiver is twice as high as in an FDD receiver. Thus, for equivalent conditions, the SNR for a TDD system is 3 dB worse than that of an FDD system. As a result, the FDD system has approximately 3 dB more receiver sensitivity (unless the average transmitter power in both systems is the same). The receiver sensitivity difference is actually more than 3 dB since the transfer switches add about a 1 dB of insertion loss [53]. (A duplexer in an FDD system adds a 3 dB insertion loss). Furthermore, since a TDD system operates at twice the bandwidth, there is more spectral regrowth (increase of adjacent channel interference caused by an increase of transmission power) or sideband regrowth. The power difference between the TDD and FDD systems is 3 dB since the power spectral density levels are the same while the bandwidth changes by a factor of two. This results in an approximately 3 dB larger output power backoff. The total effect of these factors is summarized in Table 5.1 below.

Table 5.1: TDD and FDD System Loss Comparison

Parameter	TDD Loss Amount	FDD Loss Amount
Bandwidth	-3 dB	
Transfer Switch	-2 dB	
Duplexer		- 3 dB
Power Backoff	- 3 dB	
Total	**- 8 dB**	**- 3 dB**

The net effects summarized in the table give FDD a 5 dB net SNR advantage over TDD. However, this is not entirely true. For a given channel bandwidth and a given delay spread, doubling the system bandwidth can improve the reliability of the channel by increasing frequency diversity. For example, a TDD link using two contiguous MMDS channels to form a 12 MHz RF channel can produce a 3 dB improvement in system gain over a FDD link using a noncontiguous pair of 6 MHz MMDS channels [53]. This reduces the overall net for FDD (as far as hardware in concerned) to only 2 dB.

Next, the sampling rates for ADCs and DACs are halved in FDD. This reduces the cost, power consumption, and enables higher interpolation/decimation ratios. Since the sampling rate is doubled with TDD, the equalizer length for QAM is also doubled. This leads to a doubling of the symbol rate and thus, the number of operations per second goes up by four. Similarly, in OFDM, increasing the sampling rate doubles the number of samples corresponding to the delay spread. This now requires an FFT of size 2N as opposed to size N.

5.1.4 Frequency Reuse

Systems using dynamic adaptive TDD (ATDD), such as the Ripwave system, improve spectral efficiency in many LOS cases, but have harsh frequency reuse and Carrier-to-Interference Ratio (CIR) penalties when used for NLOS situations [53]. In a cellular system with similar cell sizes, the co-channel interference (CCI) is a function of the cell radius, R, and the distance to the center of the nearest cell, D. Increasing the D/R ratio increases the separation between co-channel cells and consequently, reduces the CCI. However, the channel reuse factor and overall system capacity are reduced when the D/R ratio is increased. Therefore, tradeoffs need to be made.

FDD systems utilize different transmit frequencies for the base stations and CPE units. The worst-case potential interference for an FDD system is CPE transmitters in neighboring co-channel base station cells interfering with transmissions from the local CPE sites. An example potential interference scenario is shown in Figure 5.3 below, where a CPE transmitter in Cell B is interfering with a CPE transmission in Cell A.

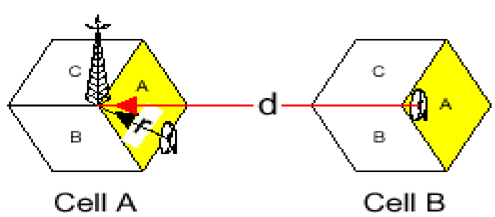

Figure 5.3: FDD Interference Scenario

This example can be extended to the 4x3 reuse pattern diagram illustrated in Figure 5.4 below.

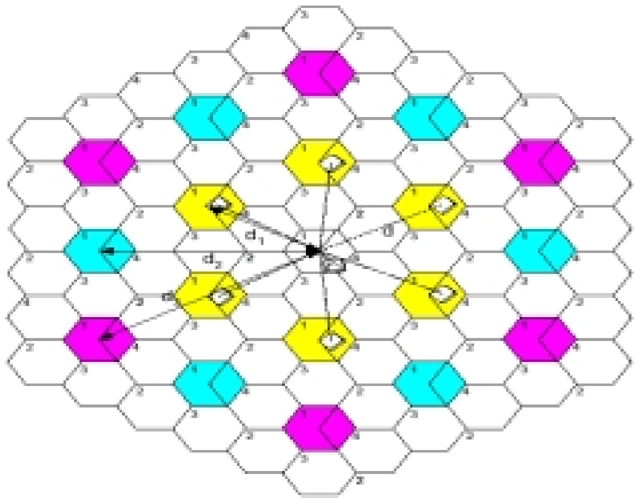

Figure 5.4: 4x3 Reuse Pattern and Tier 1, 2, and 3 Interferers

The worst-case co-channel SIR for an FDD system, using a 4x3 reuse pattern and directional CPE antennas, can be calculated as follows:

$$SIR = 10*\log [r^{-4} / \{2(d_1+r)^{-4} + 4G(d_1+r)^{-4} + 3(d_2+r)^{-4} + 3G(d_2+r)^{-4} + 2(d_3+r)^{-4} + 4G(d_3+r)^{-4}\}],$$

where d_1 = distance from tier 1 interferer, d_2 = distance from tier 2 interferer, d_3 = distance from tier 3 interferer, G is a constant equal to the inverse of the joint antenna discrimination, $(\alpha\beta_{ant})^{-1}$ = 1/1000, and r = the cell radius (5 miles). The joint antenna discrimination, $\alpha\beta_{ant}$, for a 120° sector base station antenna and a planar 20° CPE antenna is typically 1000 (30 dB) and has been assumed for the analysis. The path exponent of 4 results from NLOS being assumed between the base station site and the neighboring co-channel CPE sites. Therefore, the worst case SIR can be calculated to be 21.7 dB.

TDD systems use the same transmit frequency for both the base station and CPE sites. ATDD uses traffic-adaptive time slots, rather than fixed time slots, for upstream and downstream transmissions. ATDD systems do not coordinate base station and CPE transmissions between co-channel cells, and so the local BTS site is subject to interference from both neighboring co-channel BTS and CPE transmitters. The worst-case co-channel interference for an NLOS ATDD system can be shown to be the BTS transmitters in neighboring BTS cells interfering with transmissions from the local CPE sites. Figure 5.5 below, shows interference from the co-channel transmission in Cell B interfering with a CPE transmission in Cell A.

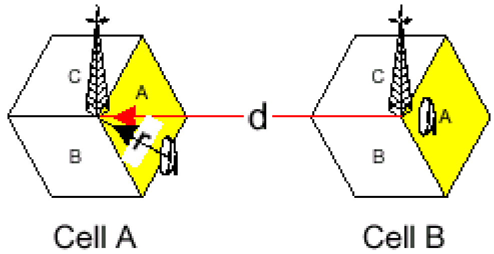

Figure 5.5: ATDD Interference Scenario

The co-channel calculation for an ATDD system includes both LOS elements (path loss exponent = 2) and NLOS elements (path loss exponent = 3 to 4). For these calculations, the power loss formula given in [37] will be used:

$$P_r = P_0(d / d_0)^{-n},$$

where P_r is the received power at a distance and P_0 is the power received at a distance d_0 from the transmitter. The distance d_0 is used in large-scale propagation models as the close-in distance. However, we will be using it as the interception distance, where the path loss slope changes from LOS to NLOS [53]. The interception distance, also known as the reference point, must be chosen such that it lies in the far-field region and d_0 is chosen to be smaller than any practical distance used in the communication system. The reference distance for practical systems using low-gain antennas in the 1-2 GHz region is typically chosen to be 100 m or 1 km in the outdoor environments [37]. This concept is illustrated in Figure 5.6 below.

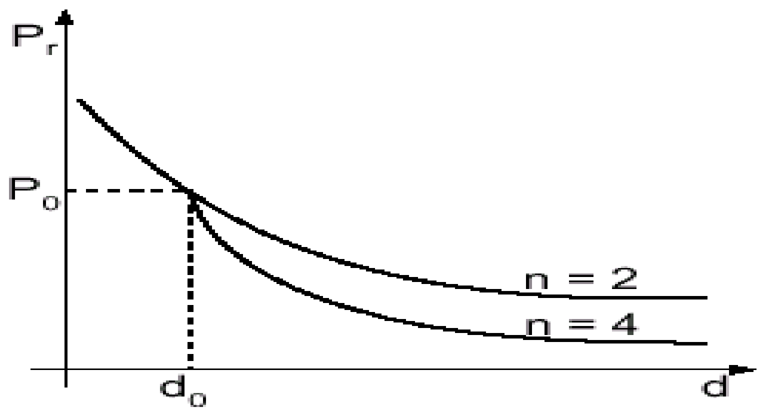

Figure 5.6: LOS and NLOS Power Loss Formulation [54]

Subsequently, the worst-case co-channel SIR can be calculated for a 4x3 reuse pattern that is calculated below. NLOS propagation is assumed between the CPE and associated base station; LOS propagation is assumed between the three tiers of co-channel base station sites.

$$\text{SIR} = 10*\log\left[(r/r_0)^{-4} / \{6G(d1/r_0)^{-2} + 6G(d2/r_0)^{-2} + 6G(d3/r_0)^{-2}\}\right] = -1.1 \text{ dB},$$

where d_1 = distance from tier 1 interferer, d_2 = distance from tier 2 interferer, d_3 = distance from tier 3 interferer, G is the inverse of the joint antenna discrimination, $(\alpha\beta_{ant})^{-1} = 1/1000$, r = the cell radius (5 miles), and r_0 is the interception radius. To achieve an SIR of 20 dB, the distance, d, would have to equal 196 miles (with a cell radius of 5 miles).

Therefore, it can be shown that frequency reuse is less effective in NLOS systems. Consequently, the spectral efficiency of an uncoordinated ATDD system can be shown to be significantly less than that of an FDD system in a typical MMDS or UNII system [53].

5.2 Coverage

Although CPEs with indoor antennas, such as the ones for general TD-SCDMA CPEs, are very attractive from the viewpoint of reducing the installation effort, they are at a disadvantage in terms of coverage area and data rate. The system impact as the CPE outdoor antenna is progressively moved to easier installation configurations from the rooftop to a portable indoor unit with a low-gain antenna is shown in Table 5.2 below. The table also lists the parameters that are modified as the antenna is moved.

Table 5.2: Antenna Configuration Results [54]

	Number of Receive Antennas	SU Antenna Gain (dBi)	Fade Margin (dB)	SU Height (m)	Building Penetration Loss (dB)
Rooftop	2	15	5	8	0
Under-the-eave	2	15	5	3	0
Indoor - window sill	2	12	5	1	6
Indoor - portable	1	3	10	1	12

In the table above, "SU" refers to Subscriber Unit (otherwise known as the CPE). The fade margin assumes a Rayleigh fading channel. The indoor portable unit is assumed to only have one broad-beam low-gain antenna. From [37], 12 dB is an average value for building penetration loss and 6 dB for window penetration loss. The indoor portable CPE antenna's fade margin will be 5 dB higher because it does not have a diversity receiver. The Navini system actually performs a little better, since it has an omnidirectional antenna and two directional patch antennas that it switches between every 10 ms and selects the best signal. This receiver diversity distinguishes the Ripwave from other TD-SCDMA systems. The receiver diversity lowers the fade margin of the Ripwave system back to 5 dB (the margin used for the other antenna configurations in Table 5.2).

Experiments in [54] illustrate the downstream performance of each type of CPE antenna and the results are shown in Figure 5.7 below.

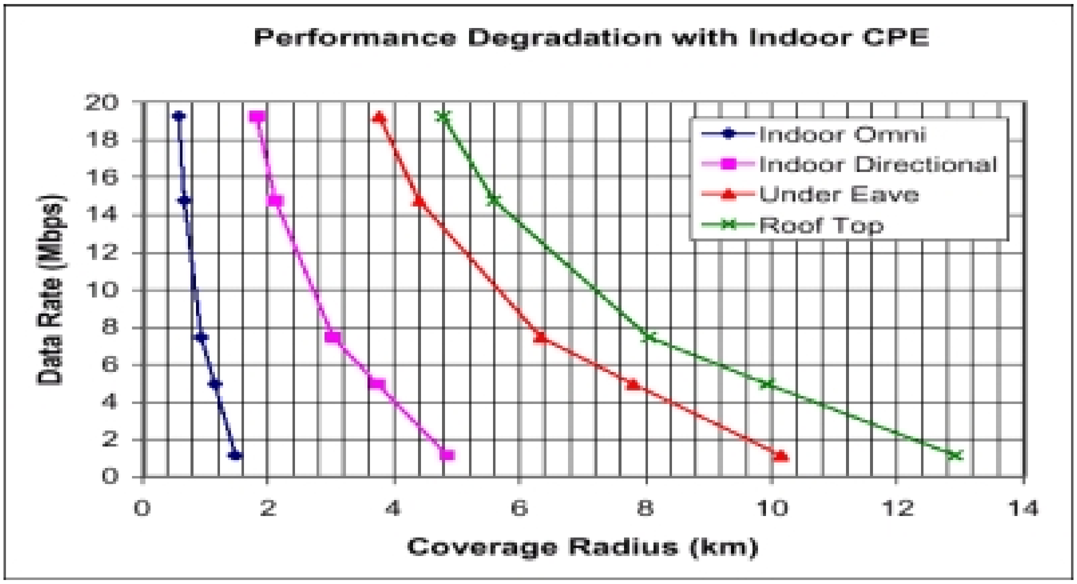

Figure 5.7: Downstream Performance with Different CPE Antennas [54]

The indoor portable CPE is only able to achieve the highest data rate of 19.2 Mbps at a range of 500 meters, and the lowest data rate of 1.1 Mbps at a range of only 1.4 km. Again, the Navini system will perform a little better than the indoor omni since it has 3-element receiver diversity. However, the results seen in Figure 5.7 are consistent with the results seen with the Ripwave system in Chapter 3. It was shown in Chapter 3 that the Ripwave system achieves a data rate of 1.1 Mbps at a range of 4.4 km and a data rate of 2 Mbps at about 1.5 km. With the rooftop antenna arrangement, the CPE can achieve a range of 13 km with a 1.1 Mbps data rate, and 4.7 km at a data rate of 19.2 Mbps.

This directly leads to a penalty in coverage and rollout costs for indoor omnidirectional antennas. Since the area relates to the radius squared, the drastically reduced ranges lead to a substantial increase in infrastructure costs. For example, Table 5.3 shows the number of cells (and hence the number of base stations) that would be necessary to provide 2.0 Mbps downstream to a 3,000-km^2 area.

Table 5.3: Cells Needed for Different Antenna Configurations

Install Type	Cell Radius (km)	Cell Area (km^2)	Total Cells
Rooftop	12	452.4	7
Under-the-Eve	9.67	293.8	10
Indoor-Windowsill	4.5	63.6	47
Indoor-Omni	1.5	7.1	422

As can be seen by the table, the infrastructure costs for an indoor omnidirectional CPE antenna are 60 times higher than for a rooftop antenna, and 40 times higher than under-the-eave antennas. The Ripwave cell radius is on the order of the indoor-omni cell radius, therefore the total cells are on the same order as well. Using omnidirectional antennas also reduces capacity; this will be discussed in the next section.

5.3 Capacity

The previous section discussed performance based on C/N – the coverage limited case. However, tolerance to self-interference dictates the system capacity since the allowable interference level sets the frequency reuse pattern. The portable indoor CPE with an omnidirectional antenna, which is used in most synchronous CDMA systems, will receive interference from other cells in all directions. This mandates a much higher frequency reuse ratio and significantly lowers system capacity.

The expression for the frequency reuse factor with a three-sector cell, directional base station antennas, and an omnidirectional CPE antenna is given in [54] as

$$N = (1/3)[(C/I) * (3.9 + 7.7 * 2^{-\alpha})]^{(2/\alpha)}, \qquad (5.1)$$

where (C/I) is the carrier-to-interference ratio (not in dB) and α is the path loss exponent. Similarly, for a CPE with a dual-channel 20° receiver (as used in VOFDM), the same three-sector cell, and directional base station antennas, the resulting expression for the frequency reuse factor is given in [54] as

$$N = (1/3)[(C/I) * (0.4 + 1.6 * 2^{-\alpha})]^{(2/\alpha)}. \qquad (5.2)$$

With these two equations, the increase in frequency reuse, which corresponds to a decrease in capacity, can be calculated

$$\text{Capacity Improvement} = \left[\frac{\left(3.9 + 7.7 \cdot 2^{-\alpha}\right)\left(\frac{C}{I}\right)_{Omni}}{\left(0.4 + 1.6 \cdot 2^{-\alpha}\right)\left(\frac{C}{I}\right)_{Directional}} \right]^{2/\alpha} \qquad (5.3)$$

Experiments in [54] that use the same 7.4 Mbps downstream data mode show that a mean (C/I) of 12 dB for a diversity directional receiver and 20 dB for a single omnidirectional receiver is required. Since the indoor CPE only has a single antenna and lacks a diversity combiner, the required C/I is 8 dB higher than the directional antennas [54]. As a result, with $\alpha = 4.4$ in Equation 5.3, the capacity per base station of a system with directional CPEs is six times greater than a system with omnidirectional CPE antennas [54]. The Ripwave system's use of transmit beamforming (with eight antenna elements) and 3-element receiver diversity results in a huge C/I advantage over the omnidirectional TD-SCDMA case. As seen in Chapter 3, the aligned interference sites can tolerate an I/C of 15 dB while maintaining an SNR of 10.5 dB. Meanwhile, the non-aligned interference sites can tolerate an I/C of 38 dB while maintaining an SNR of 10.5 dB.

Furthermore, Figure 5.8 below illustrates the coverage probability as a function of C/I with omnidirectional CPE antennas and different frequency reuse patterns.

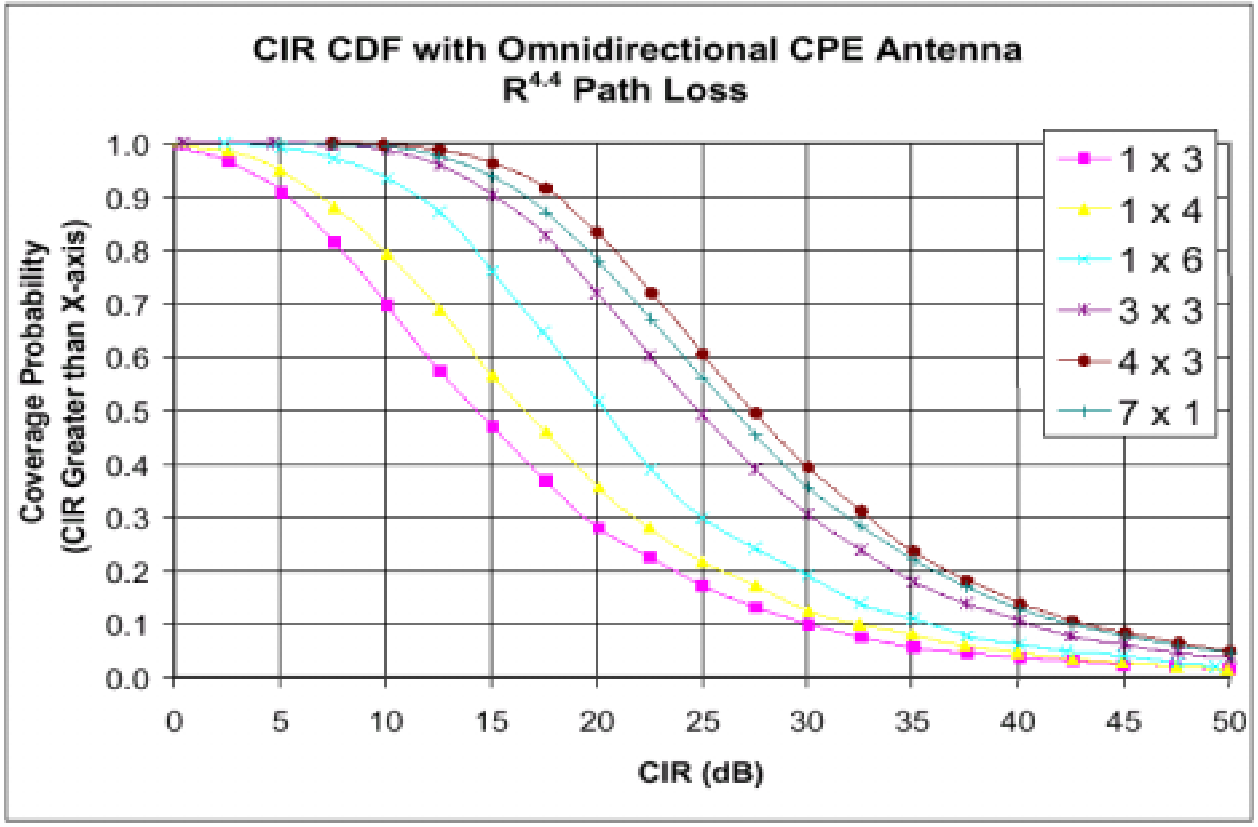

Figure 5.8: CDF of C/I with Omnidirectional CPE Antennas [54]

In the figure, the different curves represent the different frequency reuse patterns that can be used. A log-normal shadow fading with a standard deviation of 8 dB and macrodiveristy are incorporated in the simulation. Macrodiversity enables a CPE to communicate with the fixed network by more than one radio link, i.e. a CPE can send/receive information towards/from more than one base station. Assuming the same C/I requirement of 20 dB from the previous section, it can be seen from the figure above, that even with a 4x3 frequency reuse pattern, only a little above 80% of the cell would be covered.

Similarly, Figure 5.9 illustrates the coverage probability as a function of C/I with diversity directional 20° half power beamwidth (HPBW) CPE antennas as used in VOFDM systems.

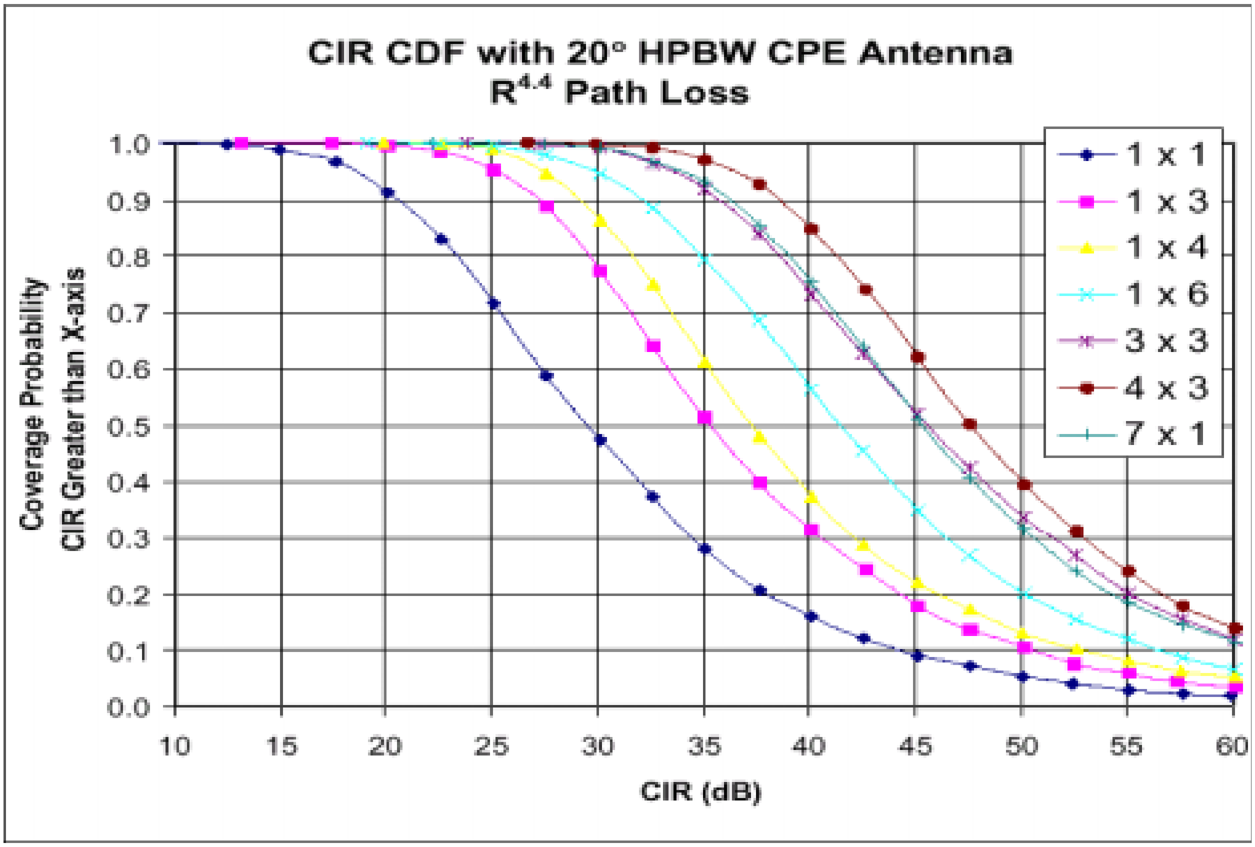

Figure 5.9: CDF of C/I with 20° Directional CPE Antennas [54]

In this case, with a 20 dB C/I requirement, complete cell coverage can be obtained with any reuse pattern greater than 1x1. Actually, a required C/I of 12 dB suffices for complete cell coverage for all the cases except for a reuse factor of 1.

The Ripwave system is also able to use a frequency reuse factor of 1 because of its superb CIR performance as shown in Chapter 3.

5.4 Spectral Efficiency

The efficiencies of CDMA systems were simulated in [55]. The quality of the system is dictated by the level of the required Signal-to-Interference ratio (SIR). Since a CDMA system is typically designed with a frequency reuse of one, the system is interference limited. Therefore, increasing the required SIR means that there is less interference, which reduces the efficiency of the system. In Figure 5.10 below, efficiency is taken to be the number of simultaneous active users divided by the available channels.

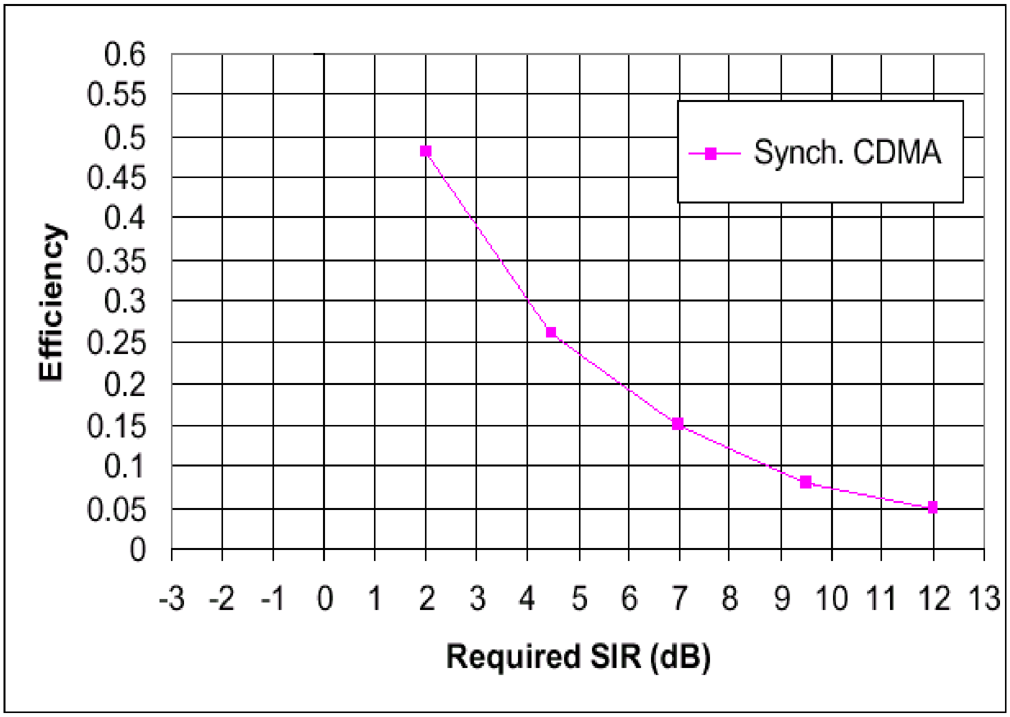

Figure 5.10: Spectral Efficiency of Synchronous CDMA [55]

The results from Figure 5.10 can now be extended to the fixed broadband wireless case. For example, TD-SCDMA uses QPSK with two-bits/symbol efficiency and ½-rate convolutional encoding. The required Eb/No for TD-SCDMA systems using block turbo codes are given in [56] as 3.5 dB for QPSK, 5.5 dB for 8-PSK, and 6.5 dB for 16-QAM.

$$\begin{aligned} \text{SIR} &= (\text{Eb/No}) + 10\log\,[(\text{bits/symbol})*\text{code rate}] \\ &= 3.5 + 10\log\,[2 * (1/2)] = 3.5\ \text{dB}. \end{aligned}$$

Using Figure 5.10, an SIR of 3.5 dB yields an efficiency of 0.35. To meet the out-of-band emission requirements, a spectral shaping factor of 1.2 is employed. Now the spectral efficiency (b/s/Hz) can be calculated

$$\text{Spectral Efficiency} = (\text{efficiency})\,(\text{bits/symbol})\,(\text{code rate})\,(\text{spectral shaping})^{-1}$$
$$= (0.35)\,(2)\,(1/2)\,(1.2)^{-1} = 0.29.$$

This analysis was extended to the different modulation schemes of TD-SCDMA and the results are presented in Table 5.4 below.

Table 5.4: Spectral Efficiencies of TD-SCDMA

Modulation	**Bits/Symbol**	**Eb/No (dB)**	**Coding Rate**	**Spectral Shaping**	**Normalized SIR (dB)**	**Efficiency (users/channel)**	**System Spectral Efficiency (bits/sec/Hz)**
QPSK	2	3.5	0.5	1.2	3.5	0.35	0.29
8-PSK	3	5.5	0.5	1.2	7.3	0.15	0.19
16-QAM	4	6.5	0.5	1.2	9.5	0.08	0.13

For example, let's take the maximum 6-to-1 downlink-to-uplink TDD ratio that can be used with TD-SCDMA (see Chapter 2). This can accommodate a traffic scenario where the downlink requires twelve times the throughput as the uplink by using a frame structure where there are 6 downlink slots using 16-QAM and 1 uplink slot using QPSK (and a switching point). The following table summarizes the data rates that would be seen for such a frame structure given different processing gains and a chip rate of 1.28 Mchip/s.

Table 5.5: Data Rates for TD-SCDMA Using 6 Downlink Slots and 1 Uplink Slot

Processing Gain (Spreading Factor)	**Downlink Information Rate (DIR) (6 slots, 16 QAM)**	**Uplink Information Rate (UIR) (1 slot, QPSK)**
1	1.6896 Mbps	0.1408 Mbps
2	0.8448 Mbps	0.0704 Mbps
4	0.4224 Mbps	0.0352 Mbps
8	0.2112 Mbps	0.0176 Mbps
16	0.1056 Mbps	0.0088 Mbps

In the table above, each time slot is 675 μs and there are 281,600 information bits per second in each time slot [Chapter 2]. Therefore, the Uplink/Downlink Information Rates are calculated as

DIR = (Timeslot Information Rate) (# of slots for downlink)

= (281,600 bps) (6) = 1.6896 Mbps, and

UIR = [(DIR) / (Downlink Throughput)] (Uplink Throughput)

= [(1.6896 Mbps) / (12)] (1) = 0.1408 Mbps.

For fixed broadband wireless, we are mostly concerned with low spreading factors to provide higher data rates. High data rates have little or no processing gain for signal separation from interferers. Now the spectral efficiency of TD-SCDMA with a spreading factor of 1 can be calculated (all values marked with a '*' are taken from Chapter 2).

Table 5.6: TD-SCDMA Coded Efficiency Calculations

Parameter	Value	Units
Chip Rate *	1.28E+06	Chips/sec
Subframe Length *	5.00E-03	sec
Burst Length *	6.75E-04	sec
Slots/SubFrame *	7	
Frame Efficiency	0.945	
Data Symbols/Burst*	704	symbols
Usable Symbol Rate	985600	symbol/sec
Bandwidth *	1.60E+06	Hz
Efficiency (PG=1)	0.62	symbol/sec/Hz
Code Rate	0.5	
Coded Efficiency	0.310	coded symbol/sec/Hz

The Frame Efficiency is calculated by

Frame Efficiency = [(Burst Length) (Slots/Frame)] / [Subframe Length]

= [(6.75E-04) (7)] / [5E-03] = 0.945.

The Usable Symbol Rate is calculated by

Usable Symbol Rate = [(Data Symbols/Burst) (Frame Efficiency)] / [Burst Length]

= [(704) (0.945)] / [6.75E-04] = 985600 symbols/sec.

The Efficiency is calculated by

Efficiency = Usable Symbol Rate / Bandwidth
= 985600 / 1.60E+06 = 0.62 .

Note that the rates and spectral efficiencies calculated above are based only on the frame structure of TD-SCDMA (and are independent of Figure 5.10). Since the there is little or no processing gain, this is now equivalent to a completely TDMA system. As explained in Chapter 2, for serial transmission of high bit rate data, TDMA transmission without spreading is applied in the TD-SCDMA frame structure [20]. Thus, it requires TDMA frequency reuse factors. Therefore, the spectral efficiency calculated above would have to be reduced by the reuse factor (since it is not 1).

The required single-channel unfaded SIR for the different modulation schemes of TD-SCDMA were calculated in Table 5.4 and are summarized in Table 5.7 below.

Table 5.7: Required C/I for TD-SCDMA (Using Block Turbo Codes)

Mode	Required SIR
QPSK	3.5 dB
8-PSK	7.3 dB
16-QAM	9.5 dB

When using these modes in a real environment, a fade margin of 10 dB (from Table 5.2) must be added to each of the required C/I figures. Then, using these new C/I numbers with Figure 5.8 and a 90% coverage probability, the frequency reuse factors can be determined. Afterwards, the system spectral efficiencies can also be determined by reducing the original efficiencies by the reuse factor. These calculations are summarized in Table 5.8 below.

Table 5.8: Spectral Efficiency Calculations

Mode	Modulation (bits/symbol)	Spectral Efficiency (bits/sec/Hz)	Required CIR (fading case) (dB)	Frequency Reuse Factor	System Spectral Efficiency (bits/sec/Hz)
QPSK	2	0.62	13.5	7	0.09
8-PSK	3	0.93	17.3	12 [54]	0.08
16-QAM	4	1.24	19.5	> 12 [54]	< 0.10

For each mode, the Spectral Efficiency is calculated by

Spectral Efficiency = Coded Spectral Efficiency (from Table 5.6) * Modulation
= (0.31) * (bits/symbol).

The System Spectral Efficiency is calculated by

System Spectral Efficiency = Spectral Efficiency / Frequency Reuse Factor.

The Navini Ripwave system would perform better than this omnidirectional TD-SCDMA system since its fade margin would only be 5 dB (instead of 10 dB). However, it uses Reed-Solomon coding instead of block turbo coding. Therefore, the required Eb/No and required SIR would be higher for each modulation scheme. Also, the Ripwave system uses a spreading factor of 32 since it operates in the 2.4 GHz band (in the ISM band, high transmit powers are not permitted, so higher received power must be realized through processing gain) as explained in Chapter 3. Therefore, its data rate and spectral efficiency will be lower. It can achieve high data rates (comparable to VOFDM) but at a cost of the limited number of CPEs one base station can support at these high data rates.

Similarly, the required single-channel unfaded C/I for the different modes of VOFDM were calculated in [54] and are listed in the table below.

Table 5.9: Required C/I for VOFDM

Mode	Required C/I
5.7 Mbps	8 dB
8.5 Mbps	13 dB
7.4 Mbps	13 dB
22 Mbps	24 dB

When using these modes in a real environment, a fade margin of 5 dB (Table 5.2) and a -3 dB adjustment for the number of receiver channels must be added to the required C/I figures (since the noise bandwidth is reduced by a factor of two for FDD systems). Then, using these new C/I numbers with Figure 5.9 and a 90% coverage probability, the frequency reuse factors can be determined. Afterwards, the system spectral efficiencies can also be determined by reducing the original efficiencies by the reuse factor. These calculations are summarized in Table 5.10 below.

Table 5.10: Spectral Efficiency Calculations

mode		Modulation (bits/symbol)	Spectral Efficiency (bits/sec/Hz)	Required SIR w/ fading	Frequency Reuse Factor	System Spectral Efficiency (bits/sec/Hz)
BW (MHz)	Data Rate (Mbps)					
6	5.7	2	0.94	10	1	0.94
6	8.5	4	1.41	15	1	1.41
6	22	6	3.70	26	3	1.23
6	7.4	4	1.22	15	1	1.22

It should be noted that 6 MHz is the proposed channel bandwidth for VOFDM systems. Therefore, it can be seen that the VOFDM system provides better than ten times the spectral efficiency as compared to TD-SCDMA for high data-rate applications.

5.5 Beamforming Versus Diversity

Spatial diversity techniques improve the performance of wireless systems. This section compares two such techniques: transmit beamforming, as employed by TD-SCDMA, and transmit diversity, as employed by VOFDM.

First of all, receive processing operations are similar for both beamforming and diversity. However, both the Ripwave and BWIF VOFDM systems use selection receive diversity, where the receiver just chooses the branch that has the strongest signal power. As stated in Chapter 3, the three-element receiver diversity in the Ripwave system improves the average carrier-to-noise (C/N) ratio by 2.6 dB.

Now, we will compare two-element transmit diversity and transmit beamforming. Figure 5.11 below shows the effective gain for a diversity transmitter operating in a flat unfading channel against a single element antenna. In this simple case, two transmitters at maximum power are used. The signal for the second antenna is a delayed version of the first one. This creates a small amount of delay spread, which is then removed by the VOFDM receiver. The delay diversity prevents coherent signal interference from the two transmitters. As a result, the signal received is 3 dB higher than in the one transmitter case.

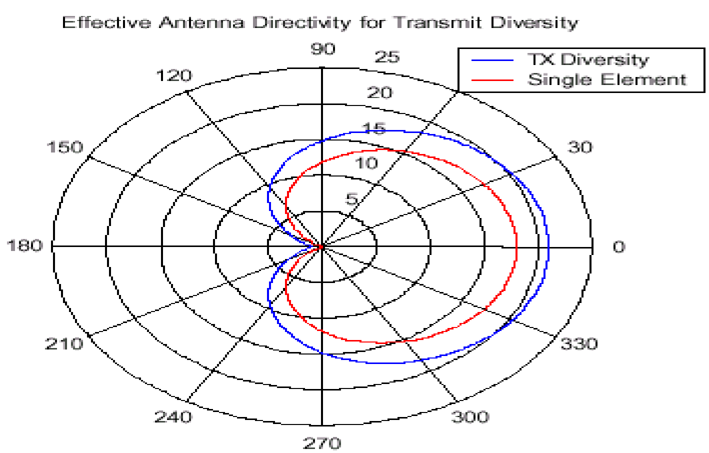

Figure 5.11: Transmit Diversity EIRP Gain [54]

The next figure shows the gain that can be achieved by transmit beamforming over a flat unfading channel. Navini's Ripwave TD-SCDMA system uses transmit beamforming. In this case, two power amplifiers (PA) are transmitting and their signals are sent to transmit antennas spaced 10 wavelengths apart. As a result, the resulting antenna array pattern has 40 lobes and if the signals arrive at the same phase, the gain over a single antenna using a single PA is 6 dB [54].

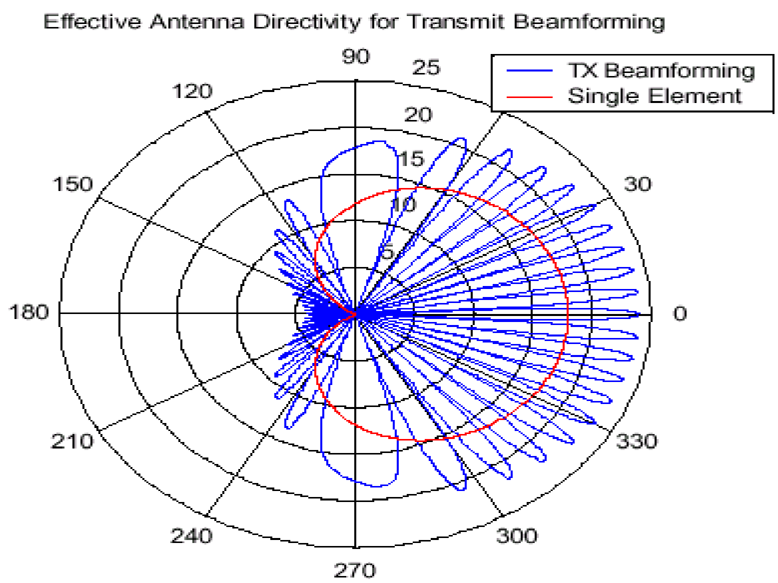

Figure 5.12: Transmit Beamforming EIRP Gain [54]

This comparison in the idealized case indicates that transmit beamforming has a 3 dB advantage over transmit diversity (with two elements). However, this advantage is at the price of using two power amplifiers.

However, in real-world scenarios, the idealized flat unfading channel characteristics will not hold. Experiments were done in [54] that simulated a field deployment using a 64-QAM signal over a 6 MHz bandwidth (6 MHz was chosen since it is the channel bandwidth for VOFDM systems). Tap magnitudes of 0 dB, -5 dB, and 10 dB and tap delays of 0 μs, 0.5 μs, and 1.0 μs were used for the simulated channel. Each tap was simulated as the summation of 50 sinusoids with random phase and random frequency. A delay diversity of 0.33 μs was used for the transmit diversity case, and the transmit beamforming case used phase-shift beamforming to maximize the resulting receiver power. Figure 5.13 shows a plot of the relative received power over time for the three transmission schemes.

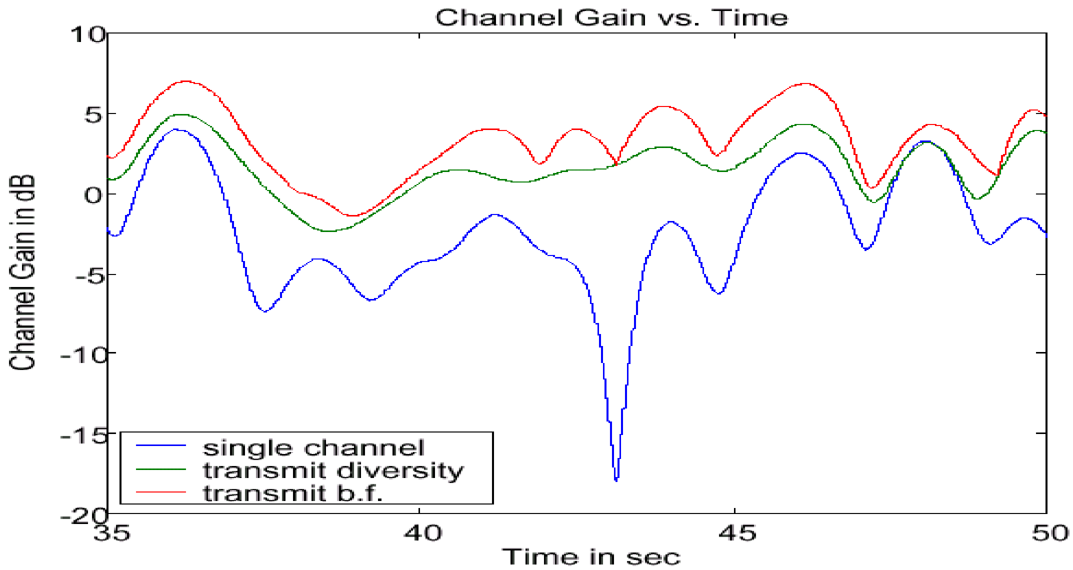

Figure 5.13: Relative Received Power for TX Diversity and TX Beamforming

Overall, slightly more gain is achieved by the transmit beamforming case. However, both the diversity and beamforming methods are effective during the deep fade seen at 43 μs (each provides over a 20 dB gain). Table 5.11 summarizes the gain obtained from transmit diversity and beamforming over a single channel (as seen in Figure 5.12).

Table 5.11: Relative Gains of TX Diversity and TX Beamforming

Transmission Type	.999 Fade RX Power	.999 Fade Gain Over Single Antenna
Single Antenna	-12.9 dB	N/A
Transmit Diversity	-5.7 dB	7.2 dB
Transmit Beamforming	-4 dB	8.9 dB

As seen by the table, for three-nines (99.9% or 0.999) fades, transmit diversity achieves a 7.2 dB gain, while transmit beamforming achieves an 8.9 dB gain over a single antenna system. The difference is now 1.7 dB, and not 3 dB as seen in the idealized case.

Also, the gain in transmit beamforming could be further increased if the number of antennas in the system were increased. However, there are the practical limitations of cost and wind loading that caps the number of antennas that can be used. This proves that transmit beamforming, as employed by the Navini system, is a powerful tool for circuit-switched TDD applications. However, for packet-switched applications (data transfers), there are implementation limitations for transmit beamforming. This will be discussed in the next section.

5.6 Throughput and Packets (MAC Layer Issues)

TD-SCDMA uses the MAC layer from the UMTS Terrestrial Radio Access (UTRA) TDD mode proposal [16]. As explained in Chapter 2, TD-SCDMA is a hybrid of TDMA and CDMA, in which users can be multiplexed in either the time or code domain. TD-SCDMA also provides a reservation-based packet transport protocol. A resource request message is sent prior to transmission, and the physical channel is allocated depending on the nature of the traffic. The allocations can be permanent, based on a set time, or based on the amount of data. Reservations are sent in the random access channel (RACH). In the case of a collision, a request is retransmitted after a random backoff time, which is a multiple of 10 ms. (This is controlled by the MAC.)

VOFDM, on the other hand, uses the Data Over Cable Service Interface Specification (DOCSIS). In DOCSIS, access to the upstream channel is controlled via a backoff window set by the headend. This includes both the initial transmission of a request and any retransmissions caused by collisions. The headend controls the initial access to the contention slot by setting an initial backoff window. The station then randomly selects a number within its backoff window [57].

Simulations to quantify the MAC layer efficiency of the TD-SCDMA system compared with the performance of DOCSIS/VOFDM system are described in [54]. The same channel bandwidth and the same reservation based scheduling algorithms were assumed for both systems. Also, all packet transmissions were non-persistent and retransmissions were based on binary exponential backoff. The traffic sources were variable length packets with exponential interarrival times intended to model variable length IP traffic. Figure 5.14 below shows the throughput-delay curves obtained by the simulations in [54].

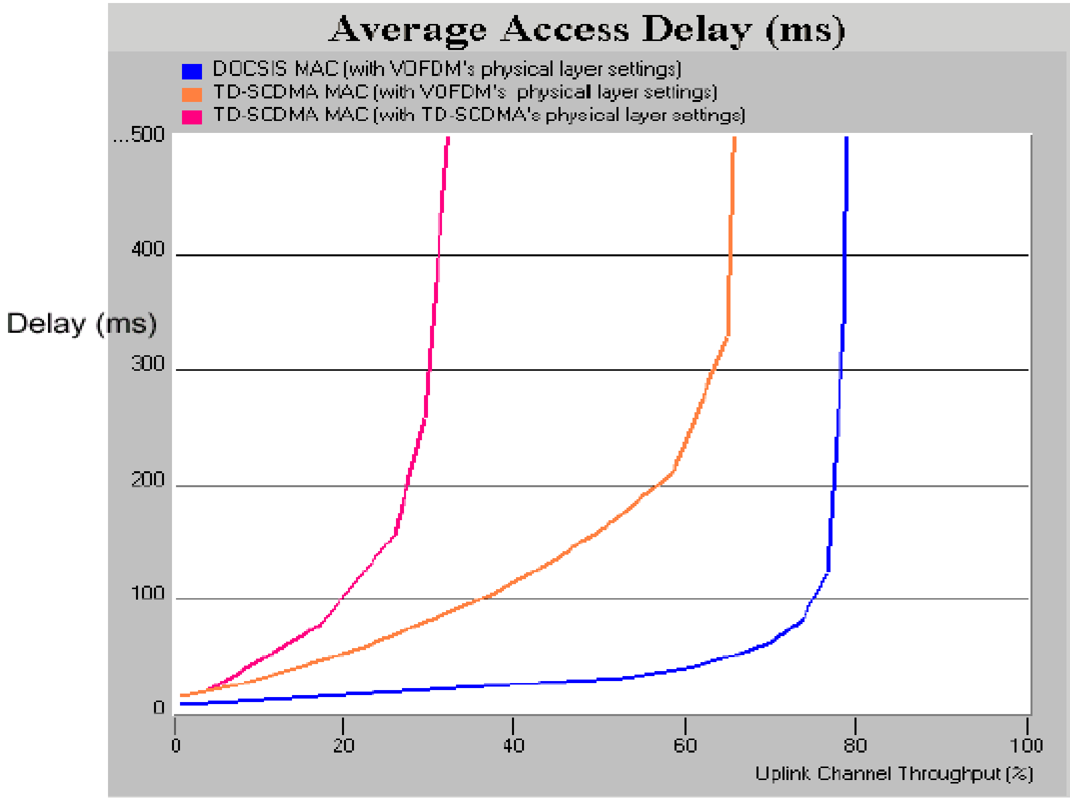

Figure 5.14: Uplink Throughput of TD-SCDMA and DOCSIS/VOFDM [54]

As can be seen from Figure 5.14, using the VOFDM physical layer settings, the DOCSIS/VOFDM system outperforms the TD-SCDMA system. For example, for a 100 ms delay, the maximum uplink throughput of TD-SCDMA is limited to 35%, while that of DOCSIS/VOFDM is 80%. This is due to the limited contention region in TD-SCDMA [54]. Since TD-SCDMA's channel rates are lower than VOFDM, the delay degradation is even worse and available user rates are much lower, when using TD-SCDMA's physical layer settings. As can be seen from the leftmost curve in Figure 5.14, the maximum uplink throughput of TD-SCDMA at 100 ms is only 20%.

The second major issue is the impact of transmit beamforming on the MAC layer of TD-SCDMA. Directing an antenna beam to a particular CPE means that one of more of the other users will not receive sufficient power to demodulate their respective received signals. This means that transmit beamforming limits IP multicasting and IP broadcasting services. One solution is to not use transmit beamforming when these services are to be used, but this has obvious disadvantages.

5.7 Channel Impairments

The performance of both VOFDM and TD-SCDMA will deteriorate under non-ideal conditions. This section will look at their respective performances under multipath, noise, and nonlinearities.

5.7.1 Multipath

OFDM systems are specifically intended to be robust with respect to multipath propagation. This is even more true when a cyclic prefix is included that is at least as long as the multipath delay spread. VOFDM actually specifies training signals for the purpose of estimating the multipath channel coefficients. The number of training signals is directly equal to the size of the cyclic prefix. Experiments carried out by AT&T Labs, Motorola, Sprint, and Cisco have never indicated a delay spread larger than 3 μs, even though the VOFDM system is designed to tolerate up to 7 μs. Thus, VOFDM's multipath performance appears to be excellent.

For a given system, the maximum delay spread that can be tolerated by the VOFDM receiver is less than the cyclic prefix length. So, to increase the resistance to delay spread, we must increase the prefix length. However, this increases the overall system overhead. So, to keep everything constant, the VOFDM burst size also has to be increased by the same proportion. This has the adverse effect of increasing the sensitivity of the system to timing, frequency, or phase errors.

So, to avoid increasing the prefix length, VOFDM systems use directional antennas at the CPE end to reduce the delay spread.

On the other hand, TD-SCDMA has no restrictions on the length of delay spread that can be tolerated. However, every CDMA system uses a rake receiver with *N* fingers to coherently detect and combine a maximum of *N* different received signal paths. Thus, the rake receiver limits the number of paths that can be combined. On the other hand, VOFDM estimates the multipath frequency response so the energy from all the paths within the delay spread limit is taken into account. So, when the multipath channel is composed of more than *N* distinct paths, the CDMA system only uses a portion of the received signal energy for detection. This can lead to a worse performance than VOFDM under the same circumstances since the unused portion of the signal will act as interference. Furthermore, each different path acts as interference for other paths in a CDMA system. This interference can become significant if the CDMA signal is transmitted over many code channels or if the spreading factor is small (as it is for the fixed broadband case). On the other hand, VOFDM does not suffer from multipath self-interference [54].

5.7.2 Frequency Offset, Phase Noise, and Timing Errors

Since an OFDM system, such as the BWIF VOFDM, detects and processes the signal in the frequency domain, it is very sensitive to frequency offsets and phase noise. Furthermore, as the OFDM burst rate decreases, the sensitivity increases [41]. There are a lot of inexpensive solutions to reduce frequency-offset errors and suppress the phase noise for OFDM presented in [40], [41], [43], [44], [45], and others. These algorithms are beyond the scope of this thesis, but it is important to note that there are inexpensive solutions to help alleviate the problems caused by frequency offset and phase noise in an OFDM system. CDMA systems, including the Navini TD-SCDMA Ripwave, are very tolerant of frequency offsets as long as the offset is smaller than the symbol rate [24]. CDMA systems are also more tolerant of phase noise than OFDM systems, even though phase noise can disturb the orthogonality of the spreading codes [24].

In the same way that OFDM is more sensitive to frequency errors, CDMA is more sensitive to timing errors and jitter since the detection and processing of the signal is accomplished in the time domain. Again algorithms exist to alleviate these problems and are presented in [58] among others, but go beyond the scope of this thesis.

A further disadvantage of operating in the time domain (other than sensitivity to timing offsets) for TD-SCDMA is that the equalization, interference rejection, and nonlinearity suppression algorithms have to operate in the time domain as well. This means that all the operations involve convolutions, which make the tasks a lot more complex than the multiplications and divisions needed in VOFDM (since it operates in the frequency domain).

5.7.3 Impulse Noise

Impulse noise in the time domain is the dual of narrowband interference in the frequency domain. OFDM spreads the energy of an impulse noise over a burst, which means that the average noise level slightly increases over a burst instead of a few symbols being totally lost. CDMA, on the other hand, absorbs the impulse noise energy over a few symbols that will be lost. For high data rate applications, such as fixed broadband wireless systems, this will increase the BER even with coding and interleaving. For high data-rate OFDM systems, the symbol interval is much shorter than the average impulse noise interval and the average narrowband interference bandwidth is also much smaller than the OFDM burst rate.

5.7.4 Peak-to-Average Power Ratio

One of the biggest disadvantages of OFDM is its high peak-to-average power ratio (PAPR). An OFDM signal consists of a number of independently modulated subcarriers, which can give a large PAPR when added coherently. The high PAPR is caused by the summation of many sinusoids in the transmitted waveform. The resulting time-domain waveform has a probability distribution that is nearly Gaussian [42]. When N signals are added with the same phase, they produce a peak power that is N times the average power. The peak power is defined as the power of a sine wave with an amplitude equal to the maximum envelope value [38]. A high PAPR means that the transmitter RF power amplifier needs to have an operating point with adequate backoff from the saturation point. If the PAPR increases, the backoff needs to be increased by the same amount. This can severely reduce the transmitted output power.

Several reduction algorithms have been published in [38], [42], [59], and others to help alleviate the PAPR problem, but goes beyond the scope of this thesis. For the BWIF VOFDM system, the backoff is 10 dB without using any reduction algorithm. This is much larger than the 2 or 3 dB backoff required for single carrier systems. In general, CDMA systems suffer from the PAPR problem also, but is at a smaller magnitude and easier to reduce [60]. However, for high spreading factors and a large constellation sizes, the CDMA PAPR approaches the OFDM PAPR magnitude. However, for broadband TD-SCDMA systems, the spreading factors are low (usually 1), so the PAPR problem is always going to be less than the OFDM case.

5.8 Summary

In conclusion, this chapter has presented a comparison between the TD-SCDMA and BWIF VOFDM systems in the areas of duplexing, coverage, capacity, spectral efficiency, spatial processing, throughput, and channel impairments. FDD requires guard bands and more complex hardware, while TDD adds overhead and cannot easily provide traffic-based adaptability as advertised. Moving the antenna indoors, as in TD-SCDMA, results in a lower cell radius and lower data rates. Keeping the antenna outside, as in VOFDM, increases the coverage area, but at larger installation and maintenance costs. The Navini Ripwave system uses selection diversity with three indoor antennas (one omnidirectional and two directional) so its performance is better than the regular TD-SCDMA portable indoor antenna. The indoor antenna also results in higher frequency reuse factors, which reduces the system capacity. It was also shown that the VOFDM system provides better than ten times the spectral efficiency as compared to TD-SCDMA for high data-rate applications. Receive beamforming and receive diversity have similar processing gains. Both, VOFDM and the Ripwave system use selection receiver diversity. On the other hand, transmit beamforming, as used in TD-SCDMA, provides a 2-3 dB advantage over VOFDM's transmit diversity. The throughput of the VOFDM system was also shown to be greater than that of the TD-SCDMA system for variable-length IP packets. VOFDM was also shown to perform better under multipath conditions. Finally, OFDM systems take a huge hit for amplifier nonlinearity, frequency offsets, and phase noise errors.

Chapter 6

Conclusions

The objective of the work in this thesis was to present the 3G standards of Time Division Synchronous Code Division Multiple Access (TD-SCDMA) and Vector Orthogonal Frequency Division Multiplexing (VOFDM) in the context of fixed broadband wireless access. The basic technologies of synchronous CDMA and OFDM were discussed, along with an example TD-SCDMA system: Navini's Ripwave 2400. Afterwards, the VOFDM and TD-SCDMA systems' field tests or simulations were reported and analyzed. This chapter summarizes those results.

6.1 The Ripwave System

Navini Network's Ripwave 2400 system operates in the 2.4 GHz ISM band and can function in either the symmetric or asymmetric TDD mode. The maximum downstream channel size is 5 MHz (ten 500 kHz subcarriers) and the maximum upstream channel size is 2 MHz (four 500 kHz subcarriers). Each subcarrier contains 32 Walsh code channels and only one CPE is assigned per code channel to take advantage of the 32-chip spreading factor (for a processing gain of 15 dB). The maximum number of CPEs that can be accommodated by one BTS is 320, with each having a total data rate of 25 kbps using QPSK. The maximum download rate than can be achieved by a CPE is 7.2 Mbps using 64-QAM and 3:1 asymmetric TDD timing.

The downlink beamforming test was consistent with theory and proved that with eight BTS antennas, an 18 dB downlink beamforming gain was possible. The uplink beamforming test was also consistent with theory and proved that with eight BTS antennas, a 9 dB uplink gain was possible. The uplink CIR test showed that an interference level of over 25 dB still resulted in a S/N of greater than 10.5 dB at the BTS. This was due to the synchronicity of the uplink signals and consequent ability to take advantage of the smart antennas. The downlink CIR test showed that an aligned interference level of 15 dB and a non-aligned interference level of 38 dB resulted in a S/N of greater than 10.5 dB at the BTS. The download data rate test verified the maximum bit rate of 2.4 Mbps (using QPSK and 3:1 TDD) and the upload data rate test verified the maximum bit rate of 1.6 Mbps (using QPSK and 1:1 TDD). The maximum allowed path loss for the downlink is 125.4 dB and 135.4 dB for the uplink.

6.2 Comparison of TD-SCDMA and VOFDM

TD-SCDMA and VOFDM systems differ in the aspects of duplexing, coverage, capacity, spectral efficiency, beamforming and diversity, throughput, and channel impairments such as multipath, noise, and nonlinearities.

6.2.1 Duplexing

While OFDM achieves duplexing in the frequency domain (FDD), TD-SCDMA does so in the time domain (TDD). FDD requires guard bands and more complex hardware (such as a duplexer), while TDD adds overhead (guard times and packet headers) and cannot easily provide the traffic-based adaptability that manufacturers advertise.

Since the base stations are often in line of sight of each other, the transmit and receive cycles of different base stations to be synchronized (otherwise co-channel interference from a neighboring base station can interfere with the uplink transmission from CPEs in a cell). This requirement for synchronization effectively cancels out the dynamic load balancing advantage of TDD. When all the transmit and receive intervals for all the LOS base stations have to be synchronous, the transmit and receive periods at a given base station can no longer be dynamically changed due to local traffic characteristics.

Also, there are frequency reuse penalties with using TDD. The worst-case co-channel SIR for an FDD system, using a 4x3 reuse pattern and directional CPE antennas, was calculated to be 21.7 dB. Meanwhile, since Adaptive TDD (ATDD) systems do not coordinate base station and CPE transmissions between co-channel cells, the local BTS site is subject to interference from both neighboring co-channel BTS and CPE transmitters. Using this assumption, the worst-case co-channel SIR for a TDD system, using a 4x3 reuse pattern, was calculated to be –1.1 dB.

6.2.2 Coverage

Moving the antenna indoors, as in TD-SCDMA, results in a lower cell radius and lower data rates. Keeping the antenna outside, as in VOFDM, increases the coverage area, but at larger installation and maintenance costs. The Navini Ripwave system uses selection diversity with three indoor antennas (one omnidirectional and two directional) so its performance is better than the regular TD-SCDMA portable indoor antenna.

The indoor portable CPE is only able to achieve the highest data rate of 19.2 Mbps at a maximum range of 500 meters, and the lowest data rate of 1.1 Mbps at a maximum range of only 1.4 km. The Ripwave system achieves a data rate of 1.1 Mbps at a maximum range of 4.4 km and a data rate of 2 Mbps at about 1.5 km. With the rooftop antenna arrangement, the CPE can achieve a maximum range of 13 km with a 1.1 Mbps data rate, and 4.7 km at a data rate of 19.2 Mbps. Thus there is a penalty in coverage and rollout costs for indoor omnidirectional antennas.

To provide 2.0 Mbps downstream service to a 3000-km^2 area, the infrastructure costs for an indoor omnidirectional CPE antenna are 60 times higher than for a rooftop antenna, and 40 times higher than under-the-eave antennas. The Ripwave cell radius is on the order of the indoor-omni cell radius so the total cells are on the same order as well.

6.2.3 Capacity

The indoor antenna also results in higher frequency reuse factors, which reduces the system capacity. Since the indoor CPE only has a single antenna and lacks a diversity combiner, the required C/I is 8 dB higher then the directional antennas. As a result, the capacity per base station of a system with directional CPEs was shown to be six times greater than a system with omnidirectional CPE antennas. Assuming a C/I requirement of 20 dB for an omni-directional antenna system, it was shown that even with a 4x3 frequency reuse pattern, only a little above 80% of the cell would be covered. On the other hand, with the rooftop CPE antennas, and a 20 dB C/I requirement, complete cell coverage can be obtained with any reuse pattern greater than 1x1. Actually, a required C/I of 12 dB suffices for complete cell coverage for all the cases except for a reuse factor of 1.

The Ripwave system's use of transmit beamforming (with 8 antenna elements) and 3-element receiver diversity results in a huge C/I advantage over the omnidirectional TD-SCDMA case. The aligned interference sites can tolerate an I/C of 15 dB while maintaining a SNR of 10.5 dB. Meanwhile, the non-aligned interference sites can tolerate an I/C of 38 dB while maintaining an SNR of 10.5 dB. Therefore, the Ripwave system is also able to use a frequency reuse factor of one.

6.2.4 Spectral Efficiency

It was also shown that the VOFDM system provides better than ten times the spectral efficiency as compared to general TD-SCDMA for high data-rate applications (since high data-rate applications are burdened with using low spreading factors). The Navini Ripwave system would perform better than this omnidirectional TD-SCDMA system since its fade margin would only be 5 dB (instead of 10 dB). However, it uses Reed-Solomon coding instead of block turbo coding. Therefore, the required Eb/No and required SIR would be higher (than for the turbo-coded systems). Also, the Ripwave system uses a spreading factor of 32 since it operates in the ISM band. Therefore, its data rate and spectral efficiency will be lower. It can achieve high data rates (comparable to VOFDM) but at a cost of the limited number of CPEs one base station can support at these high data rates.

6.2.5 Beamforming

Receive beamforming and receive diversity have similar processing gains. Both, VOFDM and the Ripwave system use selection receiver diversity. On the other hand, transmit beamforming, as used in TD-SCDMA, provides a 2-3 dB advantage over VOFDM's transmit diversity. In the case of deep fades, transmit diversity achieves a 7.2 dB gain, while transmit beamforming achieves an 8.9 dB gain over a single antenna system. The key advantage of transmit beamforming is that the gain is increased for every additional antenna element. In the Ripwave system, with eight phased-array antennas, an 18 dB downlink beamforming gain is possible.

6.2.6 Throughput

TD-SCDMA uses the MAC layer from the UMTS Terrestrial Radio Access (UTRA) TDD mode proposal, while VOFDM uses the Data Over Cable Service Interface Specification (DOCSIS). Using these MAC layer protocols, the throughput of the VOFDM system was shown to be greater than that of the TD-SCDMA system for variable-length IP packets. For example, for a 100 ms delay, the maximum uplink throughput of TD-SCDMA is limited to 35%, while that of DOCSIS/VOFDM is 80%. Since TD-SCDMA's channel rates are lower than VOFDM, the delay degradation is even worse and available user rates are much lower, when using TD-SCDMA's physical layer settings.

6.2.7 Channel Impairments

VOFDM, through the use of a cyclic prefix performs better under multipath conditions than TD-SCDMA systems. The rake receiver, used in CDMA systems, limits the number of paths that can be combined. On the other hand, VOFDM estimates the multipath frequency response so the energy from all the paths within the delay spread limit is taken into account. So, when the multipath channel is composed of more than a single distinct path, the CDMA system only uses a portion of the received signal energy for detection. This can lead to worse performance than VOFDM under the same circumstances since the unused portion of the signal will act as interference. Additionally, CDMA systems can suffer from multipath self-interference while VOFDM systems do not.

OFDM systems take a huge hit for frequency offsets and phase noise errors. In the same way that OFDM is more sensitive to frequency errors, CDMA is more sensitive to timing errors and jitter since the detection and processing of the signal is accomplished in the time domain. However, inexpensive algorithms exist to alleviate each of these impairments.

Finally, one of the biggest disadvantages of OFDM is its high peak-to-average-power ratio (PAPR), which necessitates a huge amplifier backoff. For the BWIF VOFDM system, the backoff is 10 dB without using any reduction algorithm. This is much larger than the 2 or 3 dB backoff required for single carrier systems. In general, CDMA systems suffer from the PAPR problem also, but is at a smaller magnitude and easier to reduce.

6.3 Summary

In conclusion, the technologies and comparisons of TD-SCDMA and VOFDM have been presented in this thesis. In the context of fixed broadband wireless access, there is no clear-cut winner. However, as far as the important parameters of coverage (cell size) and the number of users that can be supported at high data rates, VOFDM is superior to TD-SCDMA. However, this is at a higher infrastructure and rollout cost. The benefits of each system are summarized in Table 6.1 below.

Table 6.1: Benefits Summary of TD-SCDMA and VOFDM

	TD-SCDMA	**VOFDM**
Duplexing	• No guard bands • No extra hardware • But, no dynamic load balancing	• No guard times • Worst case SIR (for 4x3 reuse pattern) = 21.7 dB (23 dB better than NLOS ATDD case)
Coverage	• No extra installation costs for CPE antennas	• Rooftop antennas increase coverage • Sixty times fewer cells needed for 2 Mbps service for a 3000 km^2 area
Capacity		• Six times greater capacity for directional CPE antennas • Required C/I is 8 dB lower for directional CPE antennas
Spectral Efficiency		• Ten times greater for 90% cell coverage
Beamforming	• 8.9 dB deep fade gain (over single antenna element) • More gain with more elements	• 7.2 dB deep fade gain (over single antenna element)
Throughput	• For 100 ms delay, maximum uplink throughput is limited to 35%	• For 100 ms delay, maximum uplink throughput is limited to 80%
Channel Impairments	• Robust with respect to frequency offset and phase noise • Doesn't suffer from large PAPR • Doesn't need a large amplifier backoff	• Robust with respect to timing errors and jitter • More robust under multipath conditions

Future work needs to be done in testing an actual hardware VOFDM system and comparing it to TD-SCDMA systems such as Navini Network's Ripwave 2400.

Appendix A

Ripwave Data Rate Calculations

Maximum Number of CPEs permitted per base station:

Max # Users = Total Subcarriers per 5 MHz * Total Code Channels per Subcarrier

= 10 * 32 = 320 users

Total Data Rate of 320 Users using QPSK:

Total Symbol Rate, $R_s = B_{occ} / (1 + \alpha)$

= [(1 subcarrier * 500 kHz each) / 32 code channels] / (1 + 0.25)

= (5.625 kHz) / (1.25)

= 12.5E+03 symbols/sec

Using QPSK, Total Data Rate, R_b = 1.25E+03 * 2

= 25 kbps

Maximum Downlink Data Rate of a CPE:

Total Symbol Rate, $R_s = B_{occ} / (1 + \alpha)$

$= (4 \text{ subcarriers} * 500 \text{ kHz each}) / (1 + 0.25)$

$= (2 \text{ MHz}) / (1.25)$

$= 1.6E+06$ symbols/sec

Using 64-QAM, Total Data Rate, $R_b = 1.6E+06 * 6$

$= 9.6$ Mbps

With 3:1 TDD timing, Downlink Data Rate = (Total Data Rate / 4) * 3

= (9.6 Mbps / 4) * 3 = 7.2 Mbps

Uplink Data Rate = (Total Data Rate / 4) * 1

= (9.6 Mbps / 4) * = 2.4 Mbps

Maximum Download Data Rate for Experiment:

Total Symbol Rate, $R_s = B_{occ} / (1 + \alpha)$

$= (4 \text{ subcarrier} * 500 \text{ kHz each}) / (1 + 0.25)$

$= (2 \text{ MHz}) / (1.25)$

$= 1.6E+06$ symbols/sec

Using QPSK, Total Data Rate, $R_b = 1.6E+06 * 2$

$= 3.2$ Mbps

With 3:1 TDD timing, Downlink Data Rate = (Total Data Rate / 4) * 3

= (3.2 Mbps / 4) * 3 = 2.4 Mbps

Maximum Upload Data Rate for Experiment:

Total Symbol Rate, $R_s = B_{occ} / (1 + \alpha)$

$= (4 \text{ subcarrier} * 500 \text{ kHz each}) / (1 + 0.25)$

$= (2 \text{ MHz}) / (1.25)$

$= 1.6E+06$ symbols/sec

Using QPSK, Total Data Rate, $R_b = 1.6E+06 * 2$

$= 3.2$ Mbps

With 1:1 TDD timing, Downlink Data Rate = (Total Data Rate / 2) * 1

= (3.2 Mbps / 2) * 1 = 1.6 Mbps

Appendix B

Glossary of Acronyms

2G	2nd Generation
3G	3rd Generation
ATDD	Adaptive Time Division Duplexing
AWGN	Additive White Gaussian Noise
BER	Bit Error Rate
BTS	Base Transmit Station
BWIF	Broadband Wireless Internet Forum
CATT	Chinese Academy of Telecommunications Technology
CCI	Co-Channel Interference
CCPCH	Common Control Physical Channel
CDMA	Code Division Multiple Access
CIR	Carrier-to-Interference Ratio
COFDM	Coded Orthogonal Frequency Division Multiplexing
CPE	Customer Premise Equipment
CWTS	Chinese Wireless Telecommunications Standard
DCA	Dynamic Channel Allocation
DECT	Digital Enhanced Cordless Telecommunications
DEMS	Digital Electronic Messaging Service
DFT	Discrete Fourier Transform
DIR	Downlink Information Rate
DOCSIS	Data Over Cable Service Interface Specification
DQPSK	Differential Quadrature Phase Shift Keying

DS-CDMA	Direct Sequence Code Division Multiple Access
DSP	Digital Signal Processor / Digital Signal Processing
DSS	Direct Sequence Spreading
DwPTS	Downlink Pilot Time Slot
ETSI	European Telecommunications Standards Institute
FDD	Frequency Division Duplexing
FDMA	Frequency Division Multiple Access
FEC	Forward Error Correction
FFT	Fast Fourier Transform
FPC	Fast Power Control
GWCS	General Wireless Communications Service
IFFT	Inverse Fast Fourier Transform
IMT	International Mobile Telecommunications
ISI	Inter-Symbol Interference
ISM	Industrial, Scientific, and Medical band
ITU	International Telecommunication Union
LAN	Local Area Network
LMDS	Local Multipoint Distribution Service
LO	Local Oscillator
LOS	Line of Sight
MAC	Media Access Control
MAI	Multiple Access Interference
MIMO	Multiple Input Multiple Output
MMDS	Multichannel Multipoint Distribution Service
NF	Noise Figure
NLOS	Non Line of Sight
ODMA	Opportunity Driven Multiple Access
OFDM	Orthogonal Frequency Division Multiplexing
OVSF	Orthogonal Variable Spreading Factor
PA	Power Amplifier
PAPR	Peak-to-Average Power Ratio
PN	Pseudo-random Noise
PRACH	Physical Random Access Channel
PSD	Power Spectral Density
PSTN	Public Service Telephone Network
QAM	Quadrature Amplitude Modulation
QOS	Quality Of Service
QPSK	Quadrature Phase Shift Keying
RACH	Random Access Channel

RF	Radio Frequency
RFS	Radio Frequency Subsystem
RMS	Root Mean Square
RRC	Root Raised Cosine
RS	Reed Solomon
SCDMA	Synchronous Code Division Multiple Access
SCM	Single Carrier Modulation
SIR	Signal-to-Interference Ratio
SNR	Signal-to-Noise Ratio
TDD	Time Division Duplexing
TDMA	Time Division Multiple Access
TD-SCDMA	Time Division - Synchronous Code Division Multiple Access
TS	Time Slot
UIR	Uplink Information Rate
UMTS	Universal Mobile Telecommunications System
UpPTS	Uplink Pilot Time Slot
UT	User Terminal
UTRA	UMTS Terrestrial Radio Access
UWC	Universal Wireless Communications
VOFDM	Vector Orthogonal Frequency Division Multiplexing
WAN	Wide Area Network
WBS	Wireless Base Station
W-CDMA	Wideband Code Division Multiple Access
WCS	Wireless Communications Service
WIMS	Wireless Multimedia and Messaging Services
WOFDM	Wideband Orthogonal Frequency Division Multiplexing

Bibliography

[1] "A Way Forward for Broadband Wireless Access – An Investigation for the Radiocommunications Agency," http://www.radio.gov.uk.topics/bfwa/document/quotient/quotient.htm, March 1999.

[2] Three-G.net, "A 3G Introduction to 3G Technology, 3G Standards, and 3G Spectrum," http://www.wales.info/3g.html.

[3] Corinex Global, "An Introduction to Technology and Services," http://www.corinex.com.

[4] "MSI's New Broadband Wireless Access (BWA) – Center of Excellence," *Metapath Software International Limited*, 1999.

[5] B. Kim, et. al., "The AT&T Labs Broadband Fixed Wireless Field Experiment," *IEEE Communications Magazine*, October 1999.

[6] H. Bolcskei, et. al., "Fixed Broadband Wireless Access: State of the Art, Challenges, and Future Directions," *IEEE Communications Magazine*, January 2001.

[7] J. W. Porter and J. A. Thweatt, "Microwave Propagation Characteristics in the MMDS Frequency Band," *Communications, IEEE International Conference on, Vol. 3*, 2000.

[8] C. Huang and R. Khayata, “Delay Spreads and Channel Dynamics Measurements at ISM Bands,” *Communications, ICC '92, Discovering a New World of Communications, IEEE International Conference on*, 1992.

[9] G. Woodward, et. al., “Outdoor-Indoor Temporal & Spatial Wideband Channel Model for ISM Bands,” *Vehicular Technology Conference,* 1999.

[10] P. de Bot, et. al., “Propagation of Broadcast Signals into Buildings at 762 MHz,” *Communications and Vehicular Technology in the Benelux*, 1994.

[11] H. Shimizu, et. al., “LOS and NLOS Path-Loss and Delay Characteristics at 3.35 GHz in a Residential Environment,” *Antennas and Propagation Society International Symposium,* 2000.

[12] J. E. Dietert and B. Rembold, “Directional Stochastic Channel Model for (N)LOS Outdoor Environment,” *Personal, Indoor and Mobile Radio Communications*, 2000.

[13] M. Opilant, “The Mobile Phone Meets the Internet,” *IEEE Spectrum,* August 1999.

[14] Y. Xiaohu and Y. Fengyi, “Developments in the 3G Mobile Communications System,” http://www.tdscdma-forum.org.

[15] M. Zeng, et. al., “Recent Advances in Cellular Wireless Communications,” *IEEE Communications Magazine*, September 1999.

[16] K. W. Richardson, “UMTS Overview,” *Electronic & Communications Engineering Journal*, June 2000.

[17] K. Kammerlander, “Benefits and Implementation of TD-SCDMA,” on *Communication Technology Proceedings, WCC - ICCT 2000*, 2000.

[18] CDMA Development Group, "Forward CDMA Channel," http://www.cdg.org.

[19] CWTS WG1, "Method and Principle of Uplink Synchronization," *TSG-RAN Working Group 1, Meeting 5*, June 1999.

[20] TD-SCDMA Forum, "Speech-, Multimedia-, and Internet-Operation of TD-SCDMA," http://www.tdscdma-forum.org.

[21] TD-SCDMA, "TD-SCDMA Radio Transmission Technology for IMT-2000 Candidate Submission," Draft V.0.4, CATT, September 1998.

[22] J. J. Blanz, et. al., "Performance of a cellular hybrid C/TDMA mobile radio system applying joint detection and coherent receiver antenna diversity," *IEEE Journal on Selected Areas in Communications, Vol. 12*, 1994.

[23] Y. Lu and P. W. Baier, "Performance of adaptive antennas for the TD-CDMA downlink under special consideration of multi-directional channels and CDMA code pooling," *International Journal of Electronics and Communications, Vol. 54,* 2000.

[24] A. J. Weiss and B. Friedlander, "Synchronous DS-CDMA Downlink with Frequency Selective Fading," *IEEE Transactions on Signal Processing, Vol. 47, No. 1,* January 1999.

[25] China Wireless Telecommunication Standard (CWTS), Working Group 1 (WG1), "Physical Channels and Mapping of Transport Channels onto Physical Channels," TS C102 v3.0.0, 1999.

[26] CWTS WG2, "Overview of the TDD harmonization and the key features of TD-SCDMA," *TSG-RAN Working Group 2, Meeting 6,* August 1999.

[27] TD-SCDMA Forum, "Smart Antennas a Key-Feature of TD-SCDMA," http://www.tdscdma-forum.org.

[28] J. H. Winters, "Smart Antennas for Wireless Systems," *IEEE Personal Communications*, February 1998.

[29] TD-SCDMA Forum, "Joint Detection a Key-Feature of TD-SCDMA," http://www.tdscdma-forum.org.

[30] P. W. Baier, et. al., "Recent Progress of Time Slotted CDMA," *IST 2001, Tehran-Iran*, September 2001.

[31] M. Beaton, et. al., "Ripwave 2400 Solution Overview Release 1," *Navini Networks Confidential Information, Draft 1*, October 2001.

[32] K. Davey, "Zero-Install Nomadic Wireless Broadband Access," December 2001.

[33] Navini Networks, "Catch the Next Wave of Broadband – Navini Ripwave," http://www.navini.com, 2001.

[34] Grabner, "Dallas Field Trial – Summary of Results," *Navini Networks Proprietary Information*.

[35] J. H. Reed, et. al., *Software Radios: A Modern Approach to Radio Engineering*, Prentice Hall PTR, Upper Saddle River, NJ, 2001.

[36] D. Maez, "nTelos Trial Network Architecture Overview," *Navini Networks Proprietary Information, Draft 0.01*, October 2001.

[37] T.S. Rapport, *Wireless Communications*, Prentice Hall PTR, Upper Saddle River, NJ, 1996.

[38] R. van Nee and R. Prasad, *OFDM for Wireless Multimedia Communications*, Artech House, 2000.

[39] U. Reimers, “Digital Video Broadcasting,” *IEEE Communications Magazine,* June 1998.

[40] J. Rinne and M. Renfors, “An Equalization Method for Orthogonal Frequency Division Multiplexing Systems in Channels With Multipath Propagation, Frequency Offset and Phase Noise,” *Global Telecommunications Conference, 'Communications: The Key to Global Prosperity’, Volume 2*, 1996.

[41] T. Pollet, et. al., “BER Sensitivity of OFDM Systems to Carrier Frequency Offset and Wiener Phase Noise,” *Communications, IEEE Transactions on , Volume 43, Issue 2, Part 3*, April 1995

[42] J. Rinne and M. Renfors, “The Behavior of Orthogonal Frequency Division Multiplexing Signals in an Amplitude Limiting Channels,” *IEEE Communications Magazine*, 1994

[43] A. Armada and M. Calvo, “Phase Noise and Sub-Carrier Spacing Effects on the Performance of an OFDM Communication System,” *IEEE Communications Letters, Volume 2, Issue 1*, January 1998

[44] T. Seki and N. Taga, “A Novel Phase Noise Suppression Technique in OFDM Receiver,” *IEEE Consumer Electronics Magazine*, 1998.

[45] M. S. El-Tanany, et. al., “OFDM Uplink for Interactive Broadband Wireless: Analysis and Simulation in the Presence of Carrier, Clock and Timing Errors,” *IEEE Transactions on Broadcasting, Vol. 47, No. 1,* March 2001.

[46] Z. Hadad, “Coded Orthogonal Frequency Division Multiple Access,” *IEEE 802.16 Session #7: Tutorial Open Forum,* May 2000.

[47] S. Buckley, “Is OFDM Ready for Prime Time,” *Telecommunications Online*, February 2001.

[48] "Overcoming Multipath in Non-Line-of-Sight High-Speed Microwave Communication Links," Cisco Systems White Paper, September 2000.

[49] "White Paper: Wide-band Orthogonal Frequency Multiplexing (W-OFDM)," Wi-Lan Inc., Version 1.0, September 2000.

[50] Flarion Technologies, "Flash-OFDM Airlink," http://www.flarion.com.

[51] E. Ayanoglu, et. al., "VOFDM Broadband Wireless Transmission and Its Advantages over Single Carrier Modulation," Document WP-1_TG-1 Version 1.2, December 2000.

[52] G. Raleigh, "VOFDM Architecture and Competitive Positioning," Broadband Wireless Internet Forum Presentation.

[53] E. Ayanoglu, et. al., "Frequency Division Duplexing and Time Division Duplexing for Broadband Wireless Applications," Document WP-3_TG-1 Version 1.2, February 2001.

[54] E. Ayanoglu, et. al., "BWIF – Bringing Broadband Wireless Access Indoors," Document WP-4_TG-1 Version 1.0, September 2001.

[55] G. Pottie, "System Design Choice in Personal Communications," *IEEE Communications Magazine*, October 1995.

[56] D. G. Williams, "BTS Capabilities Overview," IEEE 802.16.1, July 2000.

[57] E. Ayanoglu, et. al., "Media Access Protocols: Circuit Switching to DOCSIS," Document WP-2_TG-1 Version 1.1, February 2000.

[58] R. van Nee, "Timing Aspects of Synchronous CDMA," *Personal, Indoor and Mobile Radio Communications*, 1994.

[59] E. Lawrey and C. J. Kikkert, "Peak To Average Power Ratio Reduction of OFDM Signals Using Peak Reduction Carriers," *Signal Processing and Its Applications, ISSPA '99, Proceedings of the Fifth International Symposium on, Volume 2*, 1999

[60] V. Lau, "Average of Peak-to-Average Ratio (PAR) of IS95 and CDMA2000 Systems – Single Carrier," *IEEE Communications Letters, Vol. 5, No. 4*, April 2001.

Vita

Shital Ratilal Chheda was born in Bombay, India in 1978. He was raised in the suburbs of Baltimore, Maryland and graduated from Old Mill Senior High School in 1996. He continued his education at Virginia Tech, studying Computer Engineering. While an undergraduate at Virginia Tech, Shital gained valuable industry experience with a co-op at Lockheed Martin and multiple internships at the Aerospace Corporation. He graduated cum laude with a Bachelor of Science degree in Computer Engineering in 2000.

Upon graduation, Shital continued his education at Virginia Tech by pursuing a Masters degree in Electrical Engineering. As a graduate student, he worked in the Center for Wireless Telecommunications as a graduate research assistant. His research included various aspects of wireless communications, communication system design, and RF design.

Shital will have completed the requirements for the Master of Science degree in Electrical Engineering in May 2002. Upon completion, he will join Texas Instruments in Dallas, Texas as a technical sales associate.